THE MEASUREMENT OF GROUND IMPROVEMENT USING THE CONTINUOUS SURFACE WAVE METHOD

A dissertation submitted to the University of Pretoria in partial fulfilment of the Degree of
Magister Scientiae (Geotechnical Engineering)
in the Faculty
Engineering, Built Environment and Information Technology

By
Julian Venter

October 2003

ACKNOWLEDGEMENTS

I would like to thank the University of Pretoria for allowing me to use their equipment and facilities to complete this dissertation.

Mr. Richter, the owner and proprietor of Richter sand deserves a word of gratitude for his help with excavation machinery and for allowing me to complete the field work on his property.

A word of thanks also to my promotor and mentor, Prof. G. Heymann for his guidance and support even during the difficult times. Prof. C.R. Clayton must also be thanked for his advice.

My heartfelt appreciation to my fiancée, Tia van Rensburg, her mother and sister who supported me throughout the time it took to complete the research to complete this dissertation. Thanks to my cousins and friends who helped to complete the field work, and gave up their holiday in order to assist me.

My grandmother and father also deserve a word of thanks, for they never stopped believing in me.

SUMMARY

Title:	**The measurement of ground improvement using the continuous surface wave method**
Author:	**Julian Venter**
Supervisor:	**Professor Gerhard Heymann**
Department:	**Civil and Biosystem Engineering**
University:	**University of Pretoria**
Degree:	**Magister Scientiae (Geotechnical Engineering)**

Key words: Seismic, Dynamic cone penetrometer, Continuous surface wave method, Shear stiffness, Compaction, Rayleigh waves, Geophysics, Site investigation, Geophone and ground improvement.

Seismic wave testing has become increasingly popular in site investigation. This is due to the fact that the principles involved are becoming more accepted and that the equipment are becoming more available and reliable.

This dissertation presents the required theory behind one seismic test in particular, the Continuous Surface Wave (CSW) method of seismic testing. The attributes of seismic testing are presented along with a summary of various testing methods. The dissertation also demonstrates that the author developed his own system for completing this test and demonstrated that he successfully used it to measure the stiffness of two soil profiles.

The author compared the stiffness as measured using the CSW method with the strength as measured using the Dynamic Cone Penetrometer (DCP) for two soil profiles, and the in situ profile was compared to a compacted profile.

The author demonstrated that the in situ profile had a higher stiffness than the same soil after it was thoroughly compacted and that the DCP results concur. This was caused by the in situ profile being structured and the compacted profile not.

SAMEVATTING

Titel:	**The measurement of ground improvement using the continuous surface wave method**
Outeur:	**Julian Venter**
Promotor:	**Professor Gerhard Heymann**
Departement:	**Siviel en Biosysteem Ingenieurswese**
Universiteit:	**Universiteit van Pretoria**
Graad:	**Magister Scientiae (Geotegniese Ingenieurswese)**

Sleutelterme: Seismiese, Dinamiese kegel penetrometer, Kontinue golf metode, Skuif styfheid, Kompaksie, Verdigting, Rayleigh golwe, Geofisika, Veld ondersoek en Geofoon.

Seismiese golf toetsmetodes raak al hoe meer gewild tydens veld ondersoeke in geotegniese ingenieurswese. Dit is omdat die onderliggende beginsels beter aanvaar word deur die praktyk en omdat die toerusting meer bekombaar en betroubaar word.

Hierdie verhandeling gee 'n verduideliking van die nodige teorie om die Kontinue Oppervlak Golf (KOG) seismiese toets metode te verstaan. Verder word 'n opsomming gegee van die ander seismiese toets metodes wat soms deur geotegniese ingenieurs gebruik word.

Hierdie verhandeling demonstreer dat die outeur die nodige toerusting self aanmekaar gesit het om die KOG toets metode te kon toepas en dat hy bewys het dat hy die styfheid van twee grond profiele suksesvol daarmee kon meet.

Die outeur het die KOG resultate bekom van die twee grond profiele vergelyk met die van 'n Dinamiese Kegel Penetrometer (DKP). Die een

grond profiel was in situ en die ander een het bestaan uit grond van die eerste profiel wat opgegrawe en weer gekompakteer is.

Die toetswerk het bewys dat die in situ profiel stywer was as die gekompakteerde profiel omdat dit 'n effense struktuur bevat het en die gekompakteerde profiel nie.

TABLE OF CONTENTS

TABLE OF FIGURES

LIST OF APPENDICES

1 INTRODUCTION

The key to successful geotechnical design is a proper site investigation. In order to perform a site investigation the geotechnical engineer has many tools to help him in his task. One of the lesser known tools, the Continuous Surface Wave (CSW) method, uses seismic principles to obtain soil parameters. In South Africa, until recently, seismic methods have been largely overlooked as a viable tool to aid site investigation. This is as a result of poor results obtained from seismic tests performed in an era when computers were less powerful.

In this dissertation the student will show that the CSW method of seismic testing is a viable engineering tool, which can be used reliably to aid geotechnical design and quality management during construction.

1.1 THE HYPOTHESIS

This study aims to test the hypothesis that the CSW technique can be used to detect changes in soil stiffness.

1.2 EXPERIMENT

The hypothesis was tested by comparing stiffness as measured by CSW to penetration resistance from a Dynamic Cone Penetrometer (DCP) for the following cases:

- An in situ profile of soil and
- A compacted profile of the same soil.

The first Chapter of this dissertation puts forward a hypothesis followed by an outline of the experiment used to test the hypothesis.

The second Chapter serves as a literature study where the required theory is outlined. The third Chapter discusses the experimental set-up and the procedures used to collect the data.

Chapter 4 reports and discusses the information obtained during the experiment and Chapter 5, the last chapter, contains the conclusions and recommendations.

2 LITERATURE REVIEW

The previous Chapter served as an introduction as well as a statement of the hypothesis and a short explanation of the testing procedure followed.

This Chapter serves as a literature study. The principles behind seismic testing and the Continuous Surface Wave method (CSW) are discussed and an example is given. Thereafter a number of the relevant theories behind stiffness and compaction are presented followed by a discussion of the various methods of seismic testing and the applications of the CSW method.

2.1 SEISMIC PRINCIPLES

When an elastic half space is suddenly stressed at a point near the surface (for instance by a falling weight), the energy is dissipated in the form of seismic waves (Figure 2.1). Seismic waves can be divided into two groups: body waves and surface waves.

Body waves consist of P-waves or compressional waves and S-waves or shear waves. Both S-waves and P-waves are not bound to the surface but travel directly through the body.

P-waves are longitudinal waves (Figure 2.2) and their corresponding particle motion approaches uniaxial compression of the material (Griffiths and King, 1981). The velocity of P-waves is given by:

$$V_P = \sqrt{\frac{(\kappa + 4/3 \times G)}{\rho}}$$ **Equation 2-1**

Where:

V_P = The velocity of P-waves (m/s)

κ = The bulk modulus of elasticity (Pa)

G = The elastic shear stiffness of soil (Pa)

ρ = The density of the soil (kg/m^3).

S-waves are transverse waves (Figure 2.2) and their corresponding particle motion places the material under shear stress. The velocity of S-waves is given by:

$$V_S = \sqrt{\frac{G}{\rho}}$$ **Equation 2-2**

Where:

V_S = Shear wave velocity (m/s)

G = Small strain shear stiffness of the soil (Pa)

ρ = Density of the soil (kg/m^3).

Surface waves consist mainly of Love waves and Rayleigh waves. Both types of wave propagate only along the surface of the medium they travel through. Approximately two thirds of the available energy during an impact is dissipated through Rayleigh waves (Matthews et al, 1996).

Love waves, are transverse surface waves with a particle motion in a horizontal plane with no vertical component. The particle motion is perpendicular to the direction of wave motion (Milne and Lee, 1939).

Rayleigh waves have a semi elliptical particle motion in a vertical plane parallel to the direction of wave motion (Figure 2.3). The elliptical particle motion of Rayleigh waves is retrograde to the direction of wave motion (Figure 2.3). This means that the particles rotate backwards compared to the wave motion. A wheel for instance rotates forward compared to the direction of travel. Particles in a Rayleigh wave do the opposite (they rotate backwards compared to the direction of wave motion). This retrograde motion sometimes causes exploration geophysicists to refer to Rayleigh waves as ground roll (Matthews et

al, 1996). The width of the ellipse describing the particle motion is about two thirds of its height. Rayleigh waves are related to S-waves and as such their velocity is related to the velocity of S-waves. The velocity of Rayleigh waves can be related to that of S-waves by the formula:

$$V_R = C \times V_S \qquad \textbf{Equation 2-3}$$

With:

$$C^6 - 8C^4 + 8\left(3 - \frac{1-2\nu}{1-\nu}\right)C^2 - 16\left(1 - \frac{1-2\nu}{2(1-\nu)}\right) = 0 \qquad \textbf{Equation 2-4}$$

Where:

C = The constant relating the velocity of shear and Rayleigh waves

ν = Poisson's ratio.

The value of C varies between 0,911 and 0,955 for most values of Poisson's ratio found in soil. From the formula it is clear that Rayleigh waves have a slightly lower velocity than that of S-waves, and the relationship is not very sensitive to Poisson's ratio.

The strain levels associated with the particle motion of Rayleigh waves have not been measured directly but the strain is believed to be very small, less than 0,001 %, and the soil therefore behaves elastically (Matthews et al, 1996). Matthews et al (1996) also state that the shear strain associated with Rayleigh waves decreases with depth. Below the depth of one wavelength there is hardly any energy transfer due to Rayleigh waves.

Rayleigh waves are dispersive in nature. Dispersive waves have the property that their velocity depends on their frequency as well as the properties of the medium they travel through. Light waves for instance are not dispersive, because their velocity is independent of the wavelength and depends only on the properties of the medium they travel through under most circumstances.

2.2 SIGNAL ANALYSIS PRINCIPLES

The CSW and Spectral Analysis of Surface Waves (SASW) methods of seismic testing do not use time of arrival methods to calculate the Rayleigh wave velocity. This is an advantage since time of arrival can sometimes be difficult to determine. Instead, phase information is used. This has the advantage that the noise can be filtered out from the required signal and only the velocity of the correct input signal is calculated. Phase and frequency information is obtained by using the Fast Fourier Transform (FFT).

The FFT is a computer algorithm published by Cooley and Tukey (1965) and it is a shortened form of the discrete Fourier transform. The discrete Fourier transform is a discrete (or digital) form of the Fourier transform. The purpose of the discrete transform is to provide a means of performing a Fourier transform on a digitally sampled signal, instead of the analog signal received from geophones. The algorithm for the discrete Fourier transform is very laborious to calculate and hence the FFT was a big improvement in that the computer time needed was greatly reduced.

In order to perform a FFT on a signal, it must first be sampled, in this case using an analog to digital converter. In the case of the FFT the number of samples must be an integral power of 2 i.e. 2^1, 2^2,2^3 etc (Figure 2.4 has ten samples but only eight can be used in the FFT). If the sampled signal is plotted and all the dots connected (note, however, that the sampling frequency of two samples per wavelength is the minimum required but for practical purposes four to five samples per wavelength would be better as information about the purity of the required signal becomes available), a plot showing amplitude on the y-axis and time on the x-axis is obtained (Figure 2.5).

After the FFT has been performed on the sampled signal, the columns of data are obtained with the same number of rows, as there are sampled

points (Figure 2.4). The first column, marked "Time", records the exact time the particular data point is logged measured in seconds. The second column is a counter that starts with zero and ends with the number of rows minus one. The third column, marked "Frequency", is the frequency but must be calculated using the counter and time columns (this is done by dividing the counter number by the time in last row used for the FFT (0,8 seconds in this case). The third column consists of a set of imaginary numbers. These numbers are the actual result of the FFT. In order to make sense of the results two calculations have to be performed. First the absolute value (or modulus) of the imaginary numbers must calculated using the formula:

$$|I| = \sqrt{a^2 + b^2}$$ **Equation 2-5**

Where:

I = a+bi

Secondly, the argument (or amplitude) of the complex number must be calculated using the following formula:

$$\text{Argument} = \tan^{-1}\left(\frac{a}{b}\right)$$ **Equation 2-6**

From these results two graphs can be plotted (Figures 2.6 and 2.7). First, the absolute value is plotted against frequency (Figure 2.6). This graph shows the frequencies the sampled signal consists of. In the example in Figure 2.6 the sampled signal consists of only one frequency, 5 Hz. Secondly, the argument can be plotted against frequency (Figure 2.7). This shows the phase angle of each frequency, 3,14 radians for 5 Hz in the example continued in Figure 2.7. In the case of spectral analysis the phase angle is the phase angle of a harmonic at time equal to zero. This parameter is necessary since it is possible to compile an infinite number of signals from a fixed set of pure frequencies if the time position of each frequency is not specified. The phase angle is required for calculation of wave velocities for the SASW and CSW methods.

To calculate the wave velocity the phase angles for two or more geophones are plotted against distance from the geophones (see the phase test presented in the example in Appendix A and the reference plots in Appendices B and C). This plot should be a straight line with a negative slope. A best-fit straight line can be fitted through the points to minimize any distortion in the data. The Rayleigh wave velocity is calculated using the following formulas:

$$\lambda = 2\pi \frac{\delta d}{\delta \varphi}$$ **Equation 2-7**

Where:

λ = The wavelength of the Rayleigh wave

π = The ratio of the circumference of a circle to its diameter

$\delta d/\delta \varphi$ = The inverse of the slope of the phase-distance plot

and:

$$V_R = f\lambda$$ **Equation 2-8**

Where:

V_R = The velocity of a Rayleigh wave

f = The frequency of a Rayleigh wave.

2.3 STIFFNESS OF SOIL

In the previous sections the theory relating seismic principles with stiffness was explained. The following sections explain the various methods used to induce and measure seismic or dynamic stiffness. It is therefore prudent to include a section on the stiffness measured using seismic waves.

2.3.1 Stiffness measured using Rayleigh waves

It is believed that most soils behave elastically at strains of less than 0,001 % and exhibit constant stiffness (Matthews et al, 1997, Hooker, 1998 and others). Clayton and Heymann (2001) found this limit to be between 0,002 % and 0,003 % while comparing stiff and soft clays as well as chalk. Weak rocks have a more linear relationship between stiffness and strain and stiffness is largely unaffected by larger strains (Matthews et al, 1996). While still in the elastic zone the soil stiffness may be fully described using two parameters. They may be either Young's modulus of elasticity (E) and Poisson's ratio (ν), or the shear modulus of elasticity (G) and the bulk modulus of elasticity (κ). In a soil mass these parameters are related by the following equations:

$$\kappa = \frac{E}{3(1-2\nu)} \qquad \textbf{Equation 2-9}$$

and

$$G = \frac{E}{2(1+\nu)} \qquad \textbf{Equation 2-10}$$

Where:

G = The shear modulus of elasticity (Pa)

E = The Young's modulus of elasticity (Pa)

κ = The bulk modulus of elasticity (Pa)

ν = Poisson's ratio.

In practice, engineers often use the Young's modulus and Poisson's ratio stiffness parameters because they are better understood and their measurement is straightforward. It would be, however, more fundamental to use the shear modulus and bulk modulus of elasticity in terms of geotechnical engineering. This is because Young's modulus of elasticity includes the effects of volumetric change and shear distortion. Young's modulus therefore has different values for the drained and undrained

conditions (Matthews et al, 1997). The advantage of using the latter in geotechnical engineering is that the shear modulus and bulk modulus of elasticity divide the problem in two parts. The first is a shear distortion parameter only and the second is a volumetric parameter only (Matthews et al, 1997). When measuring stiffness in rock, P-waves may be used since the stiffness of rock far exceeds that of water. This implies that the stiffness measured is that of the rock. The opposite is true in soils where the stiffness of water exceeds that of the soil skeleton. In this case P-waves would measure the stiffness of water if the soil were saturated. To avoid the problem, shear waves should be used in soil since water has no shear stiffness. Therefore only the stiffness of the soil skeleton would be measured (Matthews et al, 1997).

During seismic testing such as the CSW method, the strains are less than the elastic limit, of the order of 10^{-6} to 10^{-4} % (Clayton and Heymann, 2001). This implies that the stiffness measured using the CSW method is the small strain shear stiffness or G_{max}. Figure 2.8 shows a graph relating shear stiffness and shear strain. The maximum value for stiffness at the left is the small strain shear stiffness. As the strain level increases, the shear stiffness decreases. Figure 2.8 also relates the strains generally associated with common geotechnical structures as well as the types of test needed to measure the relevant stiffness. Figure 2.8 shows that the strains related to most structures are more than 0,01 %. The remarkable attribute of this graph is that it shows the strain levels around structures in soil are much smaller than was previously thought.

Figure 2.8 would suggest that the stiffness obtained from a Rayleigh wave analysis could be used directly in design of geotechnical structures once some adjustment has been made. For instance, Matthews et al (1997) quotes various authors who published empirical relationships between shear stiffness at working strains (0,01 %) for clays. Generally the value of the ratio $G_{0,01\%}/G_{max}$ varies between 0,5 and 0,8 for clays (Menzies and Matthews, 1996). In practice it would be more accurate to calibrate the

relationship for site specific conditions. In sands and weak rocks the ratio between stiffness at working strains (0,01 %) and very small strain seems to approach unity (Matthews et al, 1997, Menzies and Matthews, 1996). Matthews et al (1997) showed the predicted settlement of foundations on chalk using various methods compared to the actual settlement. Figure 2.8 shows clearly that Rayleigh wave measurements give a very good relation to actual settlement in soft rock and could be a valuable tool in the evaluation of settlement in the design stage. When using surface wave geophysics in soils the predicted stiffness should be adapted to working strain stiffness by adapting one of the available strain softening functions.

2.4 SEISMIC METHODS OF PROFILING

The previous sections described the nature of seismic waves and also some of the data analysis techniques used to analyse seismic waves. This section describes the various seismic methods that can be used to profile soil. The advantages and limitations are also compared.

2.4.1 Up-hole

The up-hole method of seismic profiling involves drilling a hole using a suitable piece of drilling equipment. Geophones are then placed on the surface and connected to the logging apparatus (Figure 2.9). A small seismic event is then triggered in the bottom of the hole by dropping a weight into the hole or by exploding a small charge in the bottom of the hole, or using a shear wave hammer.

The seismic event time and arrival times of P- and S-waves at the surface are measured and some assumption about the travel path is made, taking into account ray path curvature if required. Since the travel path length is

known and the time of travel can be measured, the velocity of the P- and S-waves can be calculated. Having the velocity of the seismic waves and either estimating or measuring the density of the soil, the elastic properties of the soil can be calculated.

The disadvantages of this method are:

- A hole must be excavated to the required depth or depths;
- In order to obtain a profile of stiffness at depth the test must be repeated with various hole depths;
- Timing of the seismic event in the bottom of the hole may be difficult to perfect;
- Since some marker in the arriving waves must be sought to establish a time of arrival, the travel time may not be consistent; and
- Very often it is necessary to case the hole in order to keep it from collapsing (Matthews et al, 1997).

The advantages of using this method are:

- The in situ small strain shear stiffness of the soil can be measured;
- The equipment used is relatively simple;
- Only one hammer is sufficient since a frequency spectrum is not required;
- Only a single borehole is required;
- Tests can be carried out on all soil and rock types (Matthews et al, 1997); and
- The average velocity is measured in layered materials (Matthews et al, 1997).

2.4.2 Down-hole

The down-hole method requires drilling a hole and mounting the geophones in the bottom of the hole. The seismic wave source is installed on the surface (Figure 2.9). This is usually a hammer or an explosive charge.

The time it takes for the S- and P-waves to reach the geophones from the surface is measured. Having the time and making some assumption about the path travelled, the velocity of the S- and P-waves can be calculated. The down-hole method is essentially the reverse of the up-hole method.

The disadvantages of the method are:

- A hole needs to be excavated just as in the up-hole method;
- It is difficult to properly mount the geophones on the side wall in the bottom of the hole;
- Just as with the up-hole method the timing of the arrival and the seismic event can be inaccurate;
- The assumption made for the travel path may not be accurate; and
- The hole may have to be cased to prevent it from collapsing (Matthews et al, 1997).

The advantages of the method are:

- It is easier to set up a seismic source than with the up-hole method;
- Stiffness at various depths can be calculated by moving the geophones in the hole or by simply using more than one geophone at various depths in the hole;
- The velocity of P- and S-waves can be calculated;
- Only one borehole is required (Matthews et al, 1997);
- Tests can be carried out on all soil and rock types (Matthews et al, 1997);

- The average velocity for layered materials is measured (Matthews et al, 1997); and
- Higher energy sources like explosives can be used without damaging the borehole (Matthews et al, 1997).

2.4.3 The cross-hole method

The cross-hole method is performed by excavating two holes. Geophones are installed in one hole as receivers and the source in the other hole (Figure 2.9). The source generates S- and P-waves and the wave velocities are calculated between the two holes. The velocities are calculated using time of arrival techniques. This is possible since the travel paths of the waves are known and the time of arrival can be measured.

By varying the relative depths of the source and receiver in the two holes a two dimensional picture of the soil between the two holes can be obtained. This method is called cross-hole tomography.

The disadvantages of this method are:

- Two holes must be excavated;
- Mounting the geophones and the source in the holes may be difficult;
- The measurement of travel times of the seismic waves may be inaccurate;
- The travel paths may not be straight;
- Quality of data diminishes at shallow depth (Matthews et al, 1997); and
- The maximum velocity is emphasized in thin layers due to head waves (Matthews et al, 1997).

The advantages of this method are:

- A complete two dimensional picture of the soil between the geophones are obtained;
- P- and S-wave velocities are measured directly;
- The method can detect low velocity layers provided they are thick compared to borehole spacing (Matthews et al, 1997); and
- The test can be carried out in all types of soil and rock (Matthews et al, 1997).

2.4.4 Seismic refraction

Seismic refraction testing is performed by inducing P- and S-waves into the soil as a pulse and recording at various distances from the source the arrival of the refracted waves (ASTM D 5777-95). Both the source and the receivers or geophones are on the surface (Figure 2.10). This method relies on the refractory properties of seismic waves in soil. Because the soil stiffness generally increases with depth, the seismic waves are bent or refracted in the same way as light waves are bent in a lens.

The seismic refraction method of testing uses the time of arrival method to calculate the wave velocities. The time the waves take to travel from the source to the geophones can be measured and a curve can be assumed as the travel path of the waves. From this the velocity can be calculated. By placing the geophones further away from the source the stiffness at deeper levels can be measured.

The disadvantages of this method are:

- The assumptions regarding the wave travel path may be inaccurate. This can cause faulty stiffness measurements and a wrong allocation of depth to the stiffness;

- The stiffness measured is for the entire travel path and since the exact travel path is uncertain, the location of the measured stiffness is unsure;
- The analysis of travel time may not be consistent;
- The method assumes uniform and isotropic conditions when testing a layered soil. If the soil is layered or the layers deviate from the horizontal an error is introduced (ASTM D 5777-95);
- In order for a soil layer to behave as a refractor, it must have a distinguishable contrast in stiffness with depth to refract seismic waves. If this is not the case the test cannot be concluded (ASTM D 5777-95);
- The method cannot detect thin layers (ASTM D 5777-95); and
- The method can only be used when the soil layers increase in stiffness with depth. If a lower stiffness layer is encountered, the depth of the layers below it will be overestimated (ASTM D 5777-95).

The advantages of this method are:

- No excavation is required; and
- A stiffness at depth profile is obtained.

2.4.5 Seismic reflection

Seismic reflection testing is done by inducing seismic waves into the soil as a pulse and then logging the waves that are reflected by a high stiffness layer at depth (Figure 2.10) as discussed by Matthews et al (1997). The source is usually a hammer and the waves are induced on the surface. The receivers or geophones are also placed on the surface some distance away from the source. The P- and S-waves are assumed to travel straight down to the reflection surface and bounce upwards at the same angle. These waves are then logged.

The travel time for the waves can be measured and an assumption can be made about the travel path. The velocity can then be calculated.

The disadvantages of this method are:

- A high stiffness layer is required as a reflection layer;
- The different wave types can easily be confused;
- The stiffness measured is very general; and
- The analysis procedure can be very subjective.

The advantages of this method are:

- No excavation is required (Matthews et al, 1997).

2.4.6 Seismic cone

The seismic cone is a further development of the up-hole and down-hole methods of seismic testing (Jacobs and Butcher, 1996). Two geophones are permanently fixed in the tip of a cone penetrometer (CPT) (Figure 2.11). At every penetration interval where the cone is stationary between jacks, shear waves are induced into the soil at the surface by the drop of a hammer. The shear wave signal is then logged by the geophones in the CPT. Since the distance between geophones is fixed and known and the time taken for the shear waves to pass both geophones, the velocity can be calculated.

By repeating this test at every half metre or metre a proper profile of stiffness at depth can be obtained.

The disadvantages of this method are:

- The soil to be tested must be soft enough to allow penetration by the CPT;

- Depending on the application the disturbance of the soil by the CPT may be excessive; and
- The test requires that a cone be pushed into the ground, therefore the test cannot be conducted in rock (Matthews et al, 1997).

The advantages are:

- The stiffness tested at depth is the actual stiffness at that depth;
- The analysis is simple to perform;
- The test provides other geotechnical parameters in addition to stiffness (Matthews et al, 1997); and
- The averaged velocity can be measured in layered materials (Matthews et al, 1997).

2.4.7 Spectral analysis of surface waves

The spectral analysis of surface waves (SASW) involves placing geophones on the surface in a line and inducing Rayleigh waves into the soil at a point in line with the geophones (Figure 2.11). The source in this method is usually a falling hammer. By spectral analysis of the waveforms as they pass the geophones, the phase at each geophone can be determined for each frequency and consequently the velocity of each frequency. Since Rayleigh waves are dispersive, each frequency has a different velocity. This is caused by the fact that lower frequencies have longer wavelengths and as a result soil particle motion is induced deeper into the soil.

Every hammer blow will result in a range of frequencies and thus a range of wave depths. Since the wave velocity depends on the stiffness properties of the soil it travels through, it follows that lower frequencies with longer wavelengths measure stiffness at deeper depths than higher frequencies with shorter wavelengths. As a result a profile of stiffness vs.

depth can be obtained with one stiffness measurement corresponding to every frequency induced into the soil.

The depth of every stiffness (corresponding to a frequency) can be taken as one third of the wavelength corresponding to that frequency (Hooker, 1998).

The disadvantages of this method are:

- A range of falling hammers are required to fill the required spectrum to obtain a smooth profile of stiffness vs. depth with no gaps;
- The test relies on the frequencies obtained by using falling hammers. This leads to the occurrence of gaps in the tested profile (Matthews et al, 1997); and
- Because Rayleigh waves travel from surface to a depth of about one wavelength the stiffness measured in this way is the average stiffness up to that depth and not the stiffness of a particular layer. This can be an advantage at times.

The advantages of this method are:

- A stiffness vs. depth relationship can be obtained;
- The test is easy to set up and fast to perform; and
- No drilling or penetration of the soil is required.

2.4.8 The continuous surface wave method

The continuous surface wave method or CSW method is similar to the SASW method. The testing is performed by placing a series of geophones (usually 5 or 6 geophones since linear regression is performed later in the computation process) in a line on the surface of the soil to be tested (Figure 2.11). The geophone spacing depends on the wavelength to be

tested. Some empirical rules have been summarized by Matthews et al. (1996) but the essence of all those is to ensure a sufficient number of geophones are available on a single wave to properly define it through the logging process. The source is then placed on the surface in line with the geophones. Unlike the SASW method the source in this case is not a hammer but a vibrator. The vibrator can be either electromagnetic or mechanical, as long as it applies a continuous sinusoidal force consisting of only one frequency into the soil.

As discussed in the previous section, the depth at which stiffness is tested depends on the wavelength of the Rayleigh wave. High frequencies induce short wavelengths and low frequencies induce long wavelengths. By using a vibrator with a variable frequency a complete range of frequencies can be guaranteed. This ensures an uninterrupted stiffness vs. depth relationship. The second major advantage of using a shaker is that the waves are continuous, and not pulses as is the case with a hammer. The analysis is much more reliable if a continuous wave is analysed than if only a pulse is analysed. This also makes it possible to do a double check on the frequency data obtained from the spectrum analysis by directly comparing it to the frequency applied by the shaker.

The process of converting the wavelength vs. shear stiffness graph to shear stiffness vs. depth is called inversion. According to Matthews et al. (1996) there are three principle inversion methods:

- The wavelength to depth method. This method was used for the purposes of this dissertation by dividing the wavelength associated to a stiffness by three and assigning it as a depth to that particular stiffness as recommended by Hooker (1998) and Hooker (2002). Menzies and Matthews (1996) recommends dividing the wavelength by a number between two and four but states that three is a reasonable compromise. Although this method is not the most accurate of the three it is simple to perform and gives reasonable results;

- Haskell-Thomson matrix techniques (Thompson, 1950 and Haskell, 1953); and
- Finite element approaches. Menzies and Matthews (1996) gives a short description of the method.

Both of the last two methods were beyond the scope of this study and no further details are included.

The disadvantages of the CSW method are:

- The stiffness measured is the average stiffness with depth as with the SASW method;
- The required equipment is more extensive than with the SASW method;
- The depth of testing is limited to about 10 metres unless vehicle mounted vibrators are used (Matthews et al, 1997); and
- The resolution of testing diminishes with depth (ASTM D 5777-95). Technically, this is the case with all geophysical methods.

The advantages of the CSW method are:

- No excavation is required;
- The stiffness measurements obtained using this method are not affected by sampling disturbance, insertion effects or representative sampling problems (Matthews et al, 1997);
- The stiffness is measured in situ and is therefore unaffected by sample disturbance. It also takes into account the effect of fissures and fractures on mass compressibility (Matthews et al, 1996);
- The test takes relatively little time to complete; and
- It is a fast method that gives good quality results on a wide range of materials including soft rock.

2.5 APPLICATIONS OF CSW

Section 2.4 of this dissertation described the various methods that can be used to perform seismic profiling. This section focuses on the continuous surface wave method. The various applications of the CSW method are presented and discussed. The relevant technical issues associated with the applications are also discussed.

2.5.1 Measuring shear stiffness using the CSW method

The CSW method of seismic testing can be used to measure shear stiffness in situ. It is an indirect method of shear stiffness measurement since the Rayleigh wave velocity is measured and converted to shear wave velocity, which is converted to stiffness.

The stiffness measured using seismic waves is the dynamic small strain stiffness because the load supplied by passing seismic waves is dynamic and the strains associated with seismic waves of this magnitude are very small. These strains are usually less than 0.001 % and falls within the elastic zone for soils (Figure 2.8).

Figure 2.8 shows a graph plotting strain on the x-axis and shear stiffness on the y-axis. It shows that stiffness is related to strain levels and that the stiffness measured during seismic testing is measured at very small strain levels. This is sometimes referred to as G_{max} because it is the maximum stiffness in soil.

Figure 2.8 also shows the strain levels generally found around geotechnical structures.

2.5.2 Stratigraphy

The CSW method can also be used to measure stratigraphy i.e. locate layers of varying stiffness like bedrock (for example see Menzies and Matthews, 1996). Since the CSW method reliably provides a profile of stiffness at depth it follows that high stiffness layers can easily be detected.

It must be concluded that although the above mentioned authors state that the CSW method can be used to determine depth of bedrock, the only similar application found was that by Butcher and Tam (1997) to determine the depth of landfill.

They calibrated their stiffness measurements against excavated profiles and used the CSW method with success to characterize the landfill between boreholes and other exposures.

2.5.3 Measuring ground improvement

Kim and Park (1999) described a method to evaluate the density of soil before and after ground densification by using the Spectral analysis of surface waves (SASW) method. It involves normalizing the shear stiffness with respect to the normal effective stress and then finding the relationship between density and shear stiffness through bender element tests in the laboratory. This allows the density of the soil to be measured using the SASW technique. It is included in this section since the SASW technique is similar to the CSW technique and the method described above can also be applied using the CSW method.

Moxhay et al (2000) successfully measured ground improvement on three occasions using the CSW method. These tests were conducted on various combinations of silt, clay and sand with some organic material.

Andrus et al (1988) used the SASW method to successfully quantify ground improvement in granular soils.

Haegeman and Van Impe (1998) used the SASW method to quantify the level of consolidation during a vacuum consolidation of disposed sludge. The SASW method was used directly on the sludge for two tests and was performed on an HDPE (geomembrane) cover for a further seven tests. The results were compared and they found that the HDPE cover did not affect the results significantly. By comparing the stiffness with that of the expected stiffness after consolidation and other field and laboratory measurements, they were able to conclude that the material was still consolidating and that construction over the fill was not recommended at that stage.

Quantifying ground improvement is an application where the CSW method has been used successfully as it allowed the level of improvement to be measured even at some depth without being destructive.

2.5.4 Prediction of ground deformation

Ground deformation can be predicted using elasticity theory and the stiffness parameters measured using the CSW method. The CSW measured stiffness has to be adjusted using the appropriate softening function. Menzies and Matthews (1996) have found that the in situ stiffness is generally between 0,4 and 0,8 times the seismic stiffness for clays. In practice it would be more accurate to calibrate the relationship for site-specific conditions. In sands and weak rocks this number may approach unity.

As described in Matthews et al. (1997) and the section on shear stiffness earlier in this chapter, the CSW method can be used to predict ground

deformation as long as an appropriate softening function is applied and since it is non-invasive is the ideal tool for the job.

2.5.5 Rock mass assessment

Cuéllar (1997) used the SASW method to determine the level of rock deterioration behind a tunnel lining. The tests were performed on the inside of the lining on the tunnel roof and sides. Although all the mechanisms are not fully understood when using this method in tunnels, it provided usable results.

2.5.6 Monitoring a landfill

Butcher and Tam (1997) performed CSW testing with the purpose of determining the depth of an existing landfill. Since the stiffness of the waste would differ from that of the soil beneath, the boundary between soil and waste was detected by obtaining a profile of stiffness vs. depth. The CSW data was calibrated against borehole data to obtain the relative stiffness for waste and soil and afterwards evaluated against the side of the excavation. The CSW method performed well since in only 10 % of the cases the depth of landfill was underestimated.

Cuéllar (1997) used the SASW method to monitor the changes in waste properties with time. This allowed "soft" zones resulting from poor compaction or biological degradation to be identified for treatment since these zones would have lower stiffness values than the better compacted or less degraded waste.

2.5.7 Liquefaction potential

Andrus et al (1998) describes a method to predict liquefaction potential where the shear wave velocity is correlated to the cyclic stress ratio (CSR). The CSR is a measure of the shear stress required during a seismic event to induce liquefaction in soil. The advantages of quantifying liquefaction potential using the SASW (or CSW) method is that soils can be evaluated for liquefaction potential before and after improvement, enabling remedial measures to be applied effectively. Andrus et al (1988) concluded that:

"This study further supports the usefulness of in situ V_s for predicting liquefaction potential and demonstrates the potential of the SASW test for rapid delineation of weak layers."

Cuéllar (1997) also used the SASW method with success to determine low stiffness zones liable to liquefaction.

2.5.8 Quantification of sample disturbance

The CSW method has been used successfully to quantify sample disturbance by comparing field measurements of $G_{0,01}$ with laboratory measurements using bender elements as discussed by Santagata and Germaine (2002) and Lohani et al (1999).

2.6 STIFFNESS MEASUREMENT FROM THE DCP

A Dynamic Cone Penetrometer (DCP) was used as part of this study. This apparatus as well as the testing method followed are described in Chapter 3. For this study the DCP was not used to measure soil stiffness,

but only to detect changes in soil stiffness. These changes were compared to the changes in stiffness as measured using the CSW. The purpose of this section is to present the necessary theoretical background and to show that the DCP can be used to detect changes in soil stiffness with reliability.

Harison (1987) and Kleyn et al (1982) showed that a good correlation exists between the California bearing ratio (a strength parameter) and the DCP penetration resistance of soil. Harison also found that moisture content and saturation had an insignificant effect on the correlation found between the California bearing ratio and the DCP resistance.

Bergdahl and Ottoson (1988) compared results for the CPT (cone penetrometer test), the WST (weight sounding test), DP HfA (dynamic probing according to the Swedish geotechnical standard) and the SPT (Standard Penetration Test) with each other and various geotechnical parameters. They found that a good correlation exists between any of these penetration testing methods and deformation modulus for the soil.

Chua (1998) reported that various authors found some correlation between CBR and DCP penetration resistance. These correlations in general were applicable to specific soil types only. The unifying factor was that an increase in CBR (or strength) implies an increase in stiffness. It was only the exact relationship that varied. Chua (1998) also showed that the DCP testing method can be used successfully to measure soil stiffness and he presented an empirical chart that can be used to convert cone penetration index to elastic modulus.

Clayton et al. (1988) found that both vertical and horizontal effective stress have an influence on the penetration resistance of DCP testing, using a penetrometer slightly larger than the one used in this study, but the effect of vertical effective stress is much smaller than that of horizontal effective stress. They also found that the DCP penetration number can be correlated well with mean effective stress for specific materials. They further stated

based on their experience, that the DCP number is almost unaffected by stress history.

De Beer (1991) developed a method to aid in the design of road structures using the DCP. He developed an algorithm to calculate effective stiffness for road materials based on the DCP penetration number. He also calculated an R^2 of 0,76 for his algorithm based on the data he collected. The R^2 number is a measure of how well one dataset is correlated to another. An R^2 of 1 indicates a perfect fit while 0 indicates no fit at al. Although not perfect, this number indicates that a relationship exists between the DCP penetration resistance and the stiffness of sandy soil.

Kleyn and van Zyl (1988) described a method of pavement design using the DCP. The underlying assumption was that a correlation exists between the DCP penetration number and the California bearing ratio. A correlation was also published.

Based on the above literature it is concluded that the DCP can be used to detect changes in soil stiffness and that it is suitable as a control to test the suitability of the CSW method to detect changes in soil stiffness.

2.7 CONCLUDING REMARKS

The CSW method of stiffness measurement is a non-invasive method of measuring shear stiffness in soils and rocks using geophysics. It is based on artificially applied vibrations to the soil through an electromagnetic or mechanical shaker. These vibrations are logged using geophones and analysed using available computer technology.

The Rayleigh wave velocity is calculated using information obtained from the geophones and applying the Fast Fourier Transform. The shear wave

velocity and shear stiffness is calculated using established elastic relationships.

Gordon et al (1996) states that: "Seismic techniques are based on sound, well established elastic theory and moduli are determined at known, although very small strains".

Based on the literature the CSW method can be used to measure stiffness of soil and rock in the field. The stiffness that is measured can be used for a variety of applications.

From the literature study it can also be concluded that the DCP test is well established and widely used in Southern Africa. The DCP (and other penetration tests) has been studied by numerous authors internationally and they have demonstrated that the DCP can be used to measure stiffness or modulus of deformation in situ.

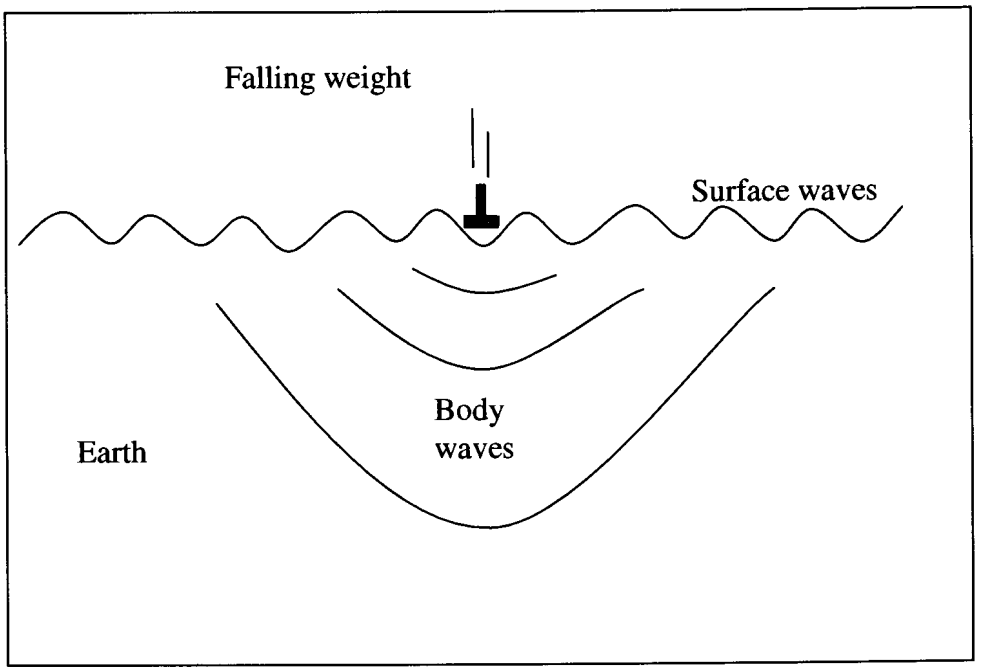

Figure 2.1 Seismic waves

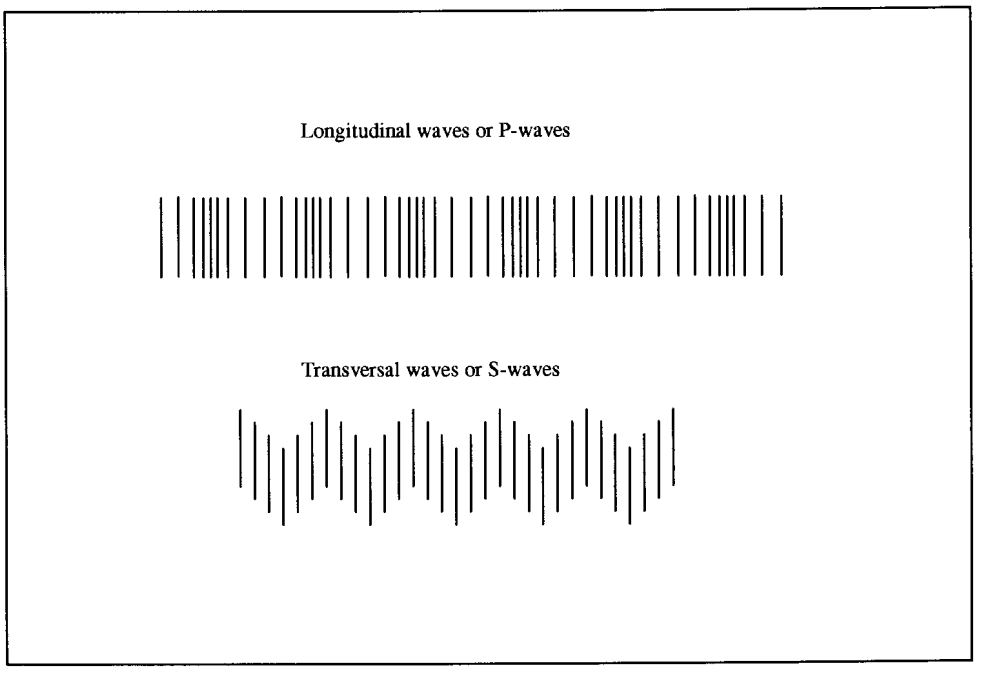

Figure 2.2 Schematic of body wave motion

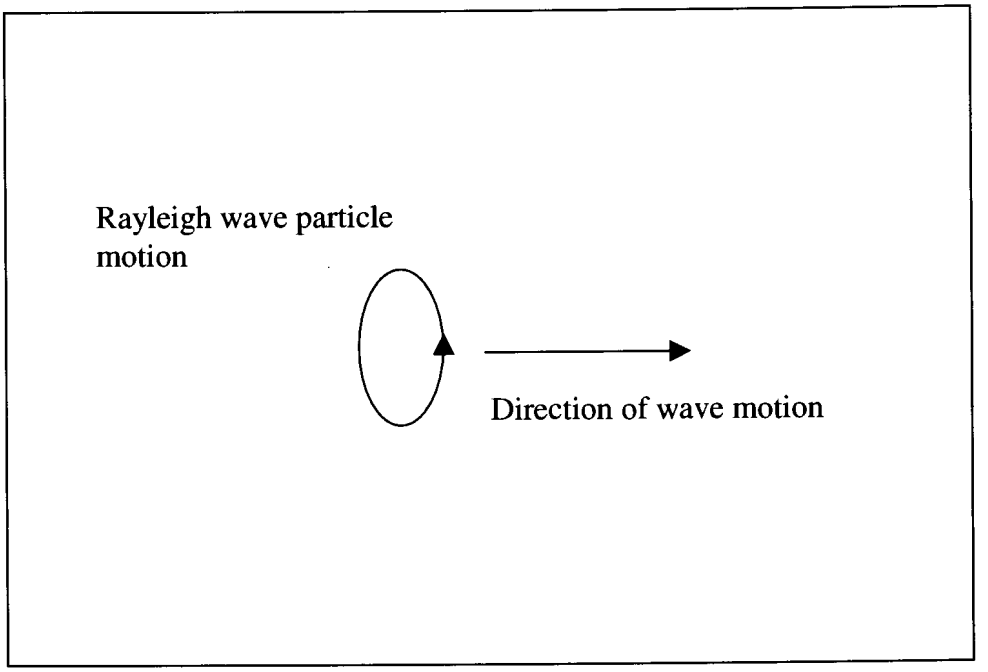

Figure 2.3 Rayleigh wave particle motion

Time (s)	Counter	Frequency (Hz)	Logged Signal	FFT	Absolute value	Argument
0.1	0	0	-0.82569	1.73210105631729	1.73210106	0
0.2	1	1.25	1.120259	6.94667478512687E-002+0.197231322317864i	0.20910721	1.23215448
0.3	2	2.5	-0.64929	-0.293552874701385+4.05414222157767E-002i	0.29633916	3.00435475
0.4	3	3.75	1.053207	-0.177520526491943+0.207692479965455i	0.27322098	2.2780287
0.5	4	5	-0.77166	-7.5344118409159	7.53441184	3.14159265
0.6	5	6.25	1.176098	-0.177520526491943-0.207692479965454i	0.27322098	-2.2780287
0.7	6	7.5	-0.65452	-0.293552874701385-4.05414222157767E-002i	0.29633916	-3.00435475
0.8	7	8.75	1.283692	6.94667478512682E-002-0.197231322317864i	0.20910721	-1.23215448
0.9			-0.77483			
1			1.278555			

Figure 2.4 Example of Fast Fourier worksheet

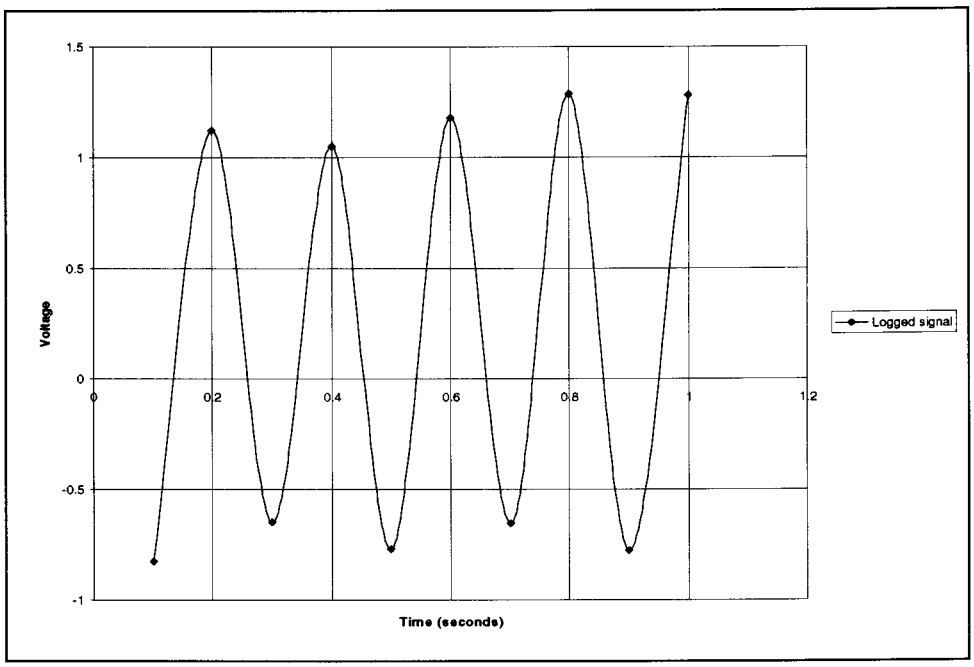

Figure 2.5 Signal obtained from sampling in Figure 2.4

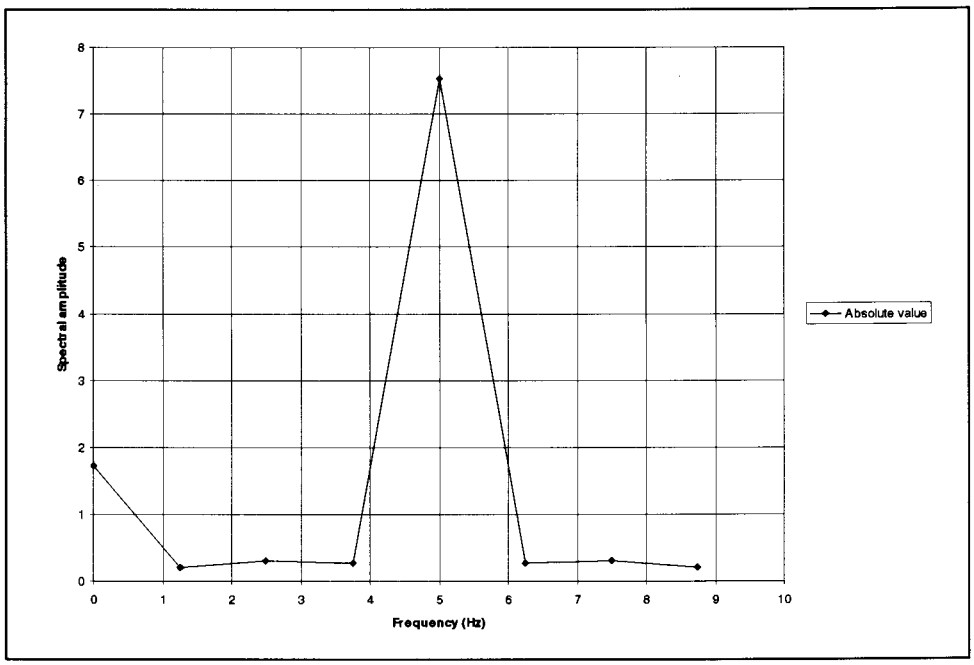

Figure 2.6 FFT as calculated in Figure 2.4

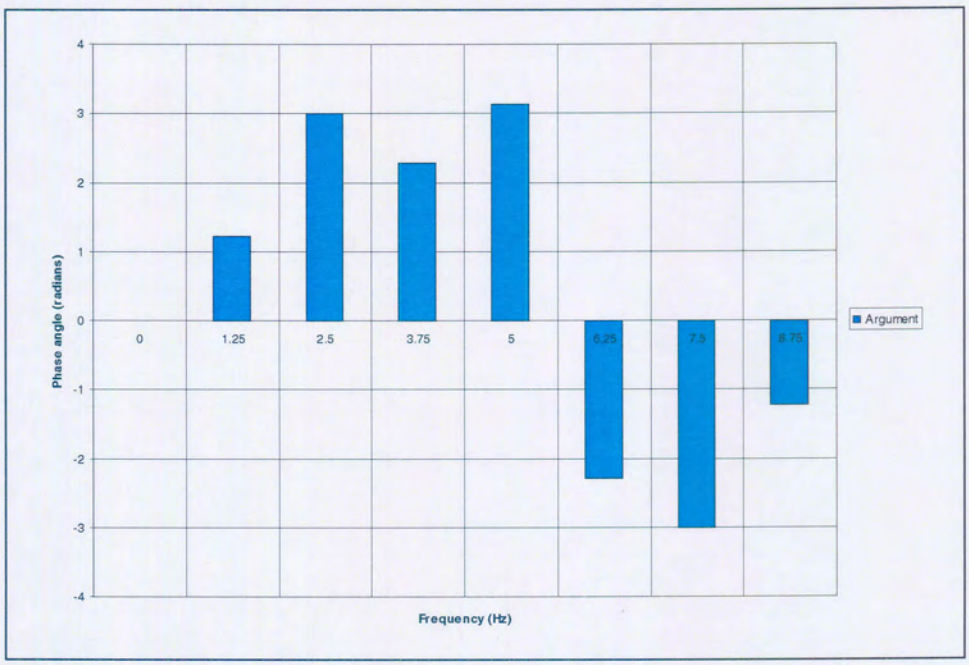

Figure 2.7 Phase angle as calculated in Figure 2.4

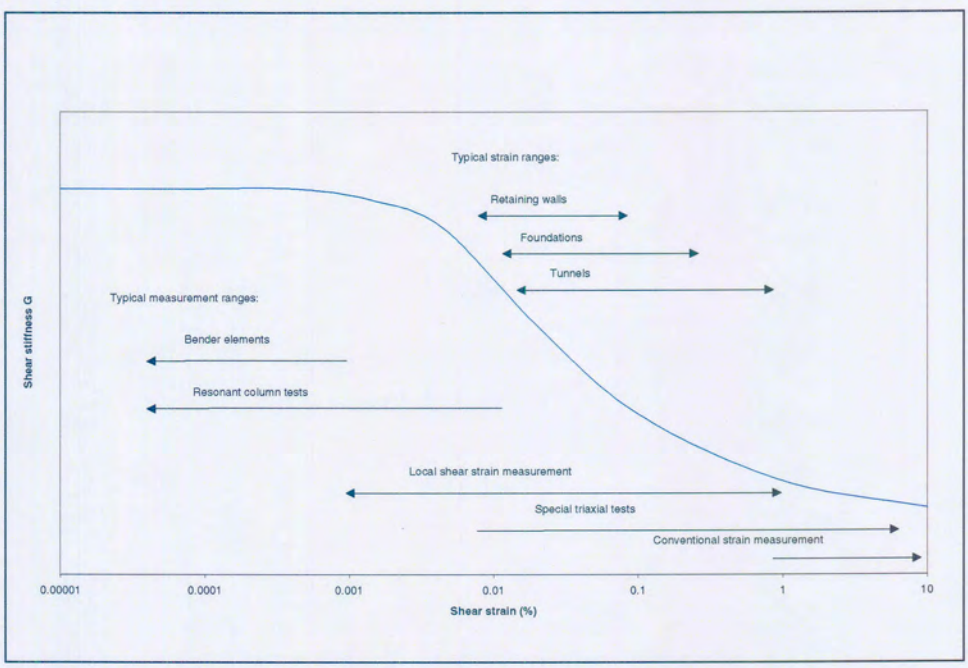

Figure 2.8 Generalized shear stiffness - shear strain graph after Hooker (1998)

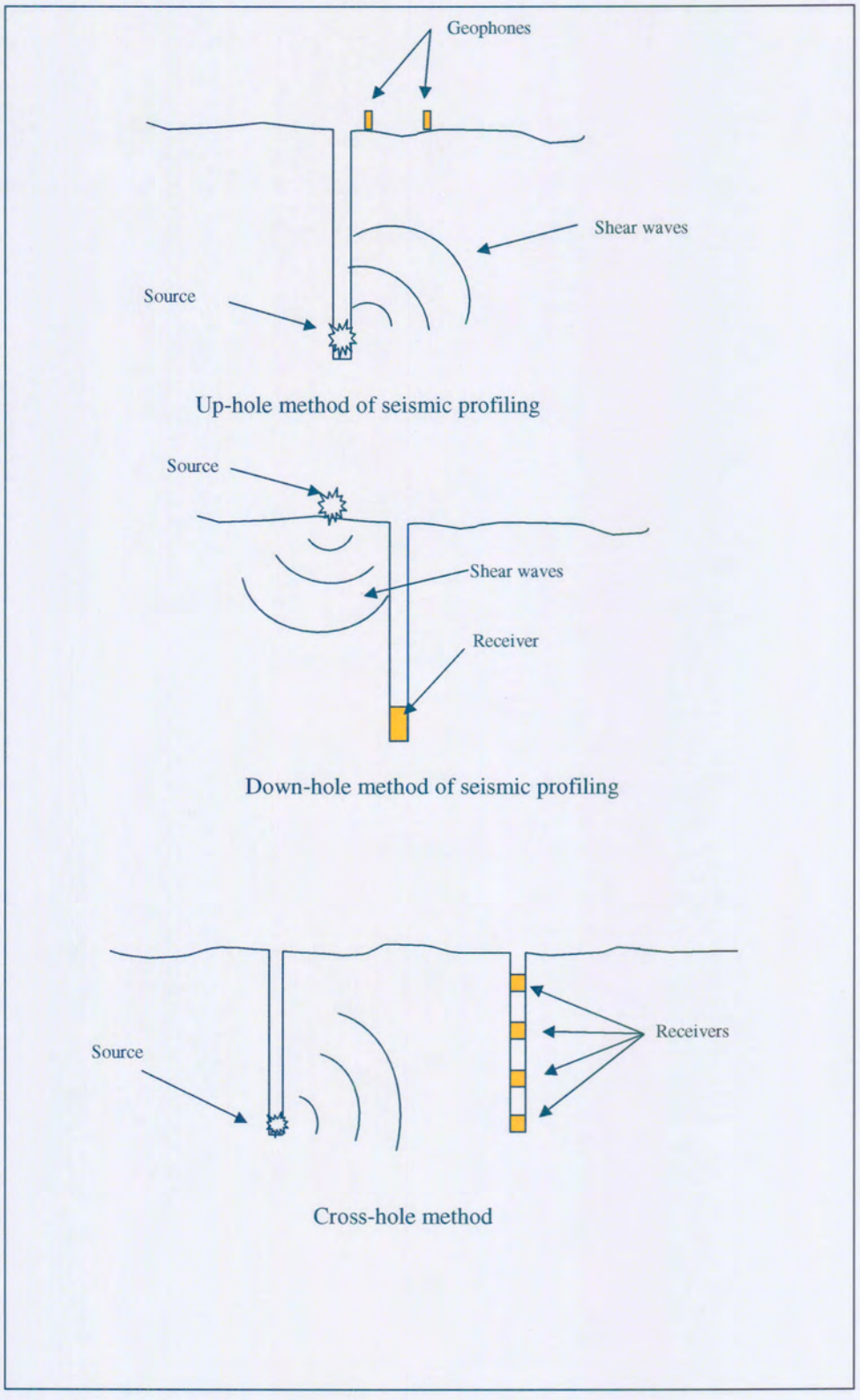

Figure 2.9 Seismic methods requiring boreholes

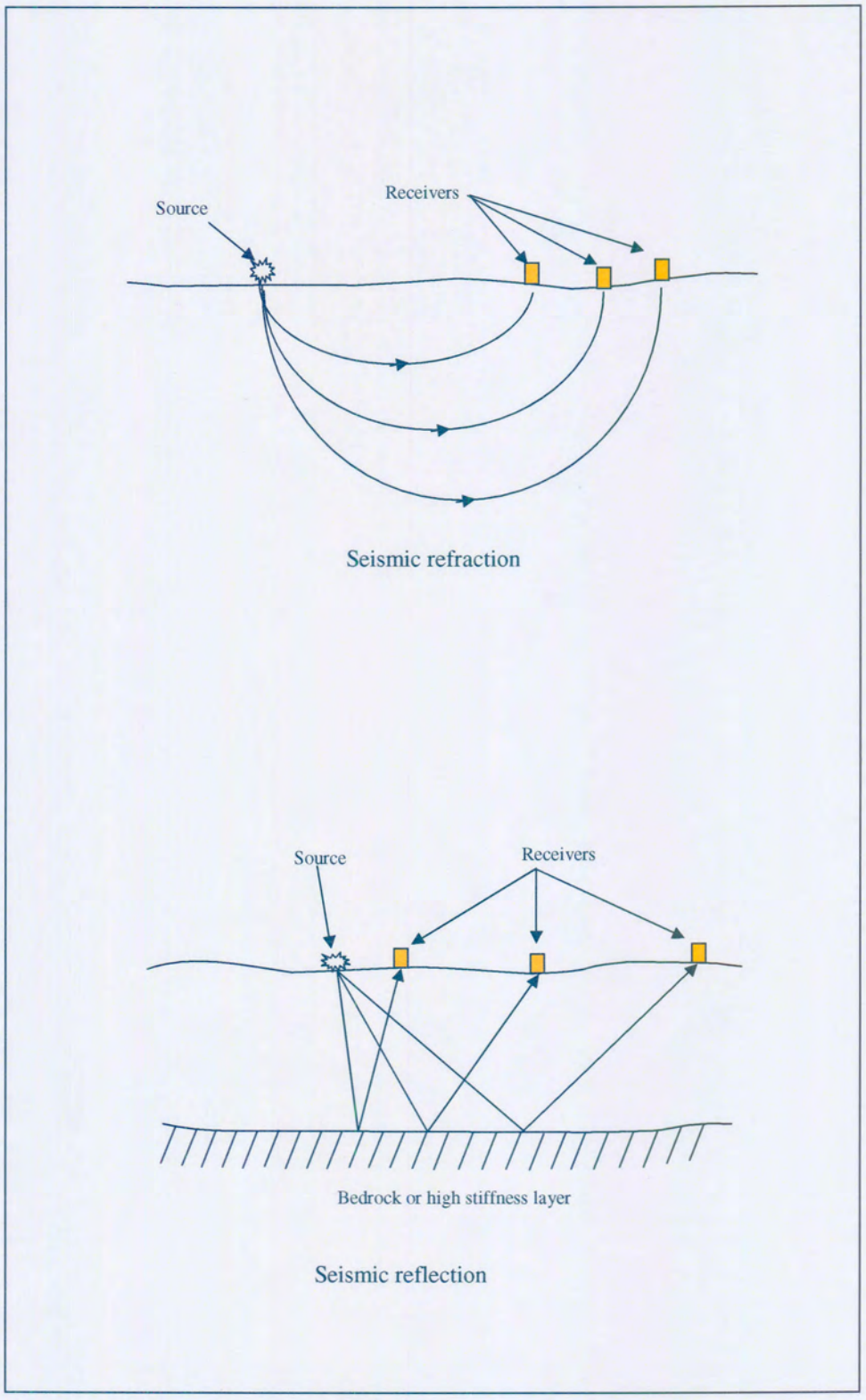

Figure 2.10 Seismic refraction and reflection

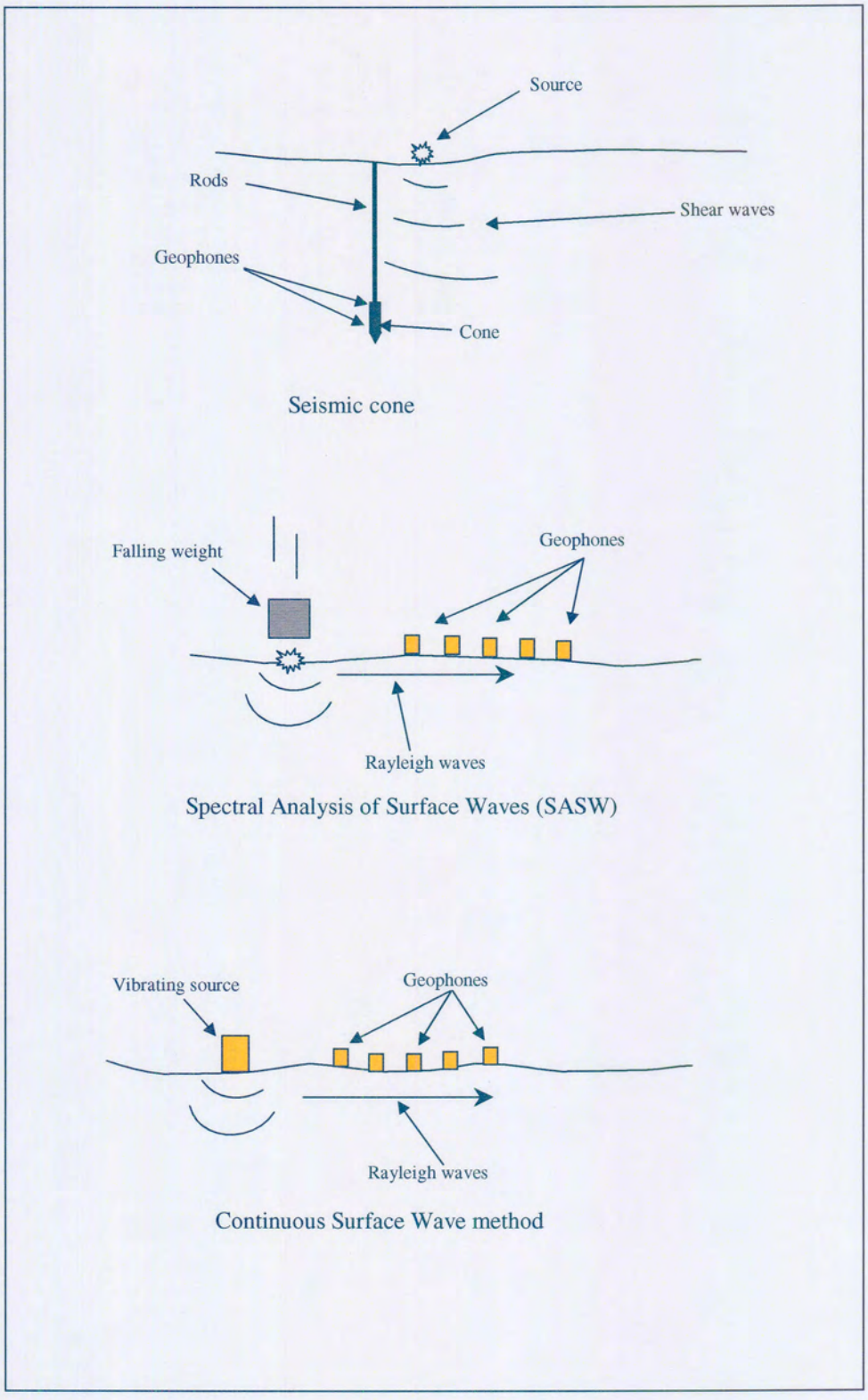

Figure 2.11 Seismic cone and surface wave methods

3 EXPERIMENTAL PROGRAMME

Chapter 2 dealt with the current state-of-the-art-knowledge of seismic testing of soils. It was explained that the CSW method of seismic testing can be used to measure small strain shear stiffness of soils without the need to excavate, and that the result of the testing is a profile of shear stiffness plotted against depth.

The aim of this chapter is to explain the equipment and the methods used to test whether the hypothesis is correct, that is whether the CSW method of seismic testing can be used to detect changes in soil stiffness. The experiment design is discussed first. Next, the test location followed by the seismic testing procedure are described together with the DCP and density testing. Results of the testing are discussed in the next chapter.

3.1 SITE DESCRIPTION

The test site is situated on a farm about 35 km North of Pretoria, South Africa. The test site comprised of a sandy soil extending down to several metres. Figures 3.17 and 3.13 show an example of the soil profile during excavation. Sieve analyses were performed on both the top and bottom layers of soil and are presented in Figure 3.16.

The site met with all requirements in that it contained uniformly graded sand and the position of the water table was deep enough as to not affect the test area even after a rainstorm in the unlikely event of it happening.

3.2 TEST PROCEDURE

A site was chosen containing a sandy soil with low cohesive properties and a reasonably uniform profile. This was done to make the effect of compaction on density easy to quantify. Furthermore, the position of the water table had to be well below the natural ground level and the probability of rain low in order to minimize the chance that water would fill the pit and soften the compacted material. The results of the seismic testing may also be influenced if the moisture content of the soil changed significantly while the testing was in progress. Therefore, it was decided to conduct the tests during the winter when the probability of rainfall was lowest.

Since the purpose of the testing was to determine whether the CSW technique could detect changes in the stiffness of soil, two tests were performed. The first test was performed on a structured in situ soil with a low density. The second test was performed on the same material after it was excavated and re-compacted, thus rendering it without structure and a higher density.

A soil exhibiting an internal structure was selected for the first sample. For the purposes of in situ testing an area 5 m wide by 10 m long was selected. The shear stiffness of the soil in the centre of the demarcated area was measured using the CSW technique of seismic testing (Figure 3.1). The penetration resistance of the in situ material was measured using a DCP (Dynamic Cone Penetrometer) and the density was measured using a Campbell nuclear density tester.

The second test site was prepared by excavating the in situ material to a depth of 1,3 m using a mechanical excavator (Figures 3.2 and 3.3), and re-compacting it in four layers (using a BOMAG 650 compactor (Figures 3.4 and 3.5)). The BOMAG compactor has a drum width of 650 mm and a total weight of 650 kg. A rolling drum type compactor was chosen instead

of a compactor with an impact or vibrating mechanism. Because of the sandy nature of the soil used in the test, this type of compactor was expected to compact the soil more consistently than compactors with dynamic mechanisms. The BOMAG was chosen because it was light enough to be transported easily and could be managed with little training. The bottom of the excavation was smoothed using spades and re-compacted. The soil was compacted using three passes of the compactor. The CSW, DCP and nuclear density tests were performed in the bottom of the excavation after the surface was smoothed and lightly compacted as shown in Figures 3.6 to 3.8.

The first layer of soil, approximately 300 mm thick, was placed and spread evenly in the bottom of the excavation using spades. After placement, the first layer was compacted using three passes of the compactor. CSW, DCP and nuclear density tests were then performed on the freshly compacted layer. The elevation of the geophones below the surface was also measured using a dumpy level. This was done in order to adjust and compare all the measurements to those of the in situ profile. The first layer was compacted a second time using ten passes of the compactor, after which the CSW, DCP and nuclear density tests were repeated.

This process of filling, compacting and testing was repeated for all four layers. The four layers were placed in such a way that the entire excavation was filled and no excavated material was left over (Figures 3.9 to 3.12). In essence, this exercise re-moulded the soil, thus rendering it with a new density, no cementation, and resulting in the erasure of any ageing effects.

3.3 SEISMIC TESTING

The CSW method was used to determine the small strain shear stiffness (G_{max}) of the soil profile. This testing method was discussed in the previous chapter.

In order to perform the CSW test, a shaker, amplifier, signal generator and other smaller pieces of equipment including the geophones, had to be procured and assembled. A laptop computer was borrowed from the Geotechnical laboratories at the University of Pretoria.

Software was developed to handle the calculations required to perform the CSW tests. In order to successfully complete CSW testing of soils, extensive test verification was performed.

The following sections present a detailed discussion of the equipment used in the study, the procedures followed to collect, process and to interpret the data.

3.3.1 Test equipment

The purpose of this section is to list the equipment used during the in situ testing of the two soil profiles and to present a detailed explanation of each listed equipment and its use.

Test equipment consisted of the following:

- A 5 kW petrol powered mobile electric generator supplying power at 50 Hz;
- A Toshiba 386 laptop computer with a data acquisition card supplied by Eagle systems;
- A connecting box with amplifier (110 times amplification);

- 5 geophones supplied by HGS Products;
- A Ling Dynamic Systems (LDS) linear electro magnetic actuator;
- A Ling Dynamic Systems (LDS) amplifier; and
- A signal generator.

The generator supplied electrical power to the actuator, the amplifier, the laptop computer and the signal generator. It was placed about 100 m away from the testing site to minimize the seismic noise caused by the vibrations of the generator motor. The seismic noise created by the generator would otherwise have masked the signal induced into the soil by the actuator, possibly affecting the test results.

Two distinct equipment groups can be identified. The first group induces Rayleigh waves into the soil. The second group logs the surface response of the Rayleigh waves.

The first group consists of the actuator, the LDS amplifier and the signal generator. The actuator vibrates at a given frequency determined by the operator, and is connected to the LDS amplifier, which in turn is connected to the signal generator. The vibrations of the actuator induce seismic waves into the soil; the phase angle and frequency of the Rayleigh wave component of the seismic waves were measured by the geophones. The actuator was placed in the centre of the test pit (Figures 3.18 to 3.20). Sprinkling fine sand underneath as bedding seated the shaker, seating was necessary in order to avoid secondary vibrations that will lower the quality of the measured signals. The actuator was also kept level by using a spirit level during seating. Both these precautions ensured reliability of results.

The LDS amplifier was used to amplify the signal from the signal generator to the actuator. This was done in order to increase the power output of the actuator, which in turn increased the amplitude of the Rayleigh waves to a measurable level.

The signal generator produces a signal in the form of a sine wave at a predetermined frequency. (The determination of the frequency is discussed in Chapter 2). This signal, after being amplified, causes the actuator to vibrate. The signal generator and the LDS amplifier were placed inside the pit close to the actuator. This placing accommodated the short connecting cable between the actuator and the LDS amplifier.

The second group consisted of a laptop computer with data acquisition card, a connecting box with amplifier and geophones.

The computer with data acquisition card was used to log and store the data collected by the geophones during the experiment. It was placed outside the test pit to simplify the pre-test set-up. The laptop computer was connected to the connecting box, with amplifier, which was custom built to amplify the signal 110 times. The connecting box and amplifier were necessary because the signal from the geophones to the data acquisitioning card was found to be too weak for measurement purposes, and as a result, the signal had to be amplified. This could be done since the signals collected from the geophones are analog. They were only converted to digital after passing through the amplifier in the connecting box. The connecting box was connected to the geophones using a co-axial cable.

The geophones measured the vertical velocity of the soil surface as a Rayleigh wave passed underneath. Geophones can also be used to measure the Rayleigh wave velocity using the difference in phase angle between geophones as discussed in Chapters 2 and 4. The geophones were seated properly, 0,5 m apart, in line with the centre of the actuator. The geophone nearest to the actuator was placed 0,5 m away from the edge of the actuator.

The equipment was connected according to the diagram shown in Figure 3.21.

3.3.2 Collection of CSW data

This section presents the procedure used to collect the data. The chronological order of data collection is presented first followed by discussing each separate action involved.

The data was collected in the following order:

- The signal generator was set to the correct chosen frequency;
- The LDS amplifier was switched to the correct amplification setting;
- The signal was logged by the laptop computer and displayed on screen at the discretion of the operator;
- If the signal of all five geophones was satisfactory, a Fast Fourier Transform (FFT) was performed and the signal purity of the data in the frequency domain was evaluated. If the signal was found to be pure enough it was saved to file. If not, it was discarded. In the event where the signal was discarded, the actuator was re-seated and the process repeated until a signal of good quality was obtained; and
- This process was repeated for all the chosen frequencies.

The Rayleigh wave frequencies chosen for the tests, were chosen to allow reasonably continuous stiffness vs. depth graphs to be created. As discussed in Chapter 2, the choice of frequency influences the depth of the Rayleigh wave, and as such the depth to which the measured stiffness is assigned.

The logging frequency for every Rayleigh wave frequency was selected to ensure that the correct number of data points was obtained to describe each Rayleigh wave. If too many data points are obtained per wave form, the frequency resolution diminishes. The implication of this occurrence is that a wider range of frequencies can be recognised in the frequency domain,

but the intervals between recognised frequencies become too large. If too few data points are obtained per wave form, the signal purity of that wave form cannot be measured.

The LDS amplifier was set to a sufficiently high amplification setting to ensure that a measurable signal was received from the geophones. If the amplification setting was set too high for a specific frequency, the power drain on the LDS amplifier exceeded the maximum limit and the safety trip switch was activated. If the amplification setting was set too low for a specific frequency, the Rayleigh wave amplitude proved too small for the geophones to measure. It was important that the signal from the signal generator did not exceed the maximum allowed input voltage for the LDS amplifier. If the input voltage exceeded the maximum limit, the amplified signal was no longer a sine wave but a clipped sine wave (Figure 3.22). As seen from Figure 3.22, a clipped sine wave no longer resembles the curvature of the sine wave, but a square wave. A square wave, when viewed in the frequency domain, consists of a large number of discrete frequencies as opposed to a single frequency as required by the CSW method. A second problem encountered was that the fuses of the LDS amplifier frequently burnt out. This was caused by the increased current output of the LDS amplifier in order to excite the soil with a Rayleigh wave of a given frequency. The problem was solved by setting the input signal from the signal generator to a sufficiently low level as to not induce clipping of the amplifier. The position corresponding to this level was found by measuring with an oscilloscope the position of the output signal amplification control knob on the signal generator that did not exceed the maximum allowable input signal for the amplifier. This position was marked on the signal generator for future use.

A total of 512 data points were logged for each signal using the laptop computer. The data points were displayed on the screen for inspection. 512 data points were selected because it was sufficient for the purposes of velocity and stiffness calculations to accurately describe the required

properties of the Rayleigh waveforms. As explained in Chapter 2, the number of data points necessary to perform a FFT must be an integral power of 2, i.e. 2^2, 2^3, 2^4...($2^9 = 512$).

The operator visually inspected the signal logged from each geophone on the computer screen (Appendix A). Considering that the signal induced by the actuator into the soil is a pure sine wave with a controlled and constant frequency, the logged signal should closely approximate a pure sine wave with the same frequency. If this was the case, a FFT was performed on all five data sets corresponding to the five geophones. This transformed the data from the time domain to the frequency domain (Appendix A). In the frequency domain the signal clarity and frequency were checked. Since the input frequency is known, the spectral amplitude of that frequency must be significantly higher than that of other frequencies when plotting the signal logged from the geophones in the signal domain. As a practical measure, the spectral amplitude of the input frequency should be at least twice as high as any other frequency. This proved a reliable and easy method to ensure that the input frequency equalled the output frequency. If the signals were sufficiently pure, they were saved to file. If the signals were not sufficiently pure, the actuator was re-seated and the test repeated until good quality results signals were logged. The entire process was repeated for all the frequencies logged.

Actuator frequencies ranging between 300 Hz and 10 Hz were logged at the following corresponding logging frequencies as shown in Table 3.1.

TABLE 3.1 Actuator frequencies

Actuator frequency (Hz)	300	250	200	250	100	90	80	70
Log frequency (kHz)	5	5	5	2	2	2	2	1
Actuator frequency (Hz)	60	50	45	40	35	30	27	24
Log frequency (kHz)	1	1	1	1	1	0,5	0,5	0,5
Actuator frequency (Hz)	21	18	16	14	13	12	11	10
Log frequency (kHz)	0,5	0,5	0,2	0,2	0,2	0,2	0,2	0,2

It was found that when a person sat on the actuator during testing, a great improvement in signal quality resulted. Presumably this is due to the increased weight on the shaking mechanism, which ensures that more energy is transferred to the soil. Attempts were made to replace the person by a dead weight but it did not yield the same results as it introduced vibrations or unwanted secondary frequencies. It is suggested that either a heavier, and therefore more expensive actuator be employed, or that sandbags be used to weigh down the actuator. Weighing down the actuator seems to be the more realistic and effective solution. This type of actuator was originally designed for the aircraft- and automotive industry to test equipment performance whilst subjected to various forms of vibration. During these tests, the equipment tested is mounted on a rigid frame with the actuator sandwiched between the equipment and the frame. The actuator is used to provide a source of vibration enough to vibrate heavy equipment above and beyond its own mass. Knowing the original use of an actuator, it makes sense to weigh the actuator down (sandwiched between soil and sandbag). Since the soil is not vibrated for long periods of time there is no need to arrange an extra cooling system for the actuator while weighing it down.

3.3.3 Processing of data

After the data was collected in the field, it was transferred to a faster computer for processing purposes. The processing procedure was initiated

by importing the text files containing the data into Microsoft Excel. Macros were written in Excel to automate data processing.

The macros performed the FFT on the data collected from each geophone. The results were used to compute the phase angle and power spectrum (Chapter 2) for each geophone (Appendix A).

The power spectrum was then used to select the correct frequency for further analysis. This process also served as a check at this stage as the frequency selected using the power spectrum has to correspond with the actuator frequency for the specific test.

The next step was to compute the Rayleigh wave velocity. In order to do this, the geophone spacing had to be known. The density was obtained using the nuclear density gauge.

The best way to calculate the phase difference is to plot the phase angle against the distance of the geophone from the actuator (Figure 3.23). In the event that the Rayleigh wave velocity is constant at all five geophones and the logging was successful, this plot is a straight line with a negative slope. However, as shown in Figure 3.23, this is not always the case.

Figure 3.24 shows the phase angle plotted against distance from the actuator for a single frequency. It is clear from this figure that the phase angle is a saw tooth wave (this results because the wavelength is less than the geophone spacing and all five geophones are not on the same wave), where points A to E correspond to the positions of geophones one to five. In order to calculate the Rayleigh wave velocity, a consistent phase difference between the geophones must be determined. This can be done by subtracting 2π from the phases at points D and E in the cited figure resulting in points D' and E'. A straight line can now be fitted through all five points using the least squares method as is illustrated with line A-E'. The inverse of the slope of line A-E' was then used to calculate a phase

difference for the purposes of Rayleigh wave velocity calculations. Appendices B and C presents the frequency spectrums and phase plots for all the selected frequencies during the test. The Rayleigh wave velocity was calculated using Equations 2.7 and 2.8.

If the phase angles were spread over more than two saw tooth wavelengths, the adjustment of 2π must be multiplied by an integer n in order to adjust the line A-A. When doing this, it must be remembered that the purpose is to adjust the logged signal for the fact that all the geophones are not on the same wave. At this point, one should caution against inserting fictitious waves between geophones. Only data sets for which the least squares method of regression R^2 exceeded 0,98 were selected for further analysis.

For future purposes it is recommended that the system be changed so that this analysis could be done in the field. Instead of discarding data points, the test could be repeated until a usable result is obtained.

Now that the Rayleigh wave velocity has been calculated, the shear wave velocity can be calculated using Equations 2.3 and 2.4. Considering that the Poison's ratio was not known, the factor C in Equation 2.3 was substituted with the constant value of 0,92. This substitution was warranted because C is not sensitive to Poison's ratio, where C is defined in Equation 2.4. It was also reasoned that the choice of conversion factor would not seriously affect the results of the study.

The shear stiffness (G_{max}) and its corresponding assigned depth were calculated using the density and the shear wave velocity. The depth was related to the stiffness by simply using a third of the wavelength as suggested by Hooker (1998) and others.

The processing was done in the same manner for all the frequencies of every test and the shear stiffness versus depth was plotted for every test.

3.3.4 Extraction of information from the collected data

After the shear velocity against depth was plotted for a particular test, the graph was scanned to determine whether the results were reasonable within the boundaries of known shear wave velocities for soils. Any outlying data points were discarded. This may be done with confidence because the shear wave velocity range for sand is well known and any values falling outside this range cannot be correct.

Since the CSW method measures the average stiffness to depth the graph showing shear stiffness against depth has to be smooth. This makes it reasonable to discard any data points that do not follow the general trend.

3.4 STIFFNESS TESTING USING THE DCP

The change in stiffness of the soil was tested using a dynamic cone penetrometer (DCP) (Figure 3.7). This penetrometer consisted of a cone with a 20 mm base diameter and a 60 degree cone tip angle. The cone is fitted to a 16 mm steel rod. The cone is driven into the soil with an 8 kg hammer sliding on a 25 mm diameter steel rod and a fall height of 575 mm. The amount of blows per 100 mm of cone penetration were counted. The more blows needed, the stiffer the soil.

The DCP test was performed in the natural in situ soil profile and in the material re-compacted in the 5 m x 10 m test pit. These two profiles were tested in order to compare the respective penetration resistances of each soil profile. This comparison serves as a clear indication of the difference in the stiffness of the soil before and after compaction i.e. high stiffness in situ and low stiffness after compaction.

The DCP test was performed in situ on the natural soil profile by excavating a test pit in five 200 mm stages. A penetration test was performed at each stage-bottom. In this manner, a profile of penetration resistance against depth could be obtained.

The compacted soil profile in the demarcated area was tested after each compaction stage. Each stage was tested five times at a different position in the pit and the average recorded.

3.5 DENSITY TESTING

In situ density testing was carried out using a Campbell nuclear testing device (Figure 3.25). The device was laboratory calibrated and did not deviate from the allowable tolerances during the entire testing period. The dry density and moisture content were recorded for every test. This was done in order to quantify the level of compaction. The densities were also used during the calculation of the shear stiffness of the two soil profiles.

3.5.1 Test 1 Density measurements

The density of the natural soil profile was tested in the same test pit and at the same time as the DCP tests. The density was tested at a different location in the pit as that used for the DCP test to avoid testing disturbed material.

3.5.2 Test 2 Density measurements

The compacted density was tested in the 5 m x 10 m test pit after each compaction stage to measure the change in density caused by each compaction stage. The measurements were performed using the direct method to a depth of 200 mm.

Chapter 3 presented the experimental method used while the results obtained during testing are presented in Chapter 4.

Figure 3.1 CSW testing prior to excavation (Test 1)

Figure 3.2 Test 2 and 3 excavation close up

Figure 3.3 Test 2 and 3 excavation

Figure 3.4 Compacting the third layer using a Bomag 650

Figure 3.5 Compacting the third layer of backfilled material

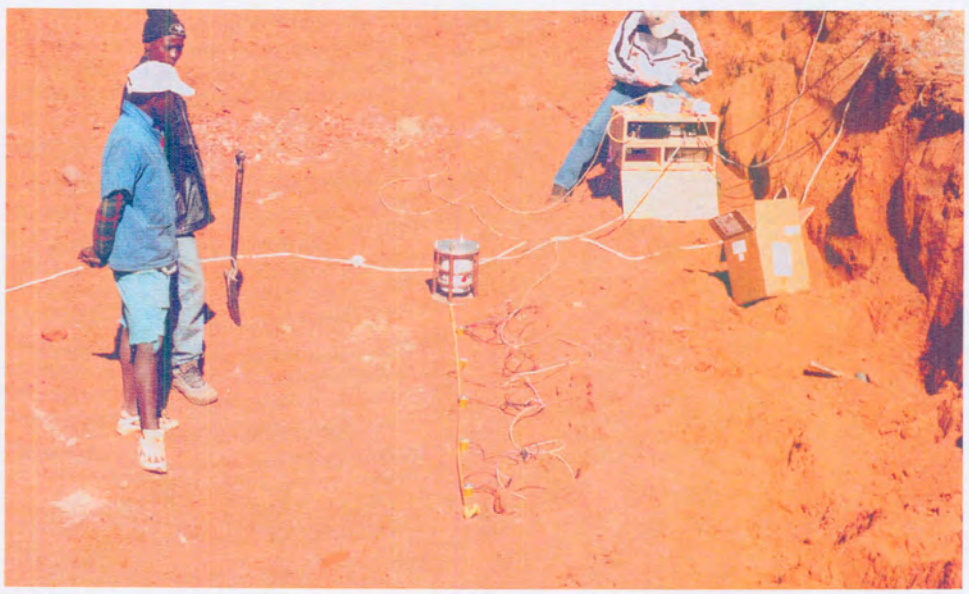

Figure 3.6 CSW testing on a loose first layer

Figure 3.7 DCP testing on a loose first layer

Figure 3.8 Density testing on a loose first layer

Figure 3.9 Backfilling the second layer by hand

Figure 3.10 Leveling the third layer

Figure 3.11 Backfilling the last layer using an excavator

Figure 3.12 Leveling the last layer using a rake

Figure 3.13 Soil profile

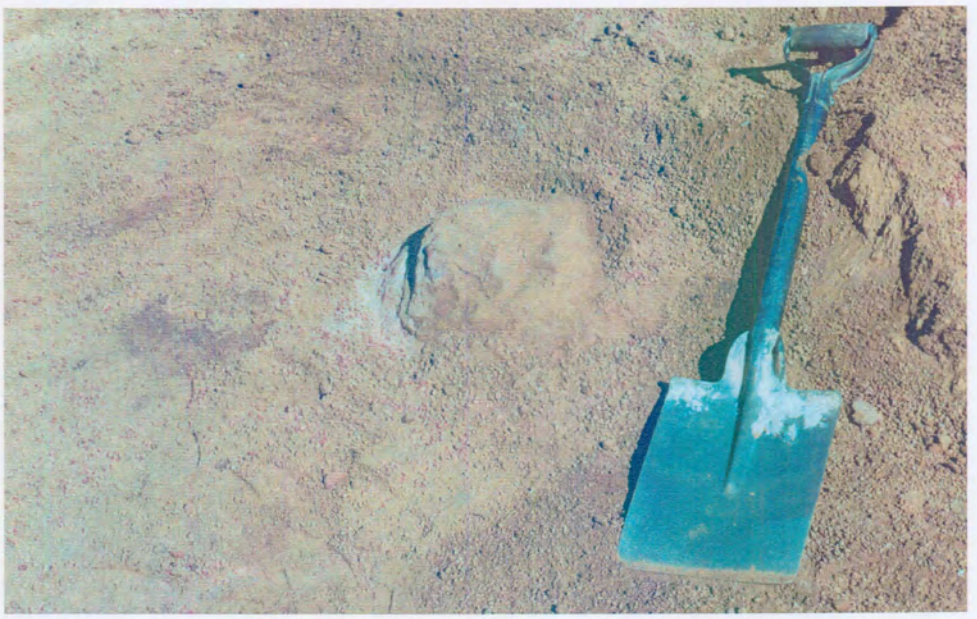

Figure 3.14 One of the sandstone cobbles found in the pit bottom

Figure 3.15 Sandstone cobble broken apart

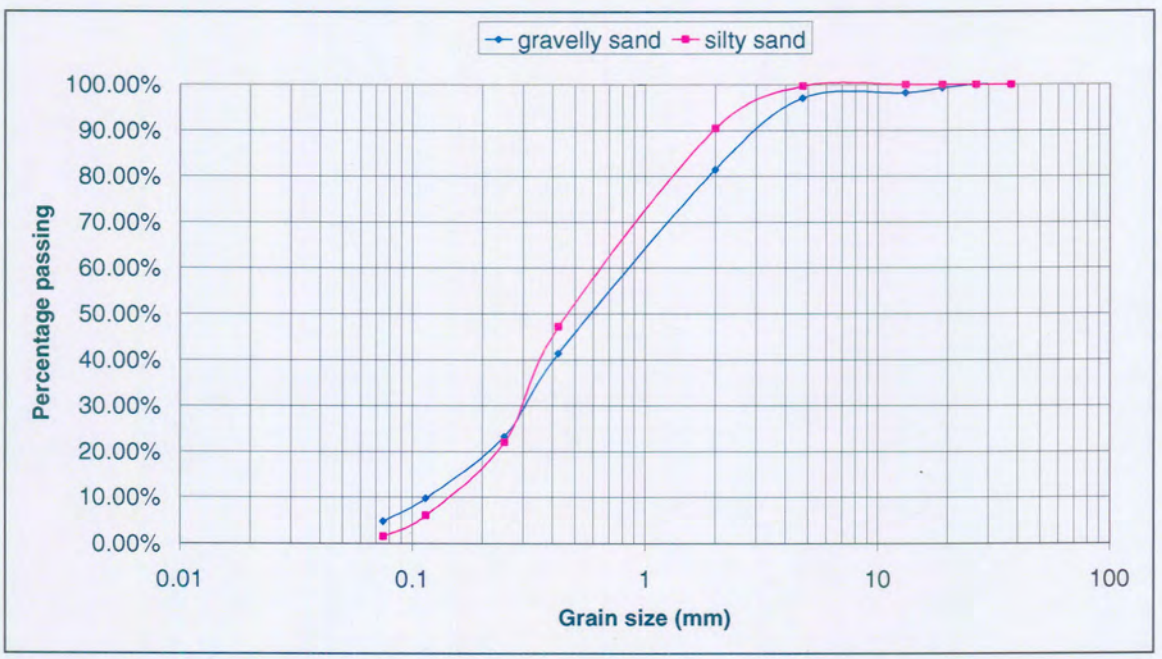

Figure 3.16 Sieve analysis of the two site materials excavated

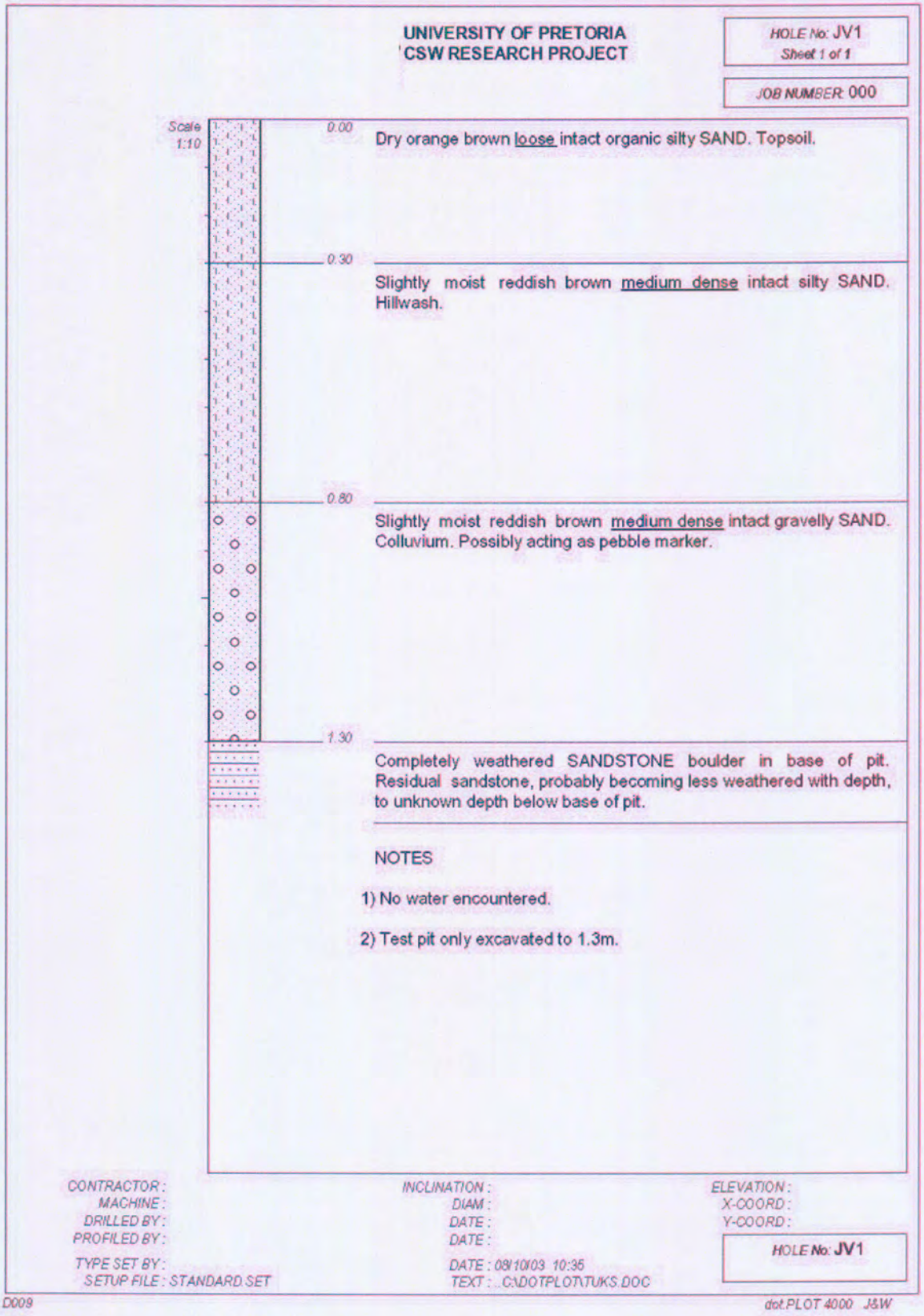

Figure 3.17 Schematic of soil profile

Figure 3.18 Preparing to perform CSW testing on second layer

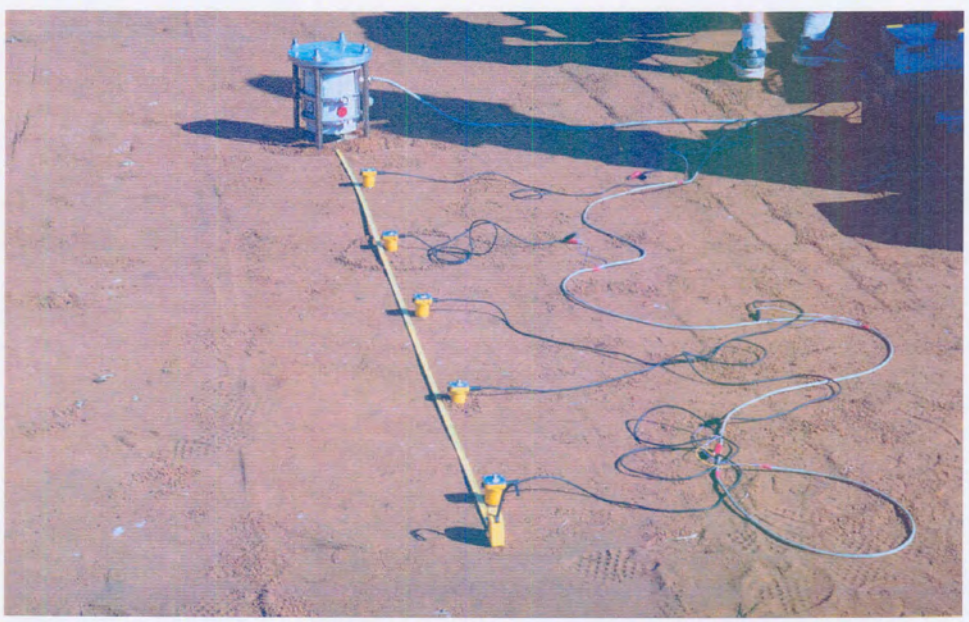

Figure 3.19 The geophones and shaker ready for testing

Figure 3.20 Preparing to perform the CSW test on the last layer

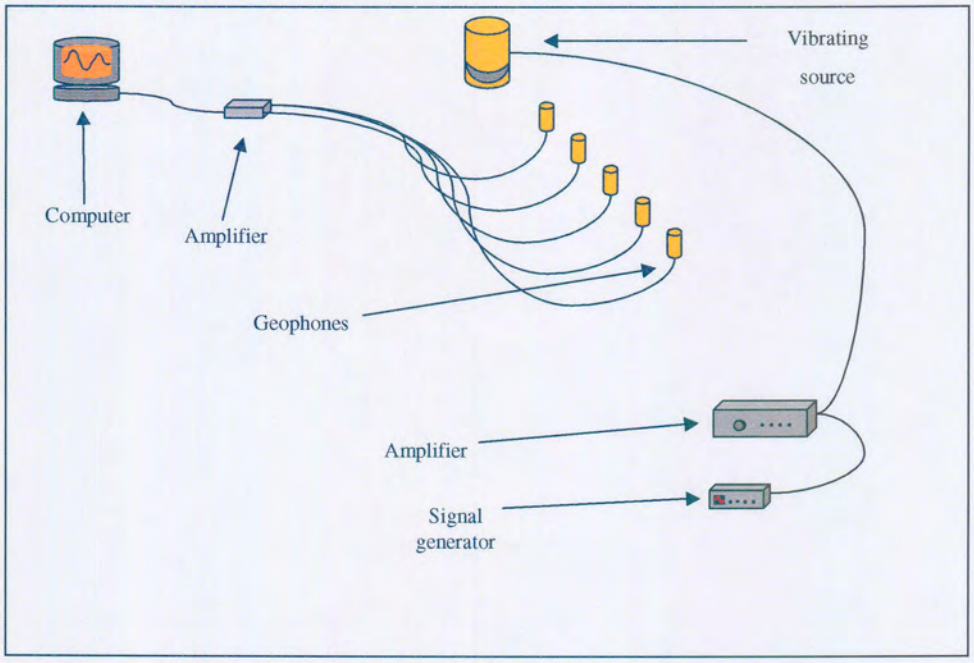

Figure 3.21 Connection diagram for CSW equipment

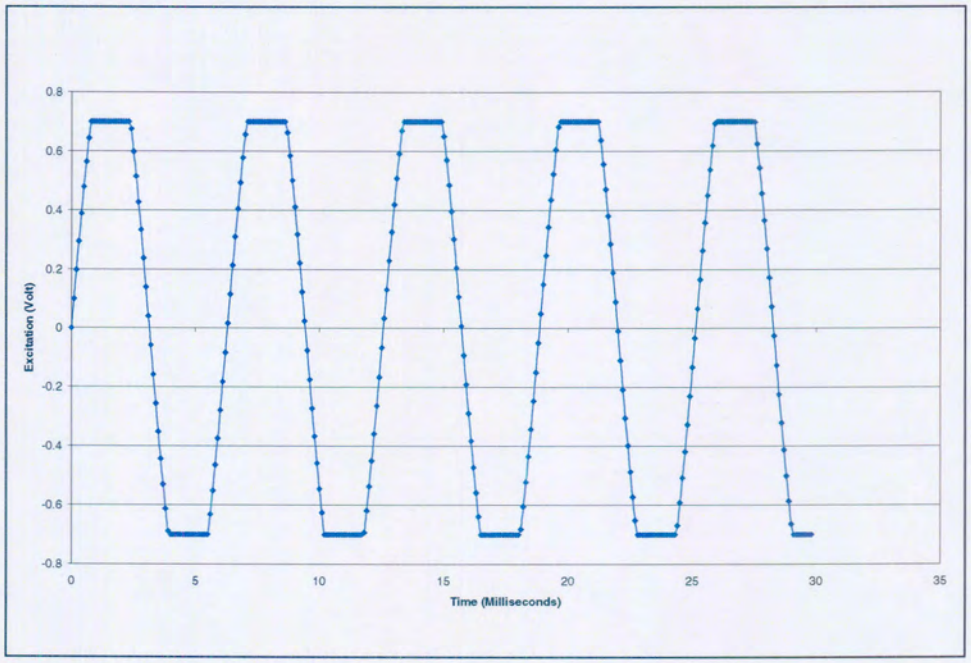

Figure 3.22 Example of a clipped sine wave in the time domain

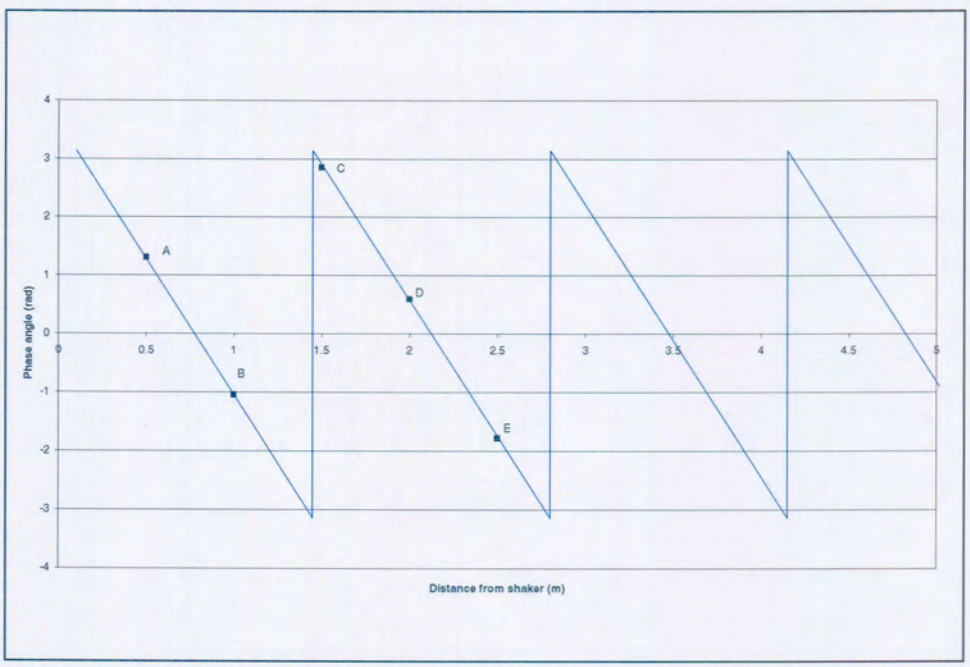

Figure 3.23 Phase vs. distance plot

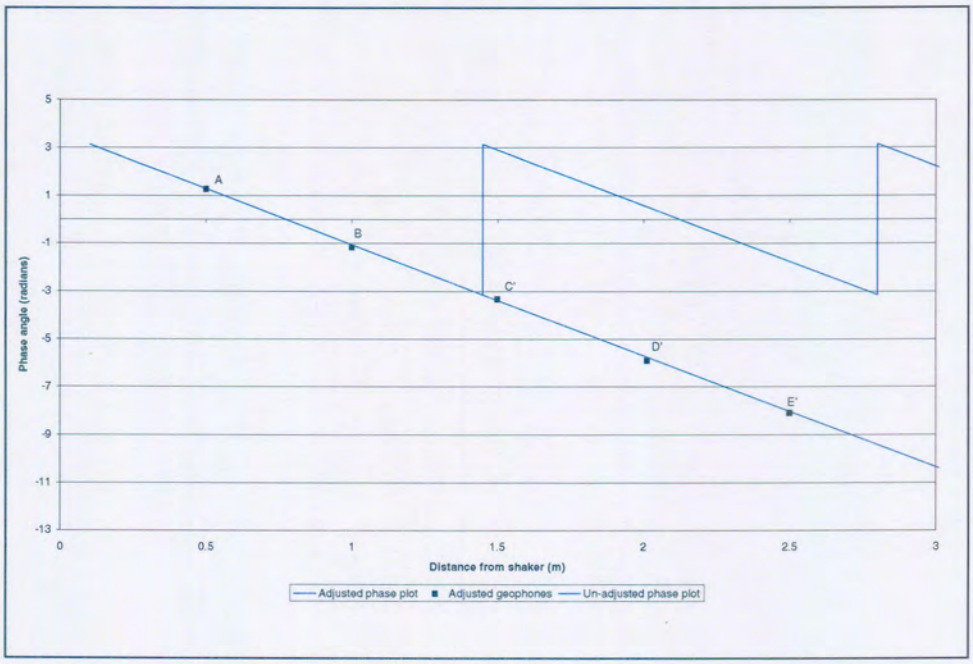

Figure 3.24 Example of an adjusted phase-distance plot

Figure 3.25 Digging the hole for in situ density and DCP measurements

4 RESULTS AND DISCUSSION OF RESULTS

In Chapter 3 the experiment design was discussed as well as the procedures used to process the data. Chapter 3 also stated that the CSW method of testing produces a profile of stiffness vs. depth. Tests were performed on in situ soil as well as on remoulded material in the field after moderate and thorough compaction.

This chapter presents and discusses stiffness vs. depth profiles obtained from the tests and compares the profiles to the DCP and density measurements on the same material.

4.1 DENSITY RESULTS

The measured densities and moisture contents are presented in Table 4.1. All the density results used in this section for comparison are dry densities of the sand. The dry density was chosen because it is not influenced by changes in moisture content of the soil. It is also generally the density used when compacting soil.

4.1.1 In situ and compacted densities

Figure 4.1 shows the density of the in situ soil for purposes of comparison. The thoroughly compacted soil profile (13 passes) is on average 12 % denser than the in situ profile. Figure 4.1 clearly shows that the removal and re-compaction of the soil has increased the density of the soil.

Table 4-1 Measured densities at depth

In situ density						
Depth (m)	0	0.35	0.5	0.73	0.98	1.23
Density Wet (kg/m^3)	1711.4	1722.6	1775.5	1895.5	1966	2022
Density Dry (kg/m^3)	1674.6	1492.6	1497.7	1578.7	1626.6	1642.6
Moisture content (%)	2.1%	15.3%	18.4%	19.9%	20.7%	23.0%
Density after three compaction runs						
Depth (m)	0.006	0.568	0.784	1.064		
Density Wet (kg/m^3)	1709.8	1733.8	1735.4	1805.9		
Density Dry (kg/m^3)	1665	1676.2	1673	1749.8		
Moisture content (%)	2.6%	3.3%	3.6%	3.1%		
Density after thirteen compaction runs						
Depth (m)	0.012	0.576	0.788	1.066	1.364	
Density Wet (kg/m^3)	1770.7	1766.5	1820.3	1935.6	2041.2	
Density Dry (kg/m^3)	1724.2	1717.8	1757.8	1876.3	1922.8	
Moisture content (%)	2.6%	2.7%	3.4%	3.1%	6.1%	

4.1.2 Density, comparison after 3 and 13 compaction runs

The soil was compacted slightly dry of its optimum moisture content of 10 %. This was done in order to minimize the effect of moisture on the CSW test results. Moisture content affects shear wave velocity only moderately and therefore, it was not tested in this experiment this was not tested. Figure 4.1 shows the density of the soil before and after it was thoroughly compacted. The figure shows that the extra compaction effort effected by the 10 runs with the compactor increased the density of the soil with an average improvement of 4,6 %. This constitutes a reduction in the void ratio from 0,84 to 0,79, which is significant for such a light compactor.

The number of compaction runs used were unrealistically high but was needed to maximise the difference between the lightly compacted and heavily compacted soils.

4.2 DCP RESULTS

The method used to collect DCP data is described in detail in Chapter 3. The recorded results are presented as blows per 100 mm of cone penetration. It is presented in this way because it makes it easier to assign penetration numbers to depths. Measured results are presented in Figure 4.2.

The figure shows results relative to the ground surface. The results were collected after each set of compaction runs and the depth adjusted relative to ground surface. This makes the results less cumbersome to interpret.

4.2.1 DCP results, in situ compared to compacted

Figure 4.2 shows that the in situ penetration resistance is generally higher than the compacted penetration resistances. There are values that overlap but it should be remembered that the DCP is an indicator test at best and the results are very sensitive to small defects like small pebbles and inhomogeneities in the soil. This result may seem contradictory at first because the in situ soil is less dense. The explanation is that the in situ soil has a long stress history and has some structure, while the compacted soil had its stress history erased. To conclude, the in situ stiffness measured using the DCP method is higher than the compacted measurements.

4.2.2 DCP results before and after compaction

Section 4.1.1 showed that more compaction effort leads to an increased density of the soil. The DCP results (Figure 4.2) indicate that the penetration resistance shows no discernable change as the density of the

soil increases. This contradicts classic soil mechanics as Hardin & Drnevich (1972) showed that stiffness increases as density increase. A possible explanation is that the increase in density was only 4,6 % as previously mentioned and the DCP may not be precise enough to reflect such a small change in density.

4.3 CSW TEST DATA

The CSW results generally failed to produce results at depths less than 300 mm. Therefore, no comparison between moderate and thorough compaction could be done as each compacted layer was approximately 250 mm thick. The stiffness comparison between in situ and compacted soil was very successful and is presented in this section.

4.3.1 In situ and final compacted lift stiffness

Figure 4.3 shows the Rayleigh wave dispersion curves for both the in situ and the compacted soils. The Rayleigh wave velocities measured during testing were faster in the in situ profile than in the compacted profile for the same wavelength. The wave velocities also increased as the wavelength increased.

Figure 4.4 shows the Rayleigh wave velocity plotted against depth below surface. As explained in Chapter 2, the depth assigned to a Rayleigh wave velocity is equal to a third of the wavelength. Therefore, Figures 4.3 and 4.4 are very similar in that the horizontal axis remains unchanged but the scale of the vertical axis is divided by a factor of three.

Figure 4.5 shows the shear wave velocity plotted against depth below surface. The in situ profile has a faster shear wave velocity than the

remoulded profile. This graph was obtained by converting the Rayleigh wave velocities in Figure 4.4 to shear wave velocities using Equation 2.3.

Figure 4.6 shows shear stiffness plotted against depth below surface. This graph was obtained by converting the shear wave velocity in Figure 4.5 to shear stiffness using Equation 2.2.

The stiffness measured in Figure 4.6 is the small strain shear stiffness as defined in Chapter 2. The figure shows that the in situ material has a higher stiffness than the compacted material. In fact, the stiffness of the in situ material is approximately twice as high as the stiffness of the compacted material. It is suggested that this is due to structure of the soil and the stress history. Other authors have observed similar reductions in stiffness (Lohani, Imai and Shibuya, 1999).

During the testing performed for this study the shear stiffness graphs indicated that the shear stiffness measured using the CSW method, has decreased after compaction as a result of the breakdown of the slight bonding between particles. Both of these profiles were tested within days of each other and there were no weather changes including rain during this period. The soil that was tested in situ was the same soil as the remoulded material.

Figure 4.1 Density profile comparison

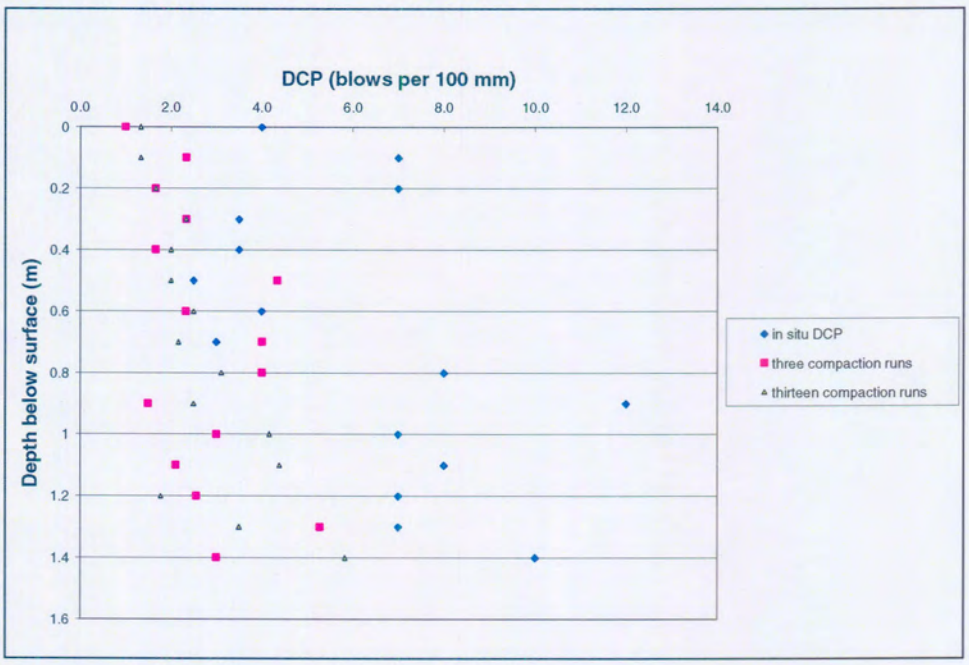

Figure 4.2 DCP profile comparison

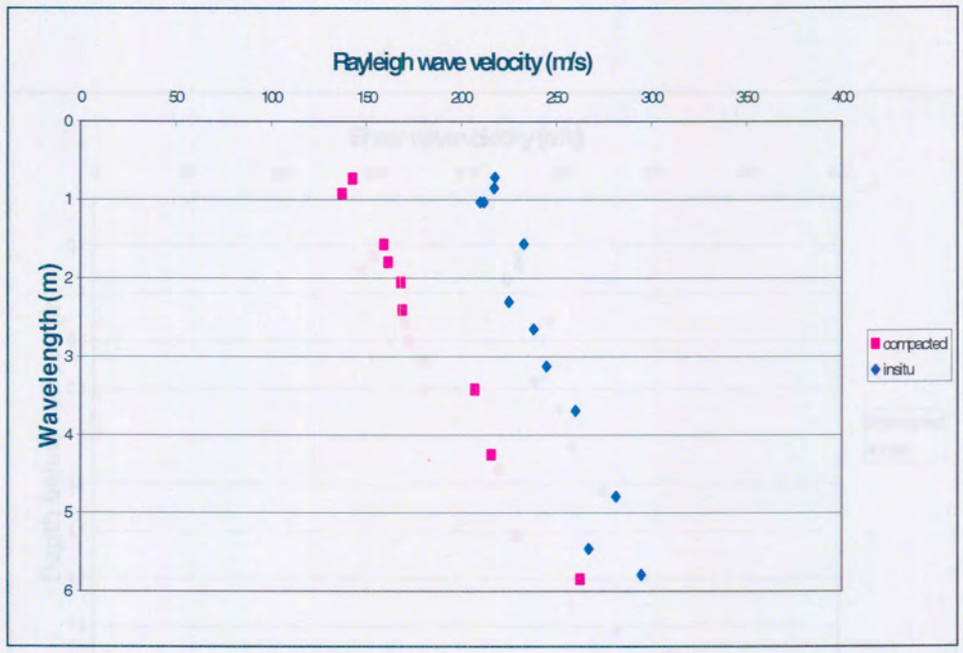

Figure 4.3 Rayleigh wave velocity vs. Wavelength

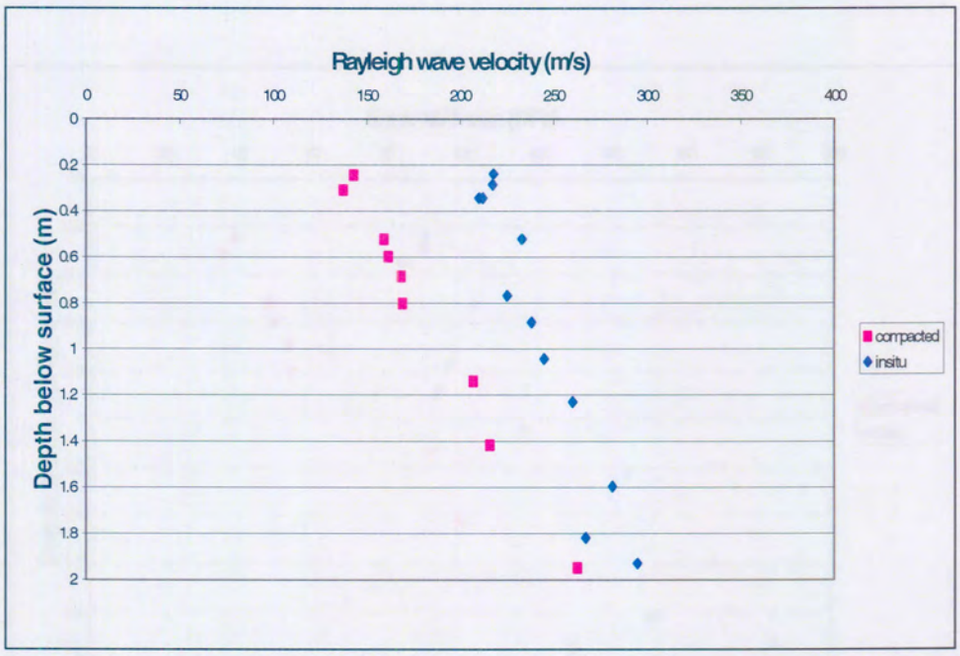

Figure 4.4 Rayleigh wave velocity vs. Depth below surface

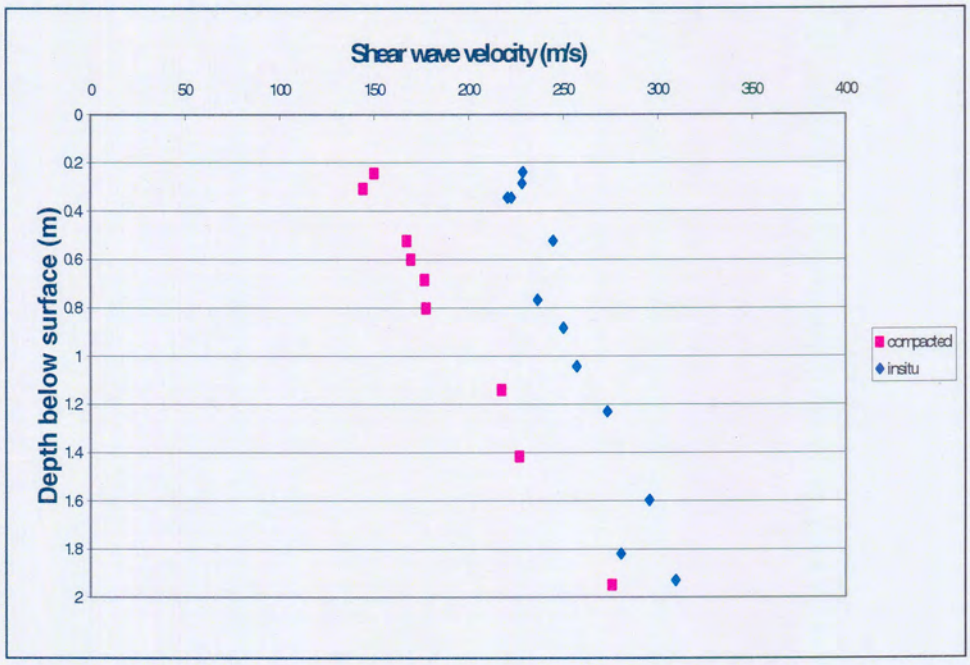

Figure 4.5 Shear wave velocity vs. Depth below surface

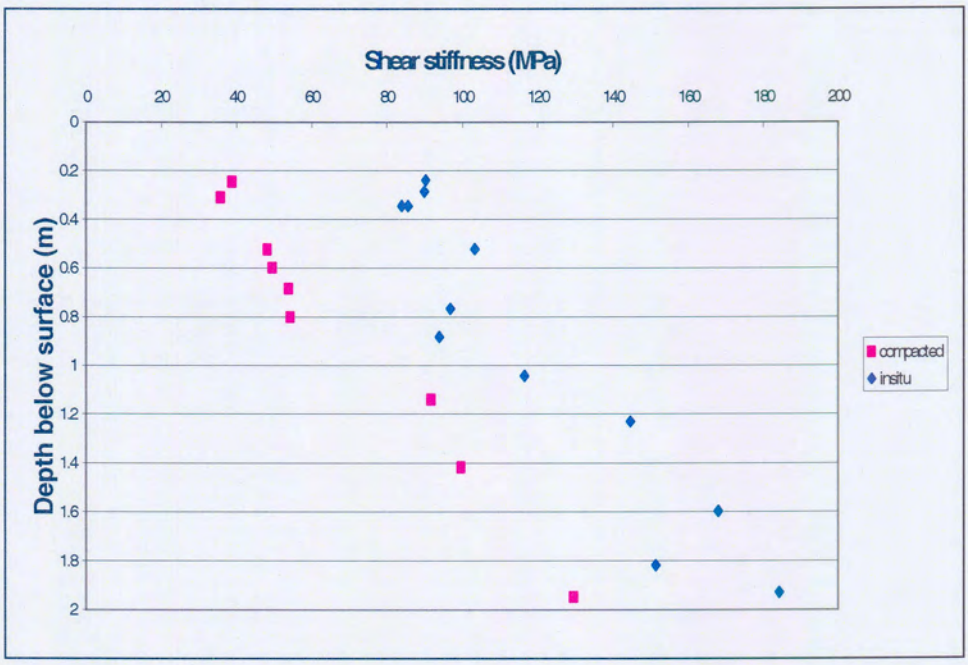

Figure 4.6 Shear stiffness vs. Depth below surface

5 CONCLUSION

Based on the results presented in Chapter 4, the shear stiffness measured using the CSW method decreased after the soil was compacted. The reduction in soil stiffness was confirmed by the DCP results as the DCP penetration number also decreased after compaction. This behaviour may be explained by the fact that the soil with bonding had a higher stiffness than when the same soil had no bonding when remoulded (excavated and re compacted).

The hypothesis stated that this study was aimed at showing that the CSW method could be used to detect changes in soil stiffness. The DCP results detected that the stiffness decreased after compaction and the CSW also showed that the stiffness decreased after compaction. Soil stiffness measured using the CSW method was however better defined compared to that measured using a DCP. Furthermore, both techniques measured an increase in stiffness with depth of soil as expected. Based on these observations the hypothesis is accepted.

During the study an interesting observation was made, namely that the in situ soil had a lower density than that of the compacted material, but the in situ soil stiffness was higher than the remoulded soil stiffness because of slight bonding between particles. Further investigation is recommended in order to quantify the effects of this phenomena and its influence on seismic stiffness testing.

6 REFERENCES

Andrus R.D., Chung R.M., Stokoe K.H. and Bay J.A. (1998). Delineation of densified sand at Treasure Island by SASW testing. *Geotechnical site characterization.* Robertson & Mayne (eds) Balkema, Rotterdam, pp. 459-464.

Andrus R.D. and Stokoe K.H. (2000). Liquefaction resistance of soils from shear-wave velocity. *Journal of Geotechnical and Geoenvironmental Engineering.* Volume 126. pp 1015-1025.

ASTM D 5777-95. (1996). Standard guide for using the seismic refraction method for subsurface investigation. *Annual book of ASTM standards*, Volume 04.08.

Bergdahl U. and Ottosson E. (1988). Soil characteristics from penetration test results: A comparison between various investigation methods in non-cohesive soils. *Penetration testing.* ISOPT-1. De Ruiter (ed.). Balkema, Rotterdam.

Butcher A.P. and Tam W.S.A. (1997). The use of Rayleigh waves to detect the depth of a shallow landfill. *Modern geophysics in engineering geology.* McCann D.M., Eddleston M., Fenning P.G., Reeves G.M. (eds). Geological Society Engineering Geology Special Publication No. 12. pp 97-102.

Chua K. M. (1988). Determination of CBR and elastic modulus of soils using portable pavement cone penetrometer. *Penetration testing.* ISOPT-1. Balkema, Rotterdam.

Clayton C.R.I., Gordon M.A. and Matthews M.C. (1994). Measurement of stiffness of soils and weak rocks using small strain laboratory testing and field geophysics. *Pre-failure deformation of geomaterials.* Balkema, Rotterdam, pp. 229-234.

Clayton C.R.I. and Heymann G. (2001). Stiffness of geomaterials at very small strains. *Geotechnique.* 51, No. 3, pp. 245-255.

Clayton C. R. I., Simons N. E. and Instone S. J. (1988). Research on dynamic penetration testing of sands. *Penetration testing.* ISOPT-1. De Ruiter (ed.). Balkema, Rotterdam, pp 415-422.

Cooley J.W. and Tukey O.W. (1965). An Algorithm for the Machine Calculation of Complex Fourier Series. *Math. Comput.* Vol. **19**, pp. 297-301.

Cuellar V. (1997). Geotechnical applications of the spectral analysis of surface waves. *Modern geophysics in engineering geology.* McCann D.M., Eddleston M., Fenning P.G., Reeves G.M. (eds). Geological Society Engineering Geology Special Publication No. 12, pp 53-62.

De Beer M. (1991). Use of the Dynamic Cone Penetrometer (DCP) in the design of road structures. *Geotechnics in the African Environment,* Blight et al. (eds.)Balkema Rotterdam, pp 167-177.

Gordon M.A., Clayton C.R.I., Thomas T.C. and Matthews M.C. (1996). The selection and interpretation of seismic geophysical methods for site investigation. *Advances in site investigation practice.* Thomas Telford, London, pp 727-738.

Griffiths D. H. and King R.F. (1981). *Applied Geophysics for Geologists & Engineers. The Elements of Geophysical Prospecting.* Pergamon Press. pp 8-64.

Harison J.A., (1987). Correlation between California bearing ratio and dynamic cone penetrometer strength measurement of soils. *Ground Engineering Group.* Proc. Institution Civil Engineers, Part 2, 83, Dec., pp 833-844.

Haegeman W. and Van Impe W.F., (1998). SASW contol of a vacuum consolidation on a sludge disposal. *Geotechnical site characterization.* Robertson & Mayne (eds) Balkema, Rotterdam, pp 473-477.

Hardin B. O. and Drnevich V. P., (1972). Shear modulus and damping in soils: Design equations and curves. *Journal of the Soil Mechanics and Foundations Division.* ASCE. Vol 98, No. 7, pp 667-692.

Haskell N. A., (1953). The dispersion of surface waves on multilayered media. *Bulletin of the Seismological Society of America.* Vol. 21, pp 17-34.

Hooker P. (1998). Seismic solution. *Ground Engineering.* February 1998, pp 28-29.

Hooker P. (2002). Measure for measure. *Ground Engineering.* October 2002, pp 26-27.

Jacobs P.A. and Butcher A.P. (1996). The development of the seismic cone penetration test and its use in geotechnical engineering. *Advances in site investigation practice.* Thomas Telford, London, pp 396-406.

Kim S. (1997). SASW method for the evaluation of ground densification of dynamic compaction. *Ground improvement geosystems, Densification and reinforcement.* Proceedings of the third international conference on ground improvement geosystems. London , June 1997.

Kim D.S. and Park H.C. (1999). Evaluation of ground densification using spectral analysis of surface waves (SASW) and resonant column (RC) tests. *Canadian Geotechnical Journal.* Vol. 36, pp 291-299.

Klein E.G., Maree J.H. and Savage P.F. (1982). The application of a portable pavement dynamic cone penetrometer to determine in situ bearing properties of road pavement layers and subgrades in South Africa. *Proceedings of the Second European Symposium on Penetration Testing.* Amsterdam. 24-27 May. pp 277-282.

Klein E.G. and van Zyl G.D. (1988). Application of the dynamic cone penetrometer (DCP) to light pavement design. *Penetration testing.* ISOPT-1, De Ruiter (ed), Balkema, Rotterdam, pp 435-444.

Lefebre G., Leboeuf D., Muhsin E.R., Lacroix A., Warde J. and Stokoe K.H., (1994). Laboratory and field determinations of small-strain shear modulus for structured Champlain clay. *Canadian Geotechnical Journal.* Vol.31, pp 61-70.

Livneh M. and Ishai I., (1988). The relationship between in situ CBR test and various penetration tests. *Penetration testing.* ISOPT-1, De Ruiter (ed), Balkema, Rotterdam, pp 445-452.

Lohani T. N., Imai G. and Shibuya S. (1999). Effect of sample disturbance on G_{max} of Holocene clay deposits. *Pre-failure deformation of geomaterials.* Balkema, Rotterdam, pp 115 – 121.

Matthews M.C., Hope V.S., Clayton C.R.I. (1995). The geotechnical value of ground stiffness determined using seismic methods. *30th annual conference . Engrg Gip. Geol. Soc. Modern geophysics in engineering geology.* Liege.

Matthews M.C., Clayton C.R.I., Own Y. (2000). The use of field geophysical techniqes to determine geotechical stiffness parameters. Proc. Institution Civil Engineers Geotech. Engng, 143, Jan., pp 31-42.

Matthews M.C., Hope V.S. and Clayton C.R.I. (1996). The use of surface waves in the determination of ground stiffness profiles. Proc. Institution Civil Engineers Geotech. Engng. 110, pp 84-95.

Matthews M.C., Hope V.S. and Clayton C.R.I. (1997). The geotechnical value of ground stiffness determined using seismic methods. *Modern Geophysics in Engineering Geology.* Geological society Engineering Geology Special Publication No. 12, pp. 113-123.

Menzies B. and Matthews M.C. (1996). The continuous surface wave system: a modern technique for site investigation. *Special lecture: Indian geotechnical conference.* Madras.

Milne J. revised by Lee A. W. (1939). *Earthquakes and other Earth Movements*. KEGAN PAUL, TRENCH, TRUBNER & CO., LTD.

Moxhay A.L., Tinsley R.D. and Sutton J.A. (2000). Monitoring of soil stiffness during ground improvement using seismic surface waves. *www.gdsinstruments.com*

Rickets G.A., Smith J. and Skipp B.O. (1996). Confidence in seismic characterization of the ground. *Advances in site investigation practice.* Thomas Telford. London, pp 673-686.

Santagata M.C. and Germaine J.T. (2002). Sampling disturbance in normally consolidated clays. *Journal of geotechnical and geoenvironmental engineering.* Vol. 128, No. 12. pp. 997-1006.

Szavits-Nossan A., Kovacevic M.S. and Mavar R., (1998). Experience gained in testing pavements by spectral analysis of surface waves. *Geotechnical site characterization.* Robertson & Mayne (eds) Balkema, Rotterdam, pp 521-524.

Thomson W. T., (1950). Transmission of elastic waves through a stratified solid medium. *Journal of applied physics*. Vol. 21, pp 89-93.

Appendix A

Example of CSW test for one frequency

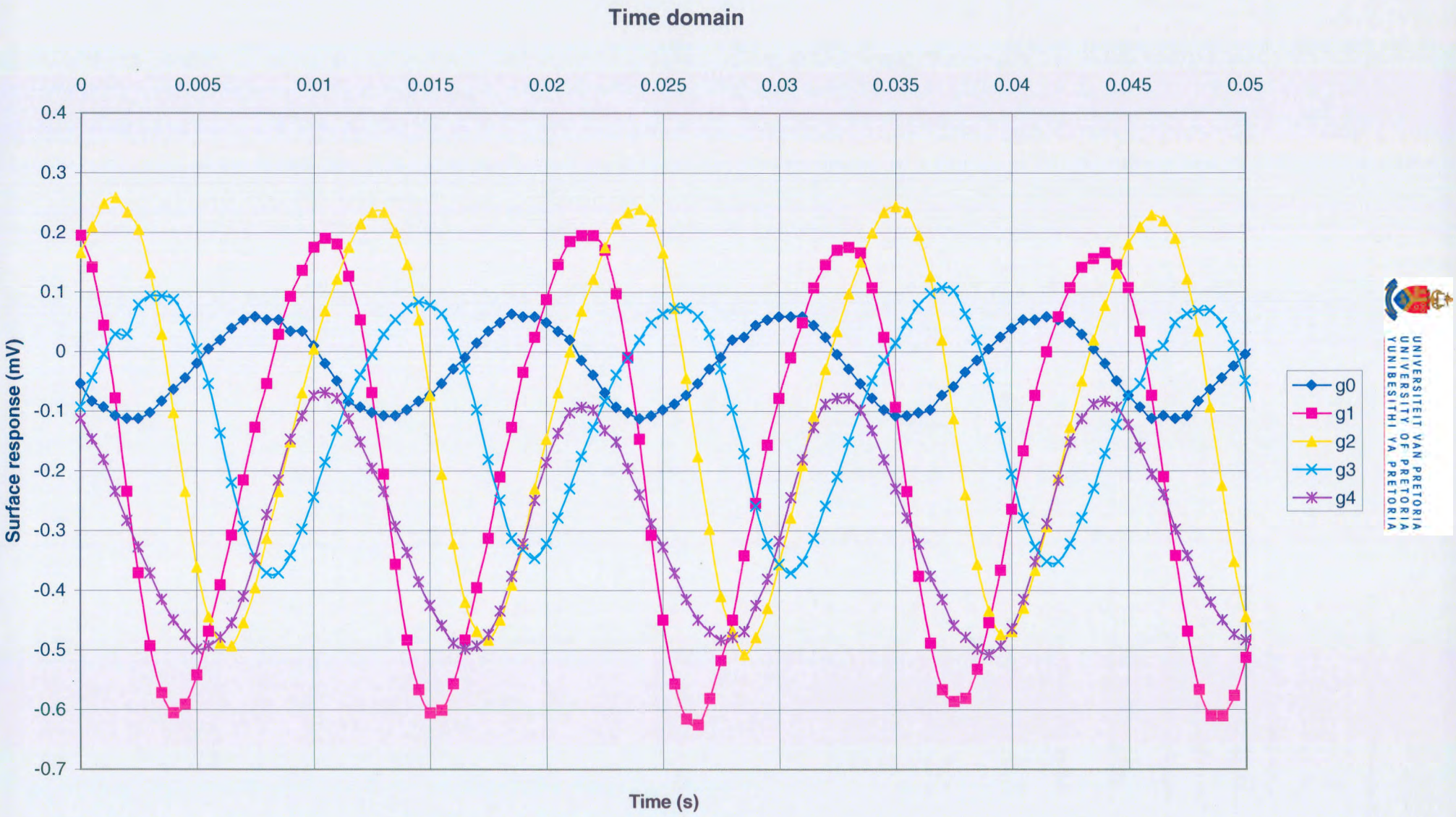

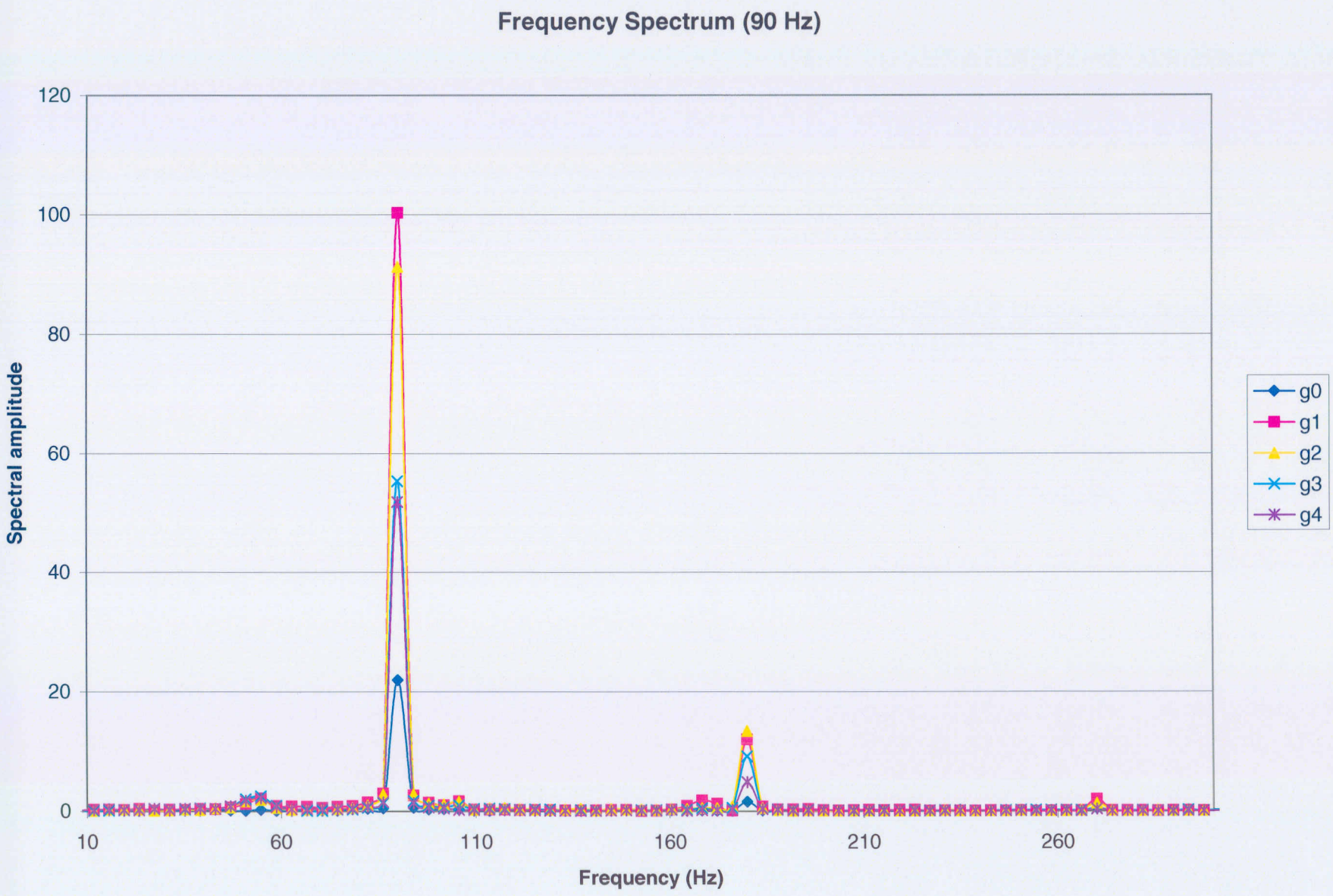

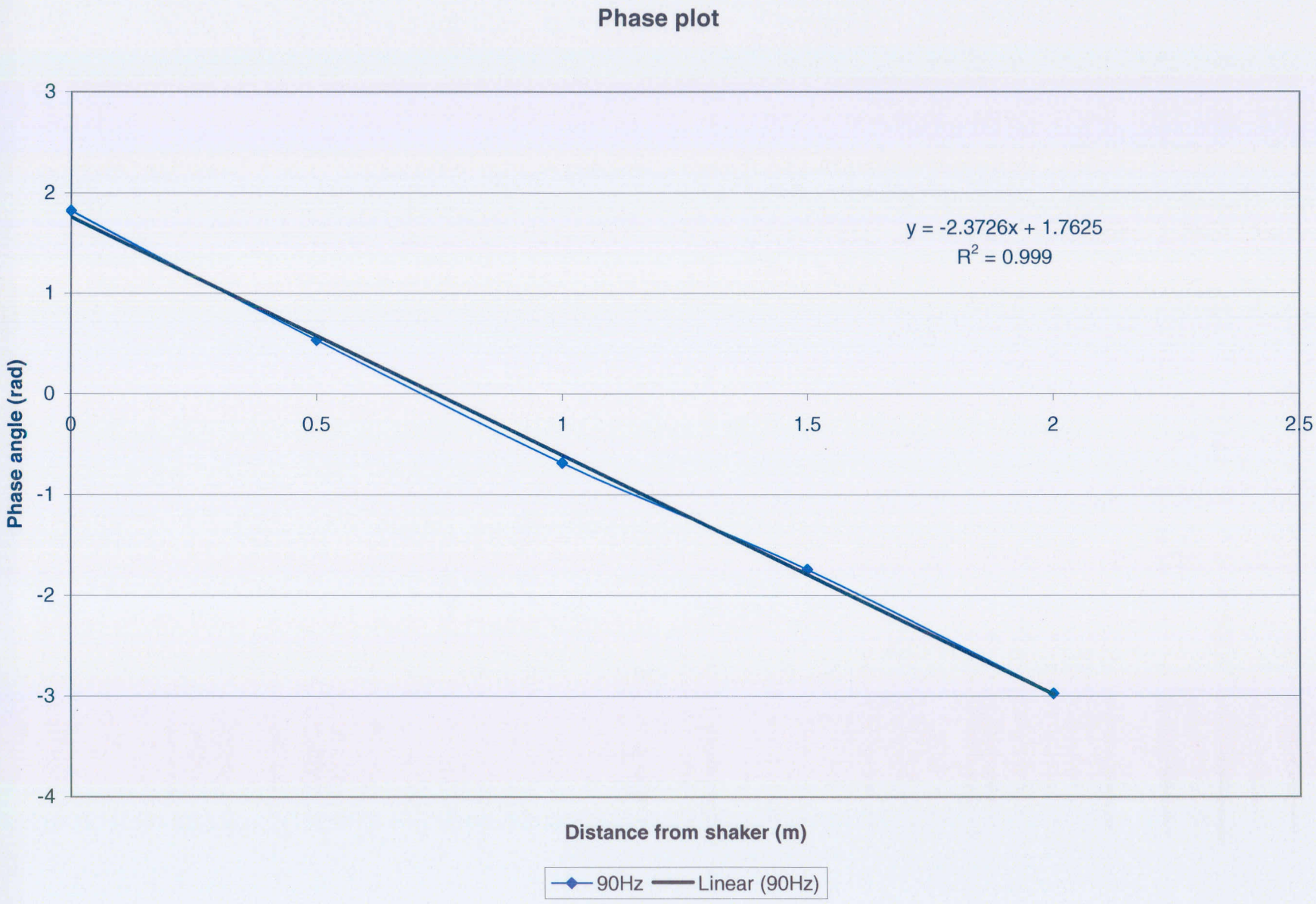

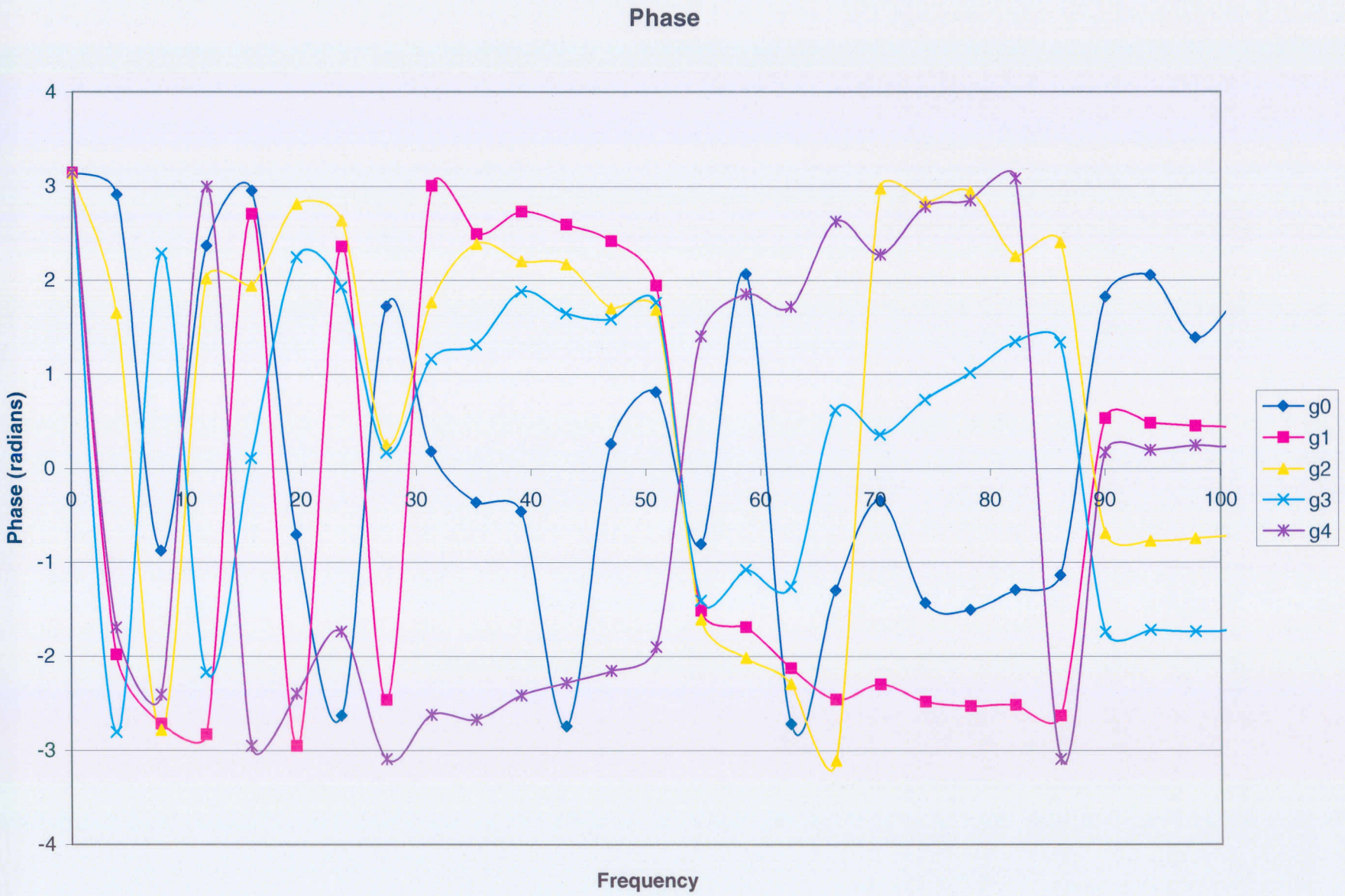

Appendix B

Phase plots and frequency spectrum for the in situ CSW testing

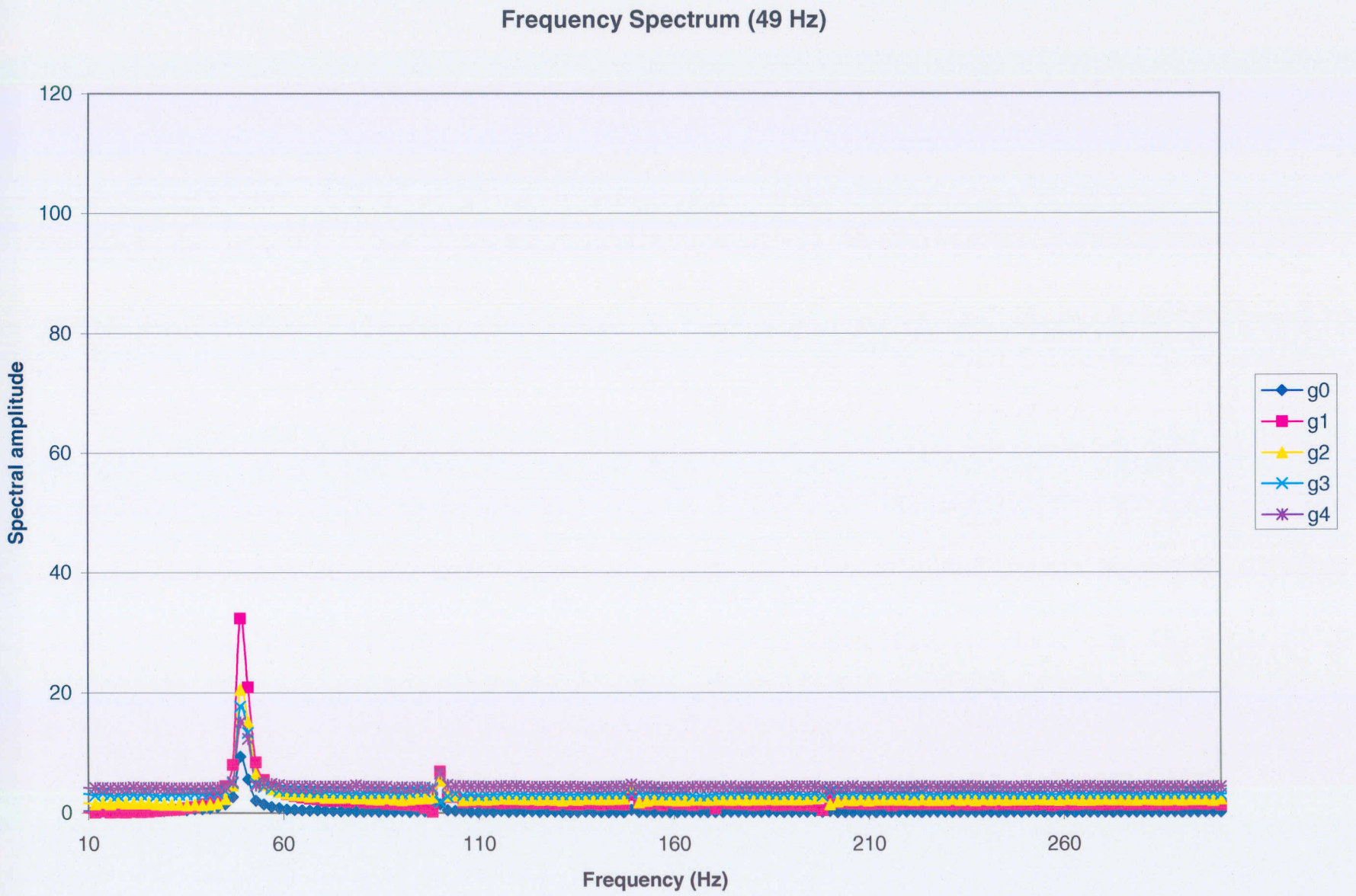

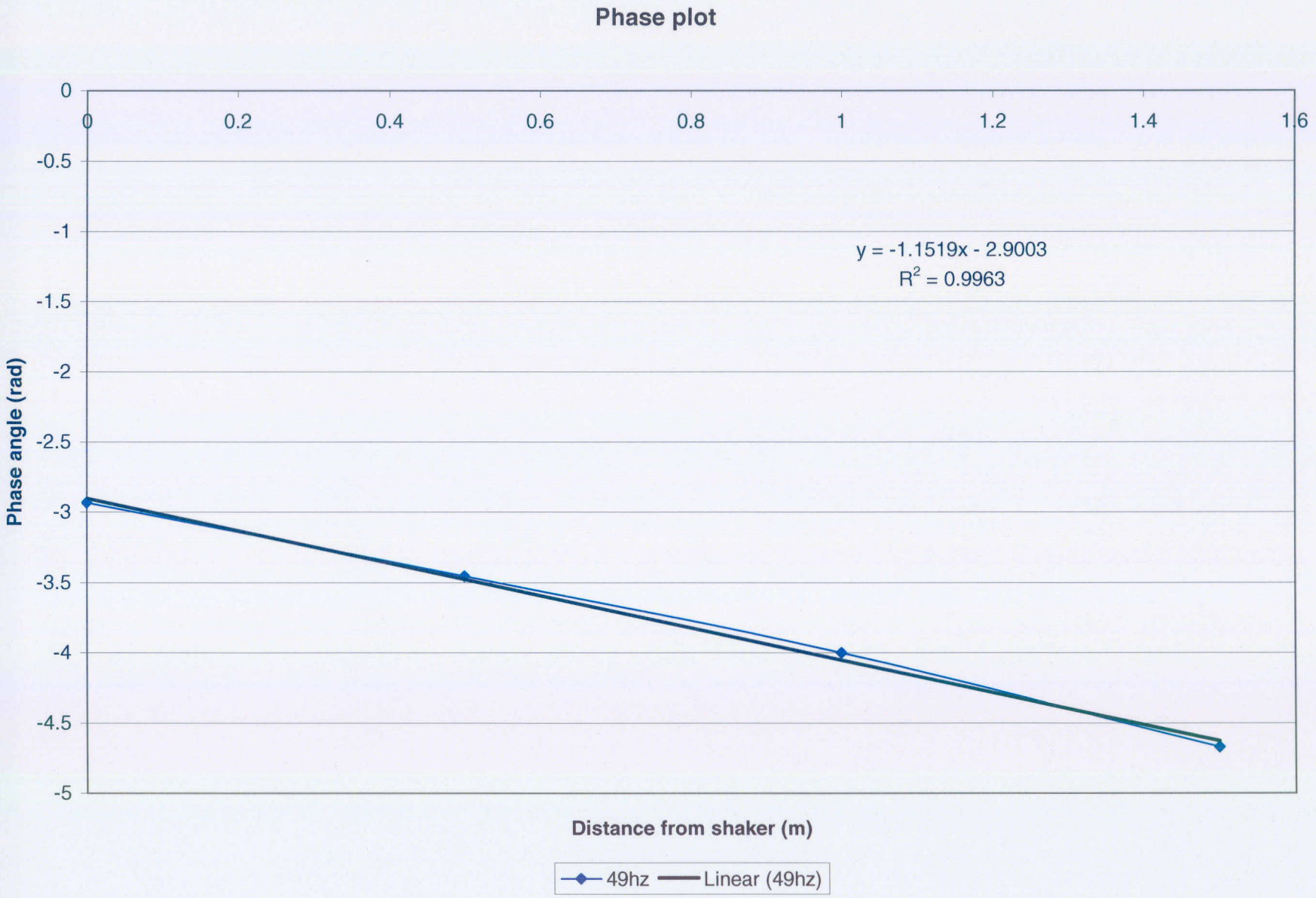

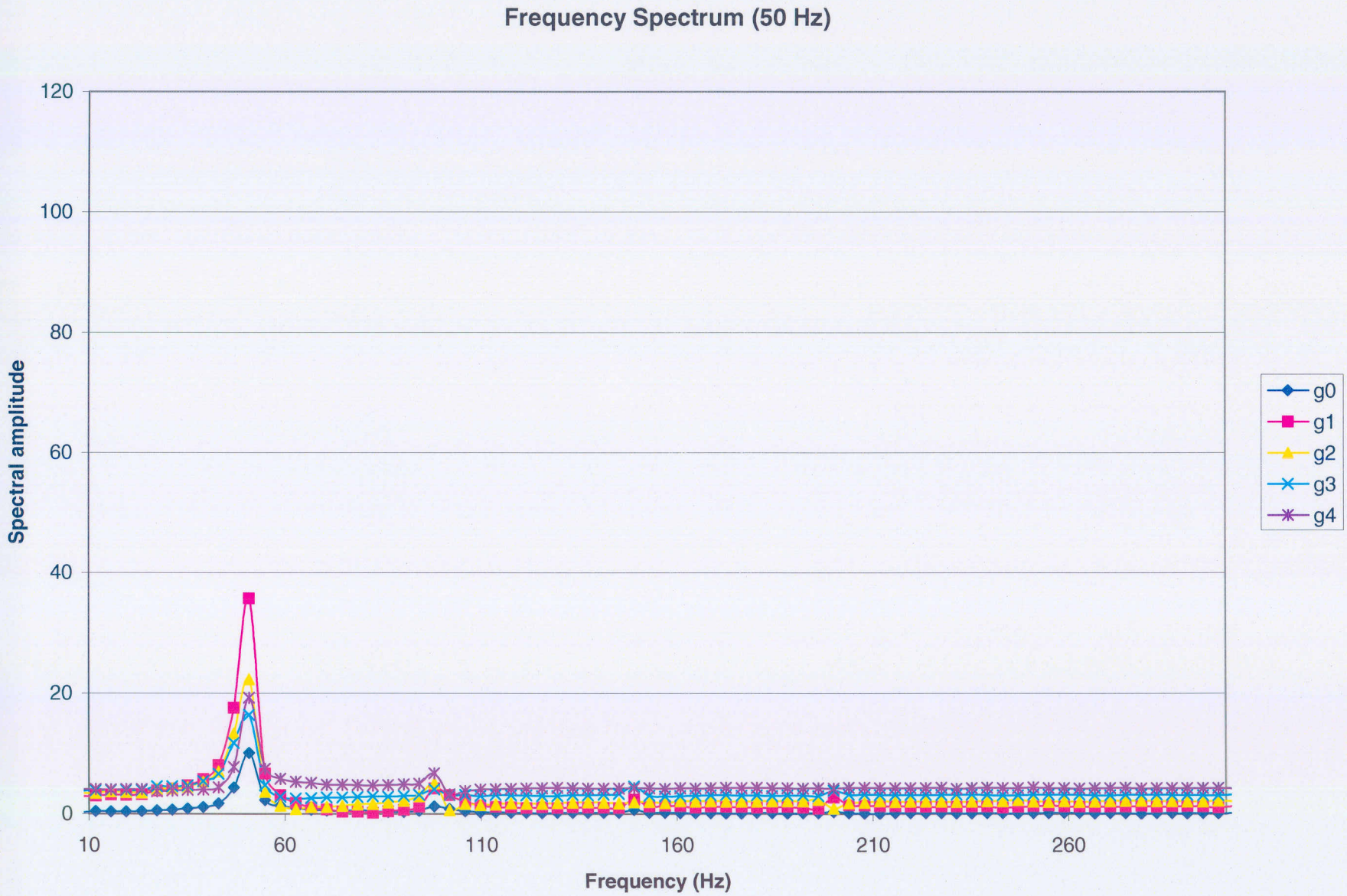

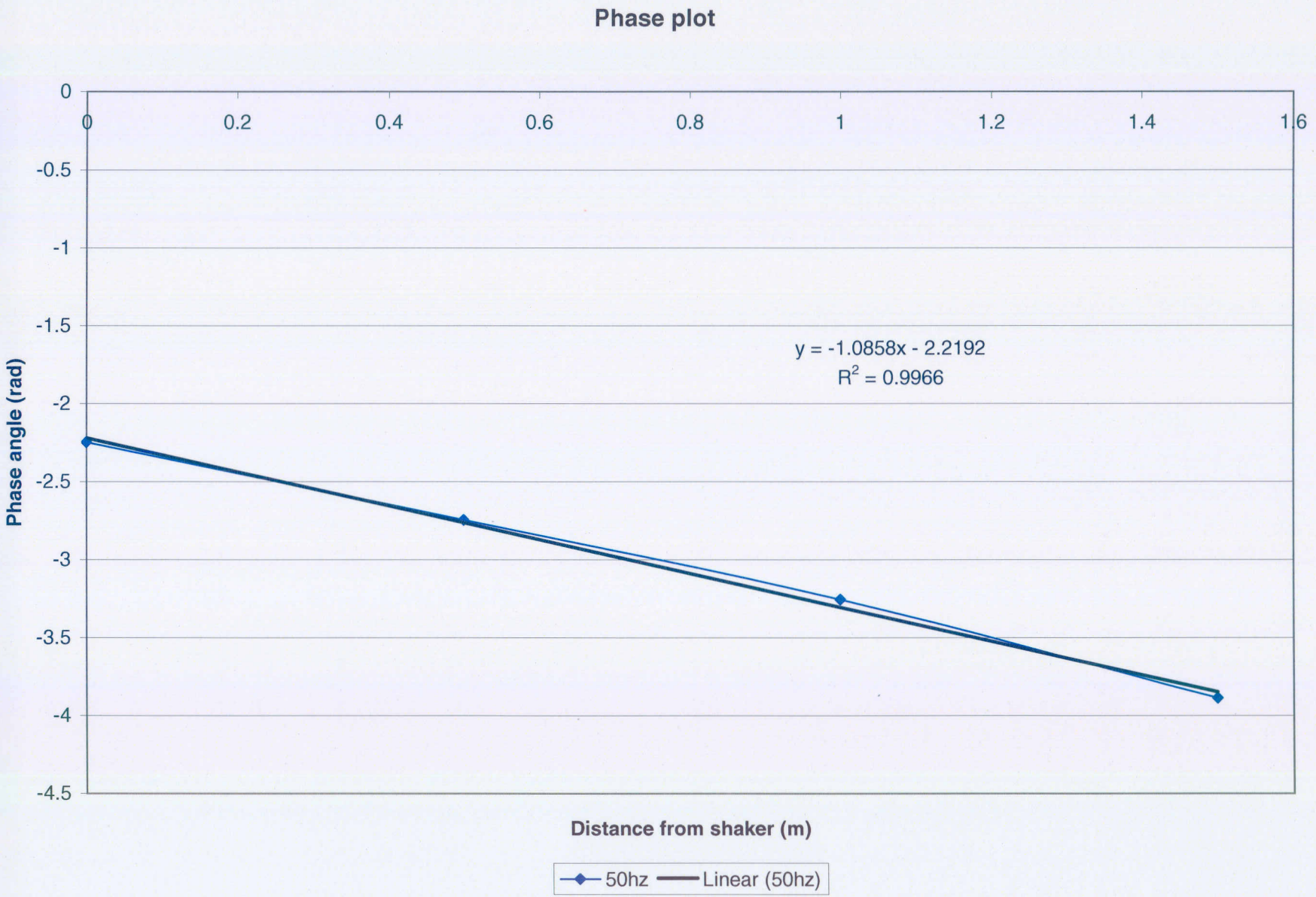

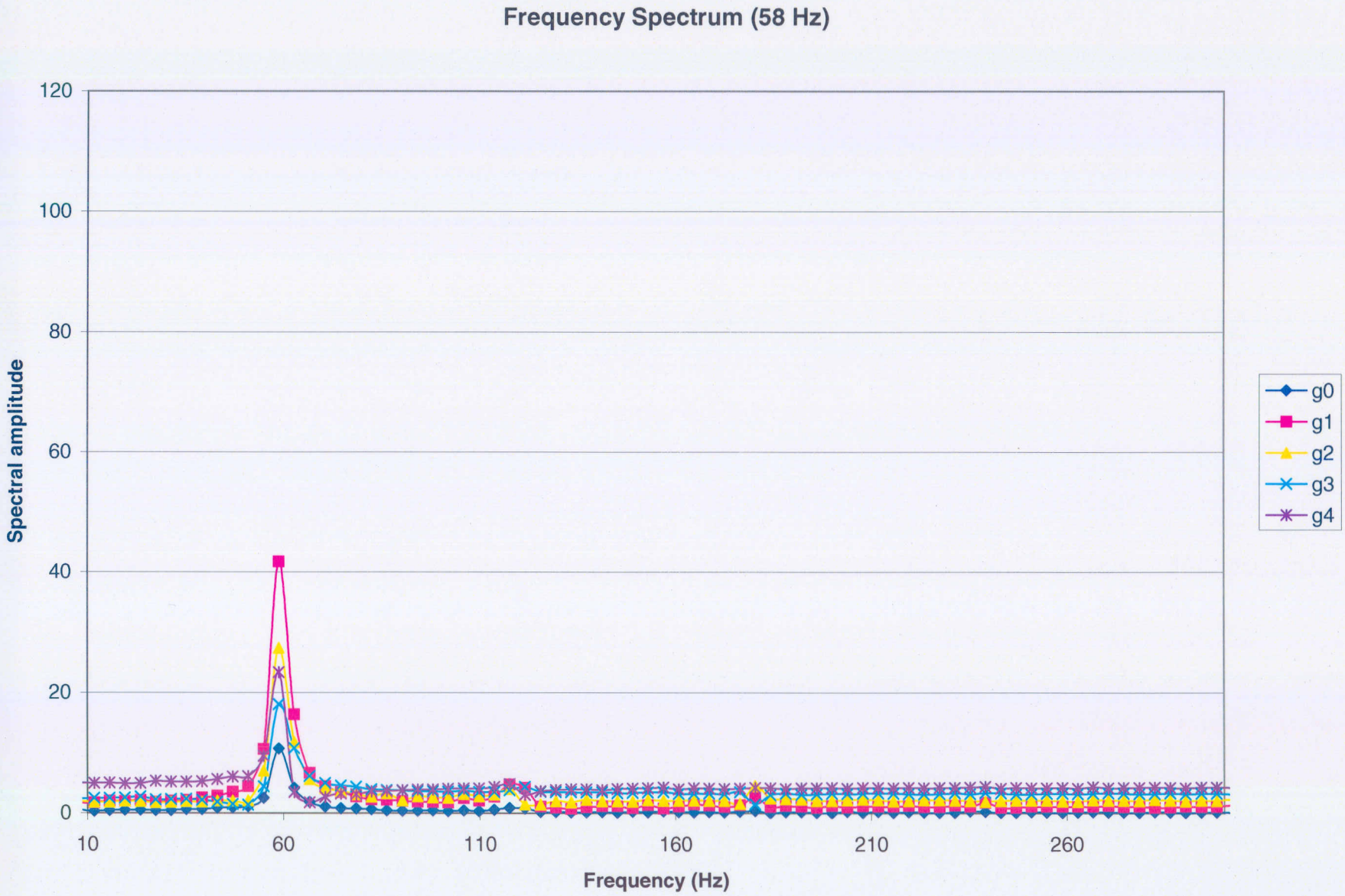

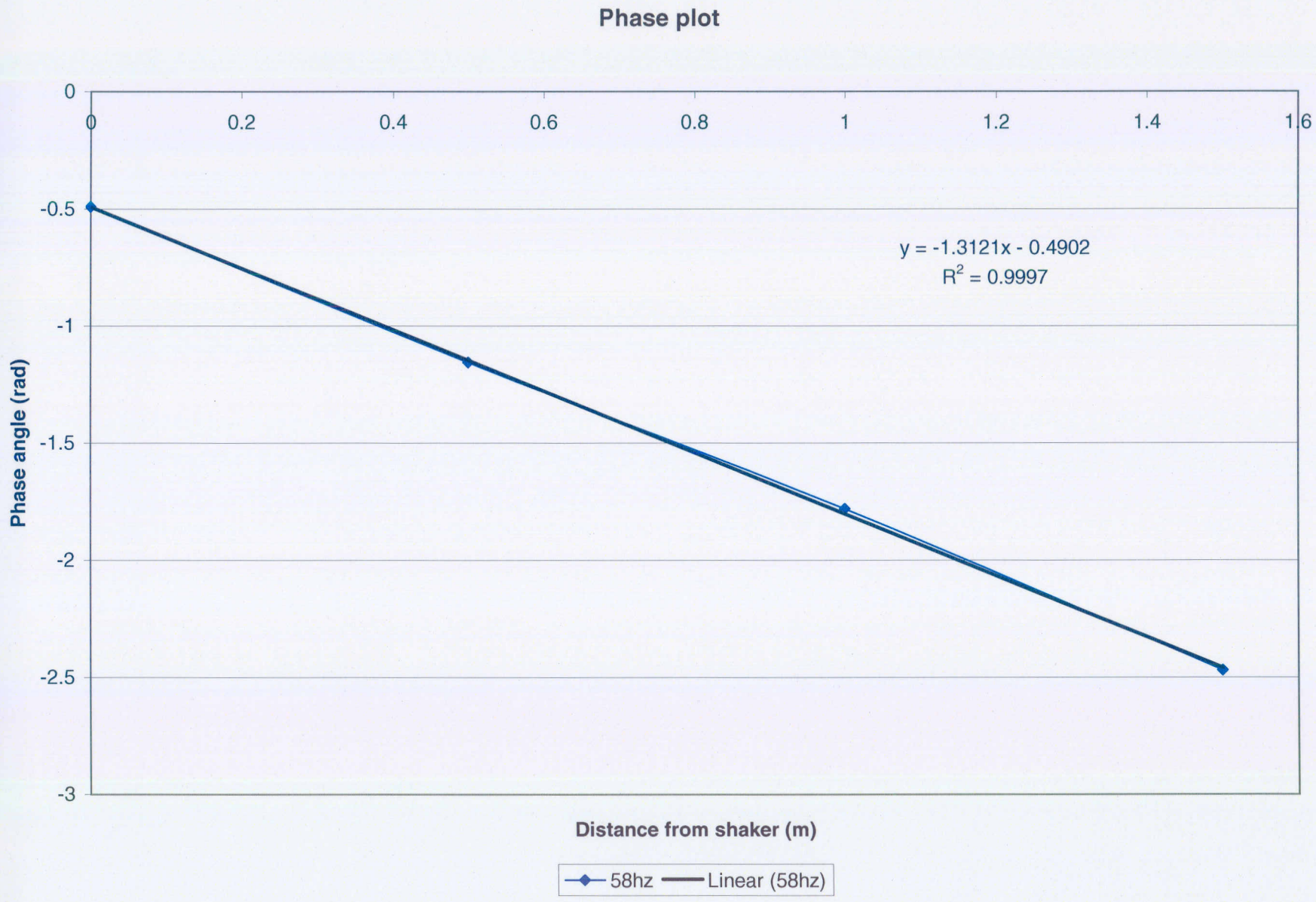

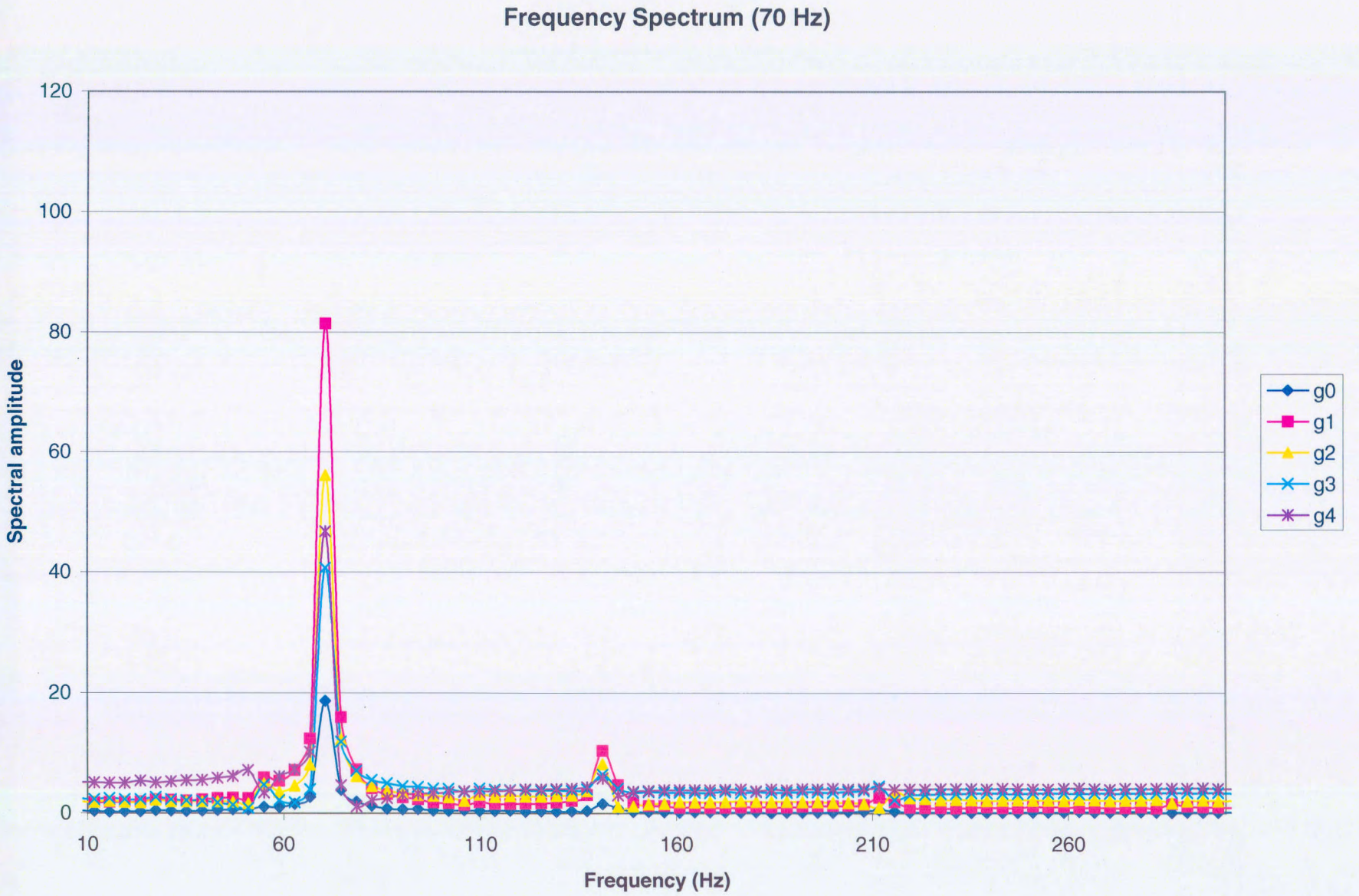

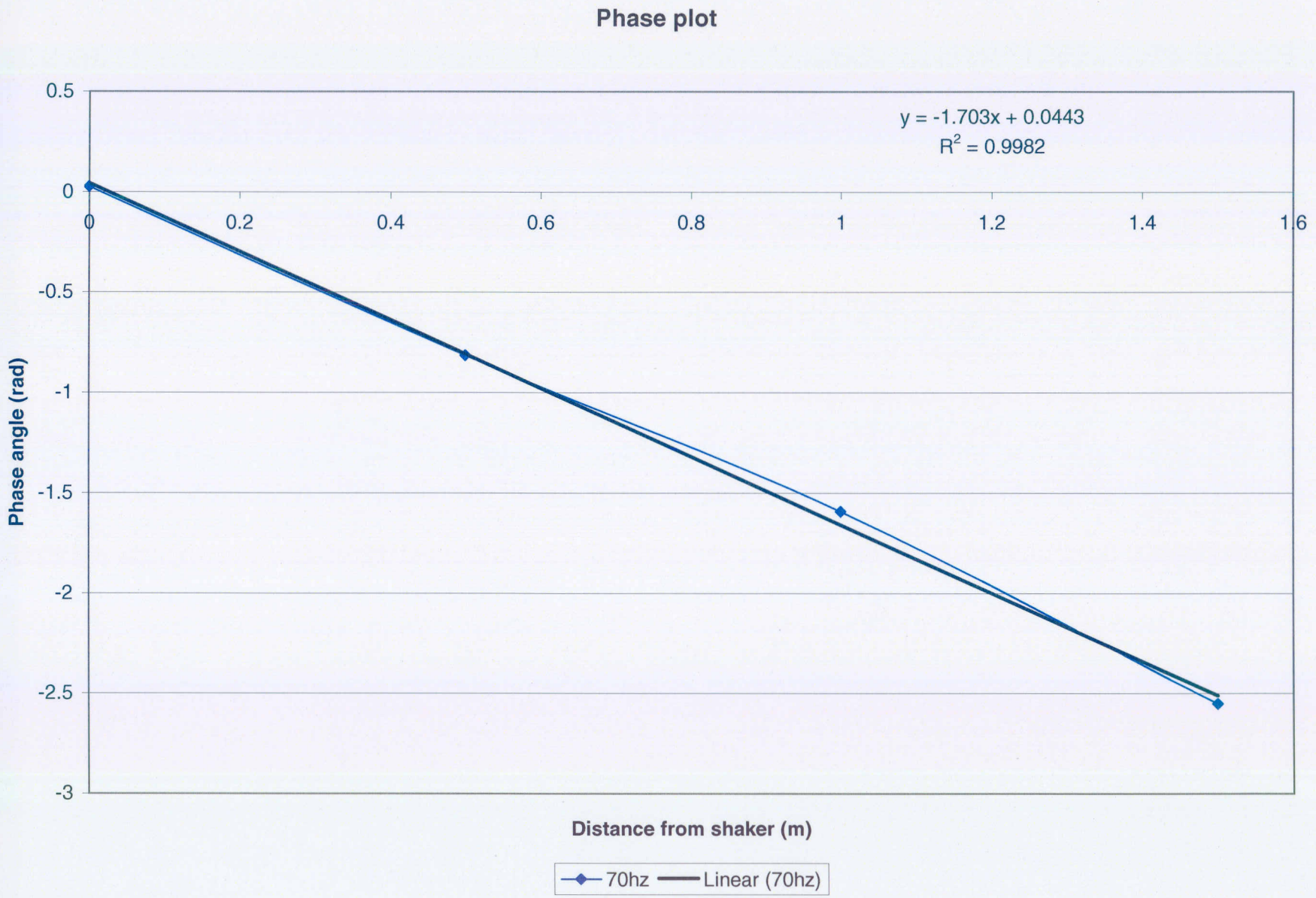

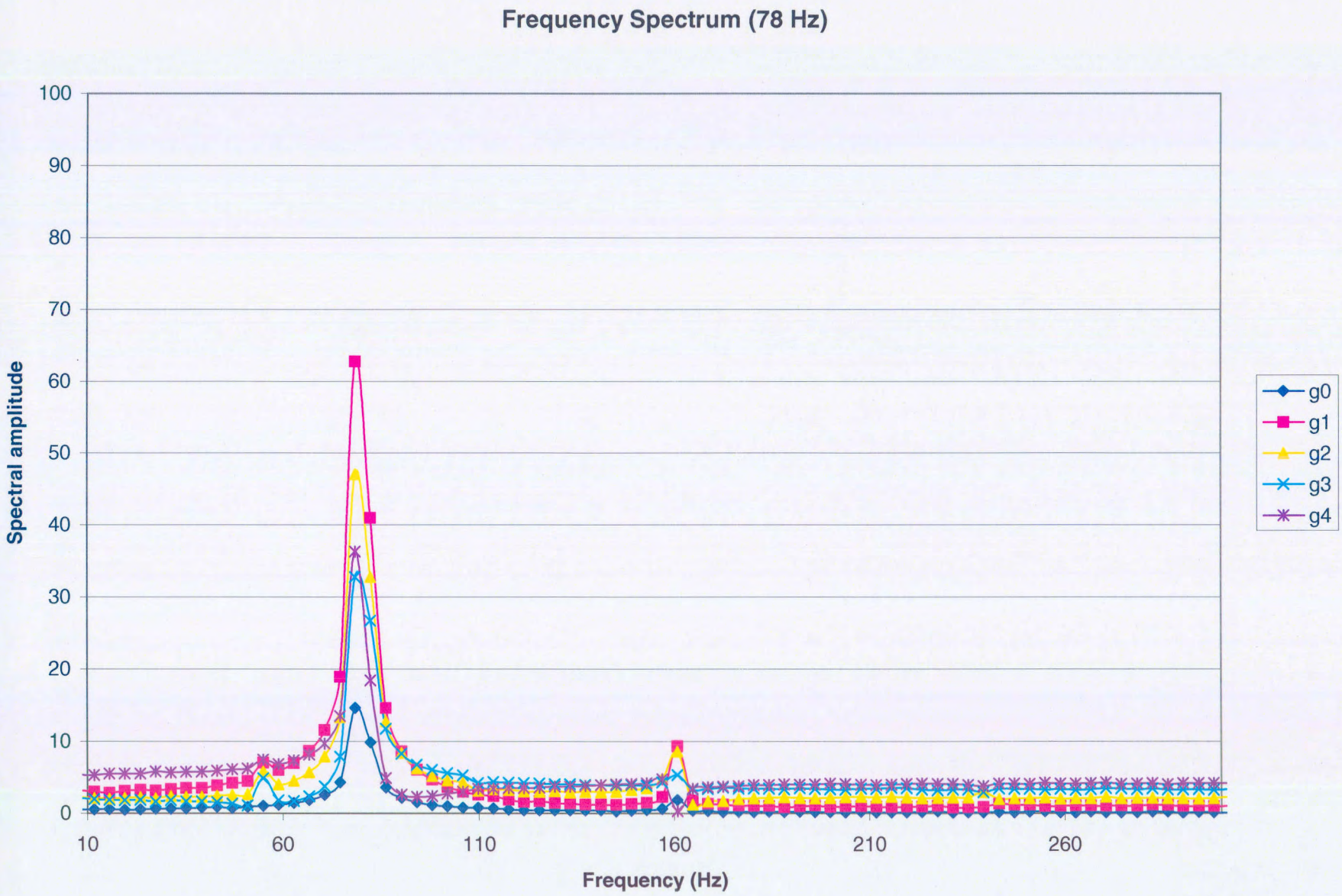

Phase plot

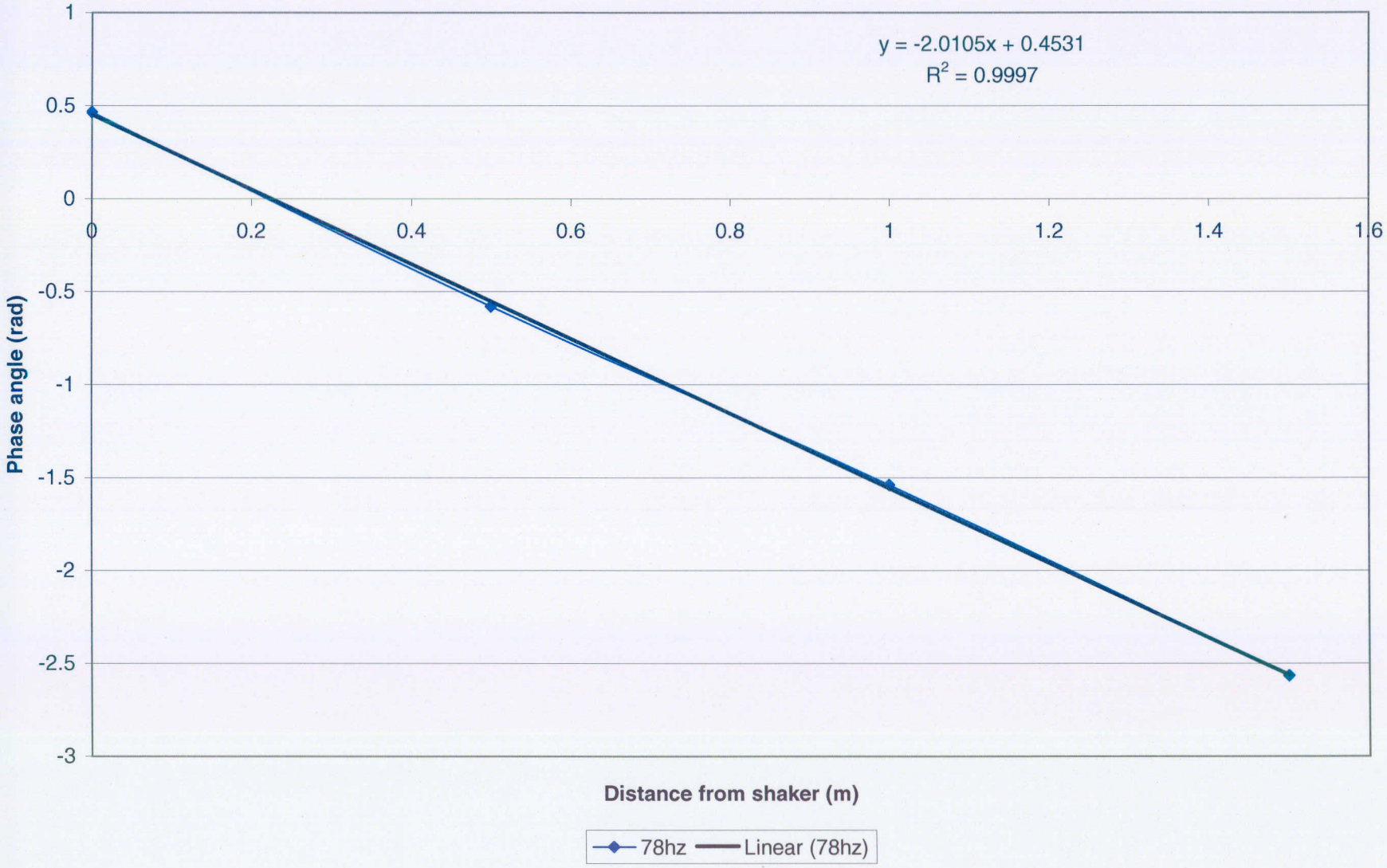

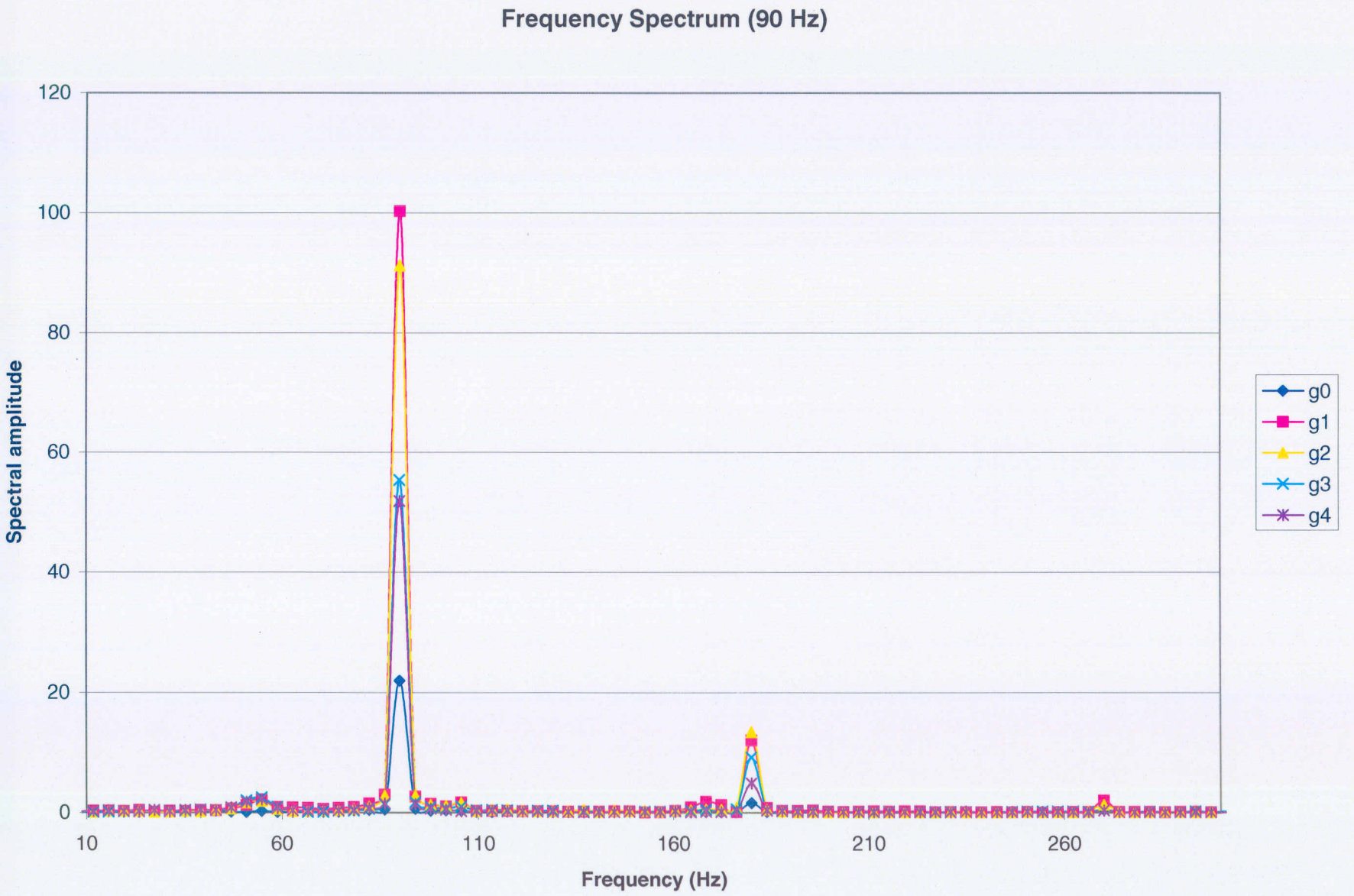

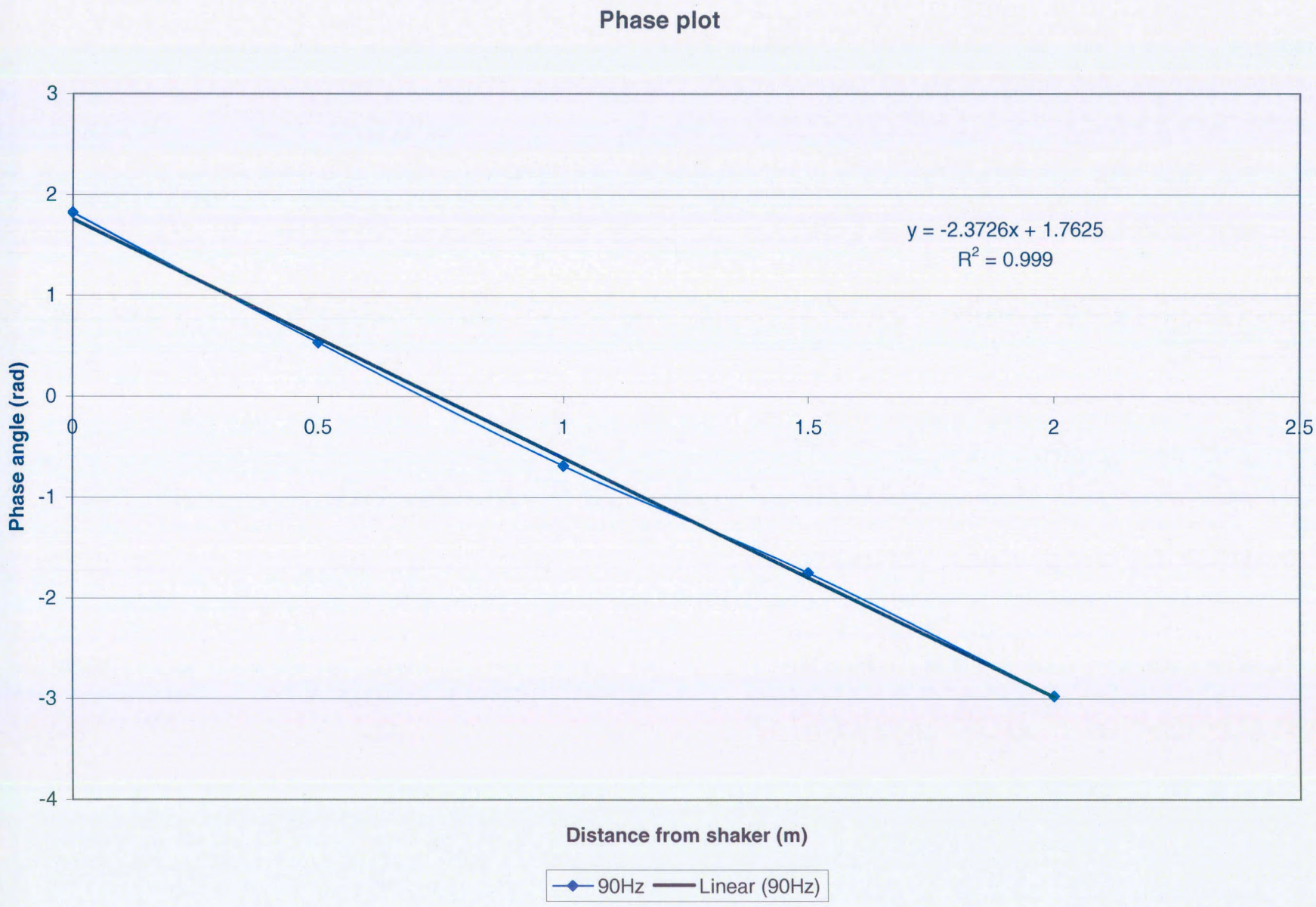

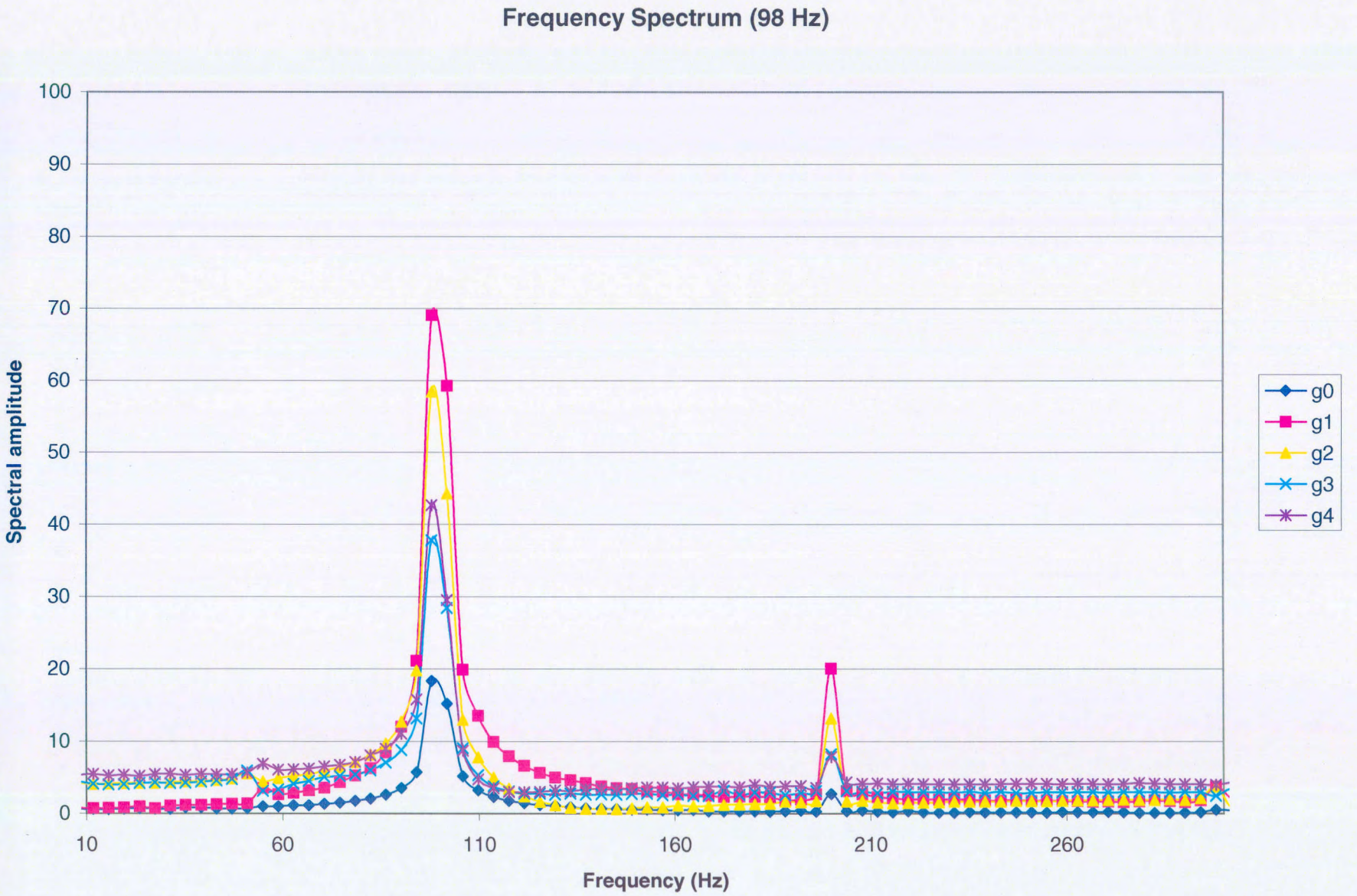

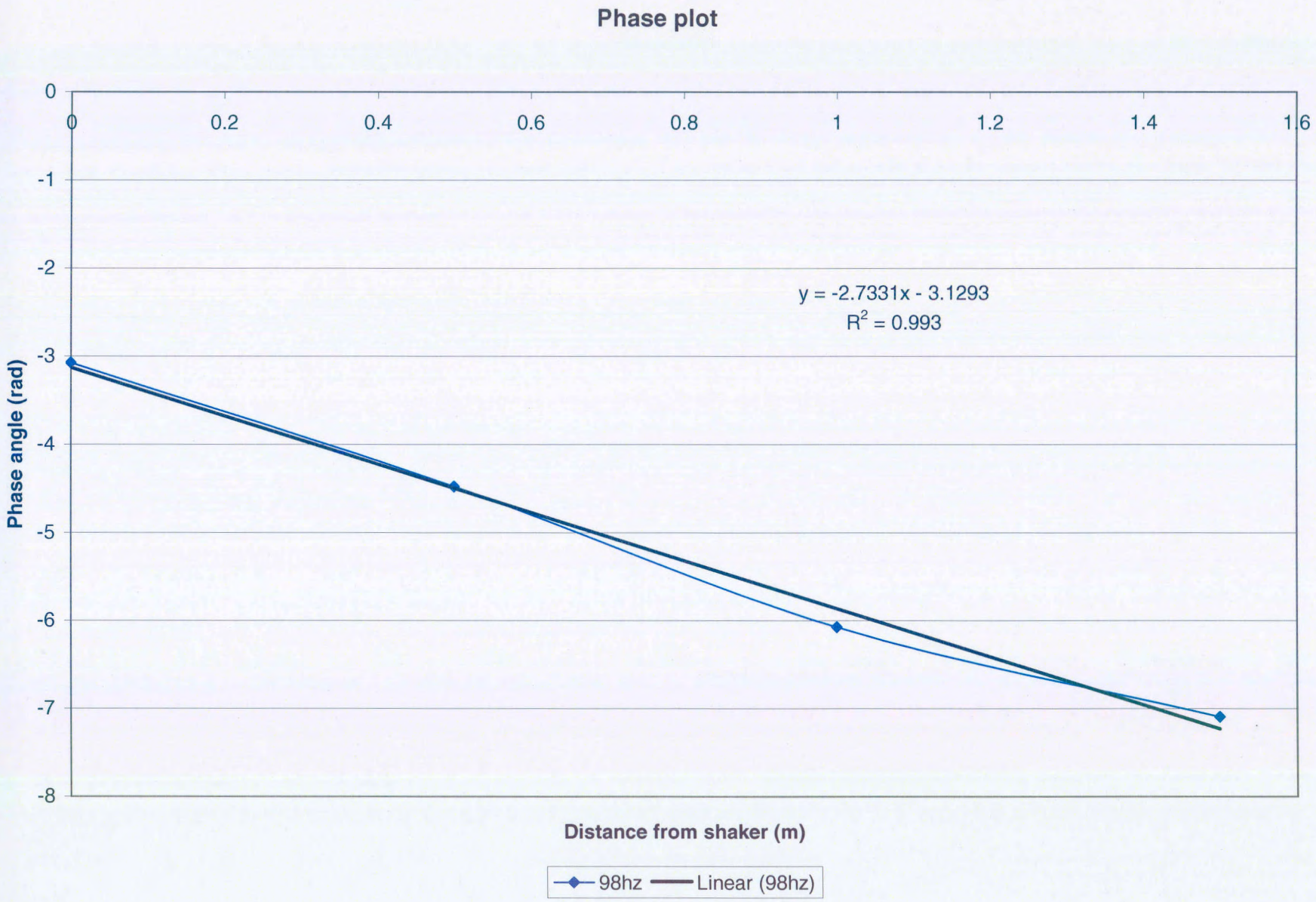

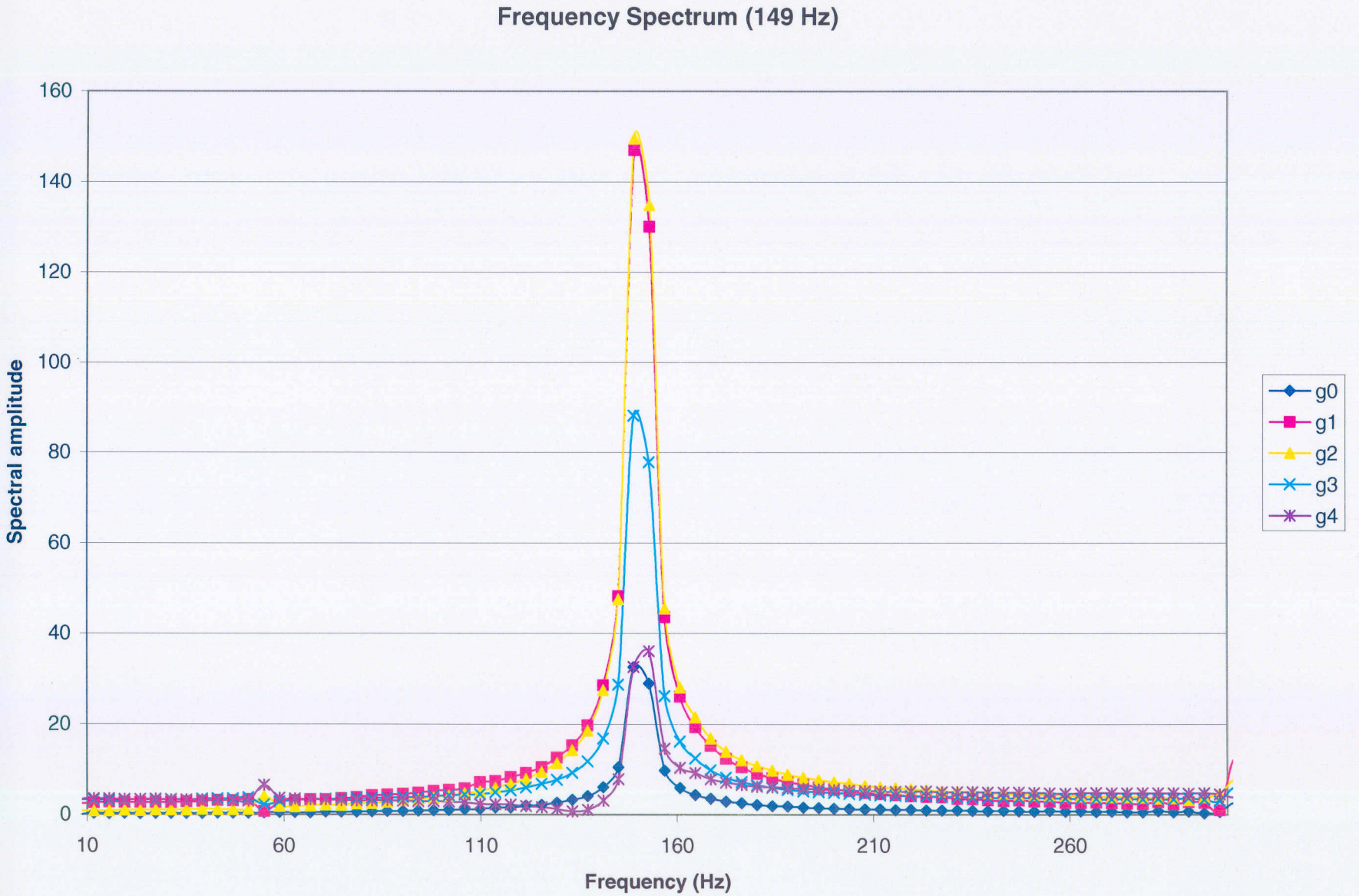

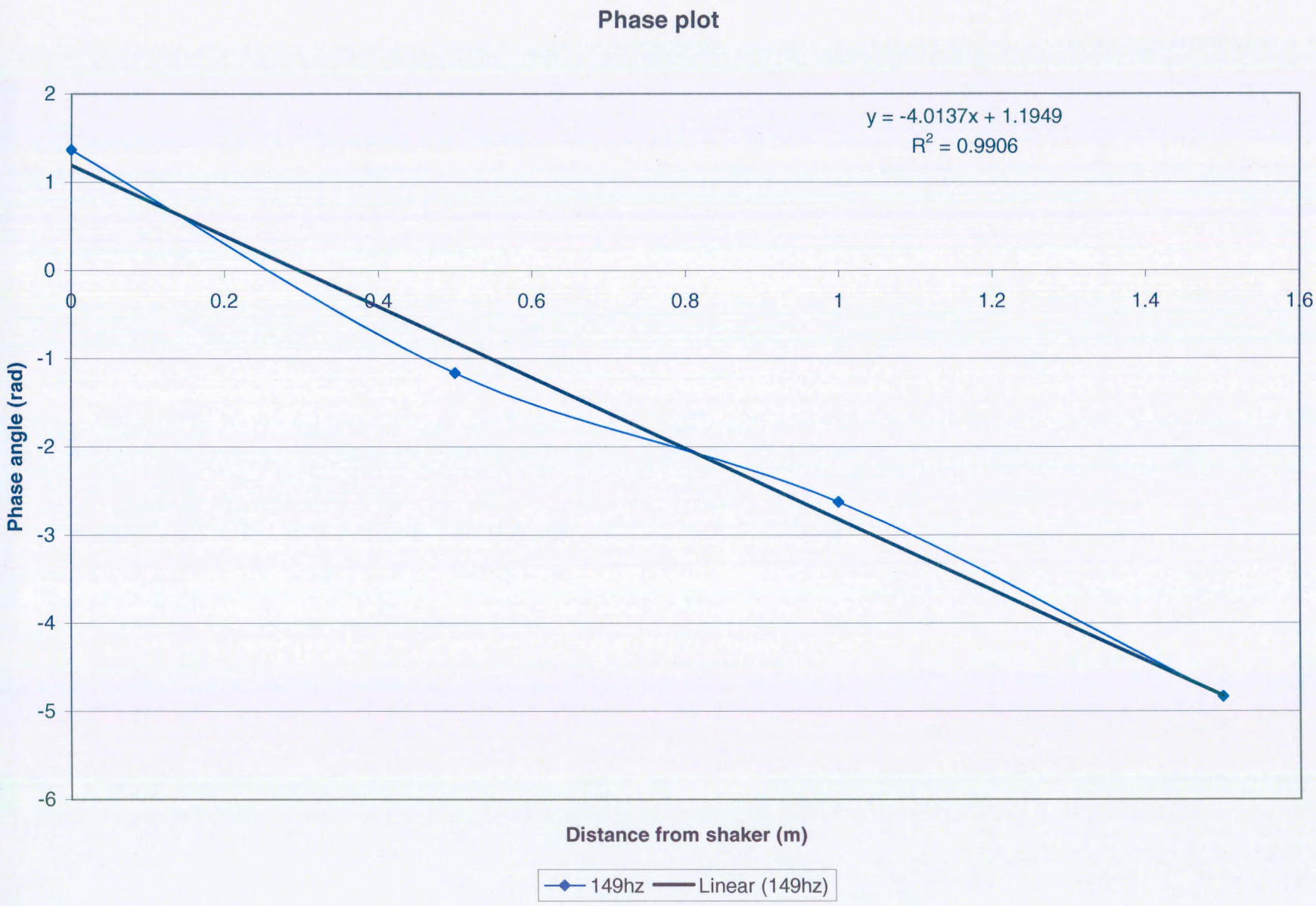

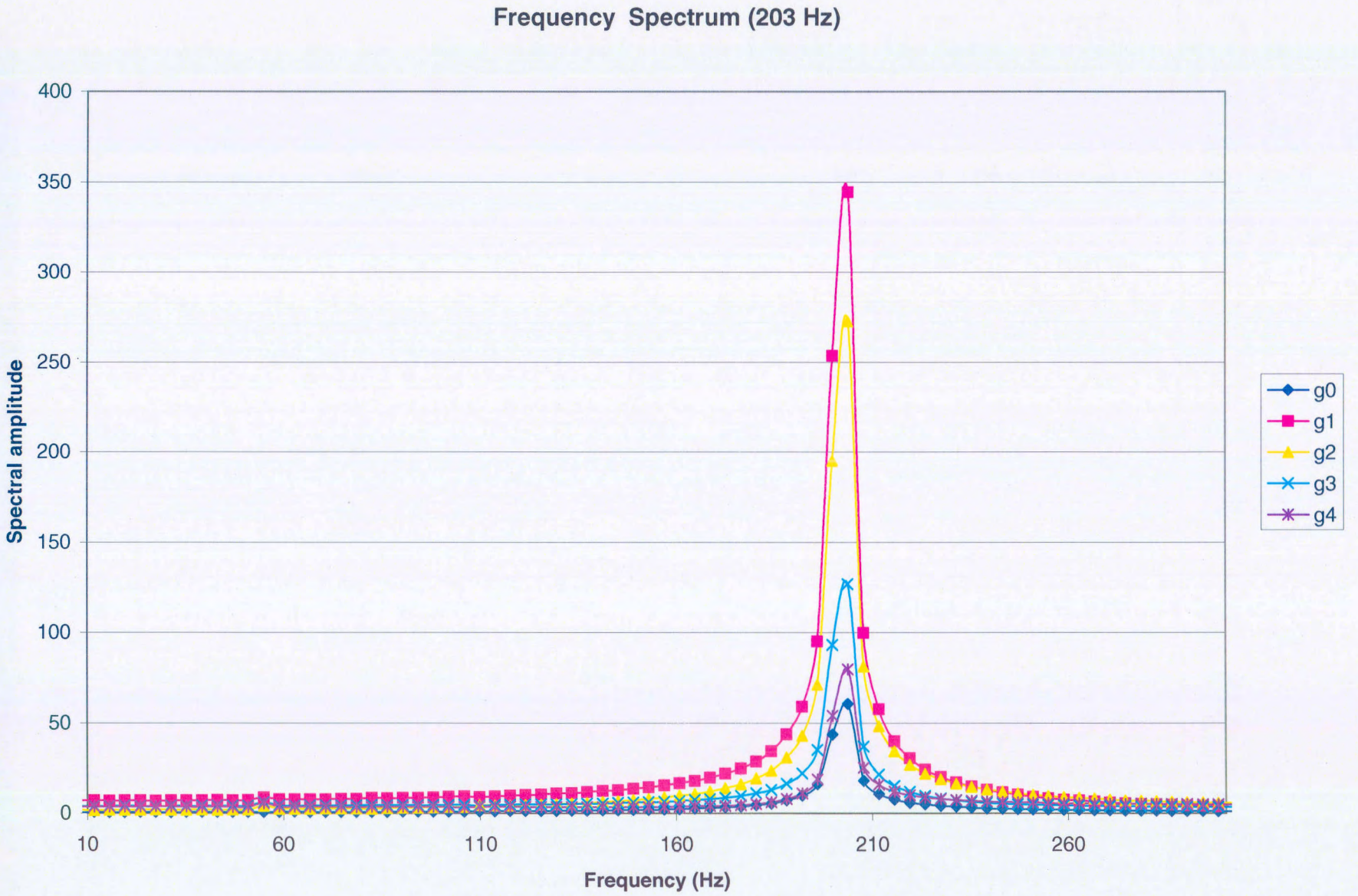

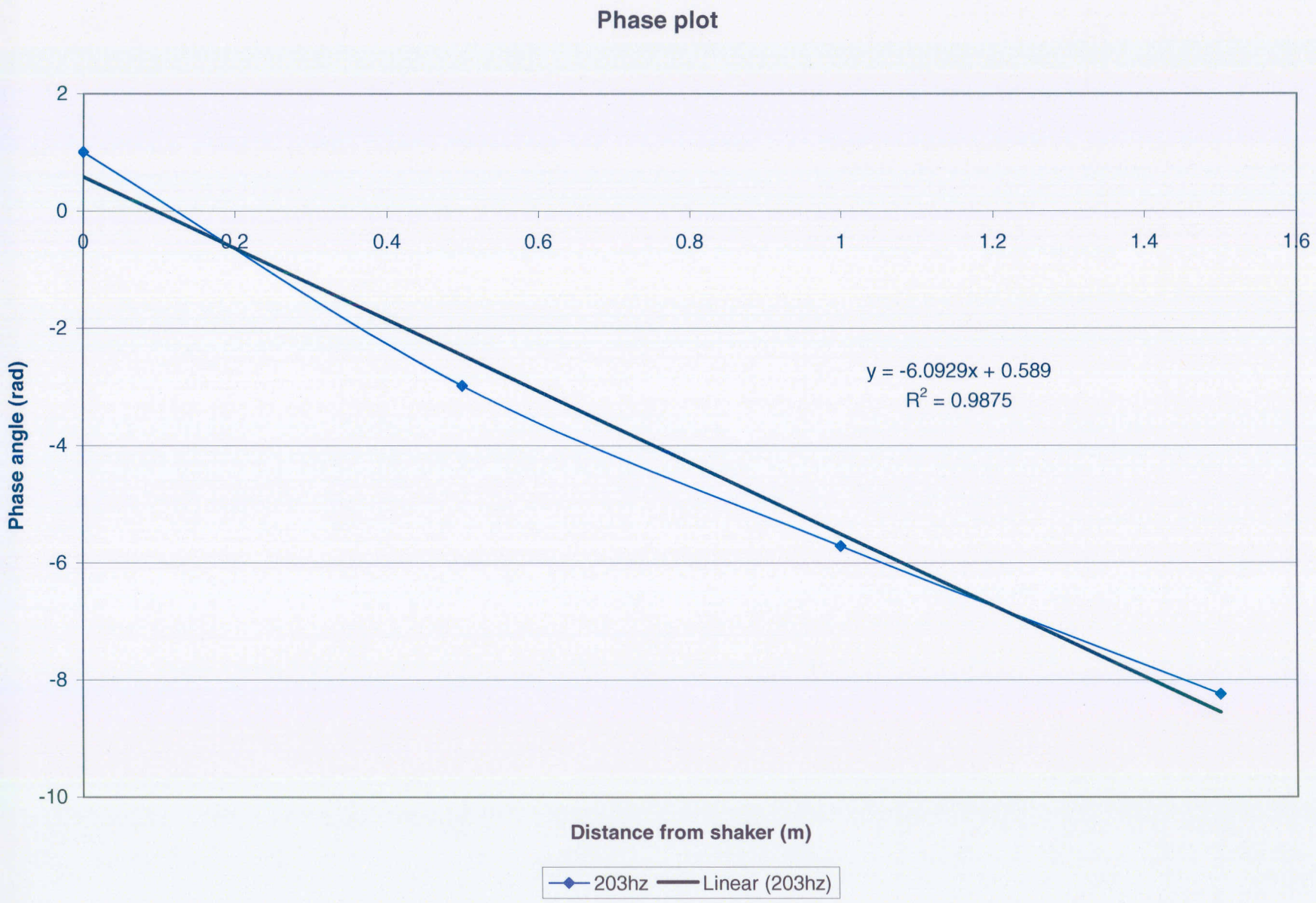

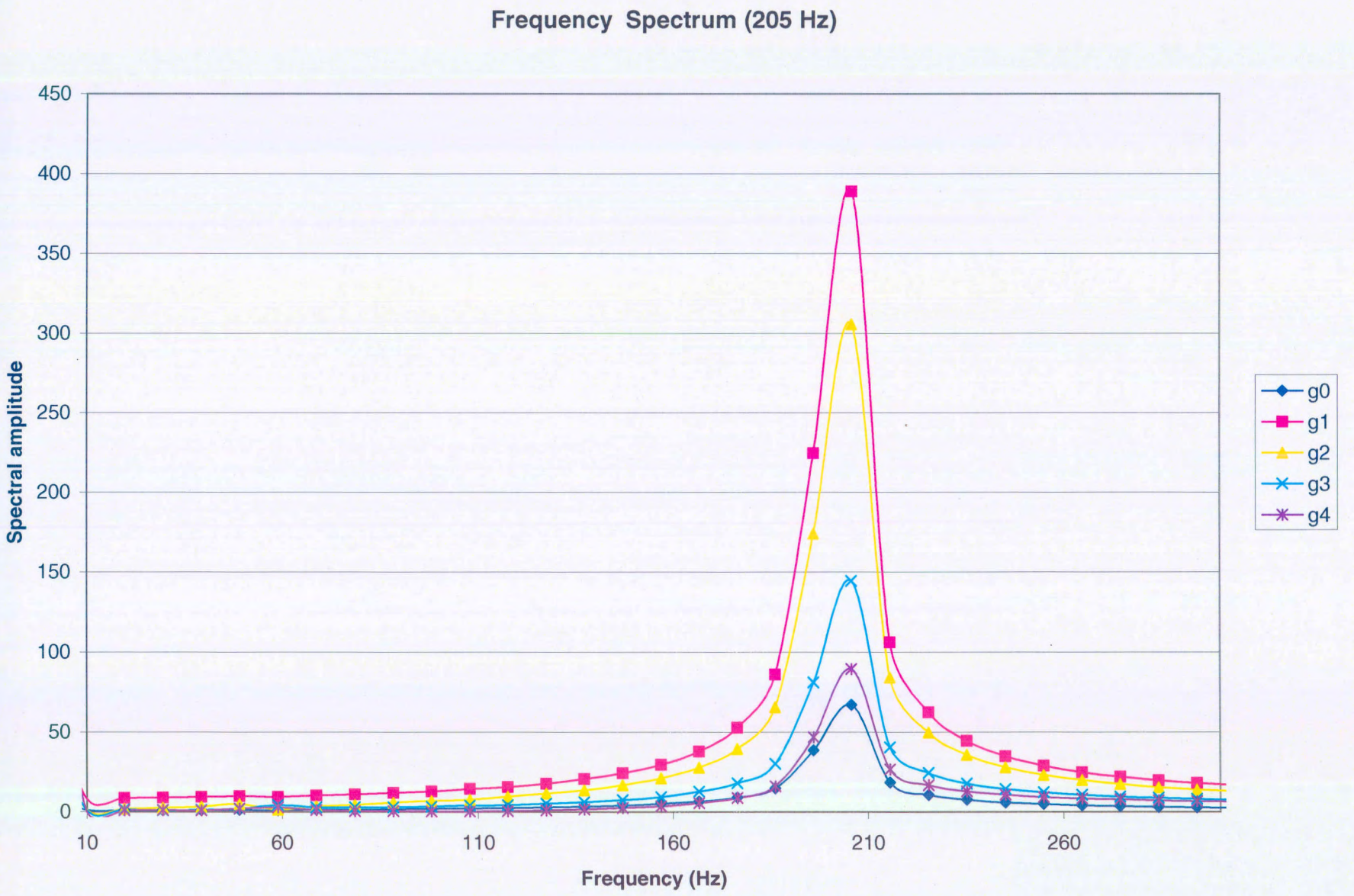

Phase plot

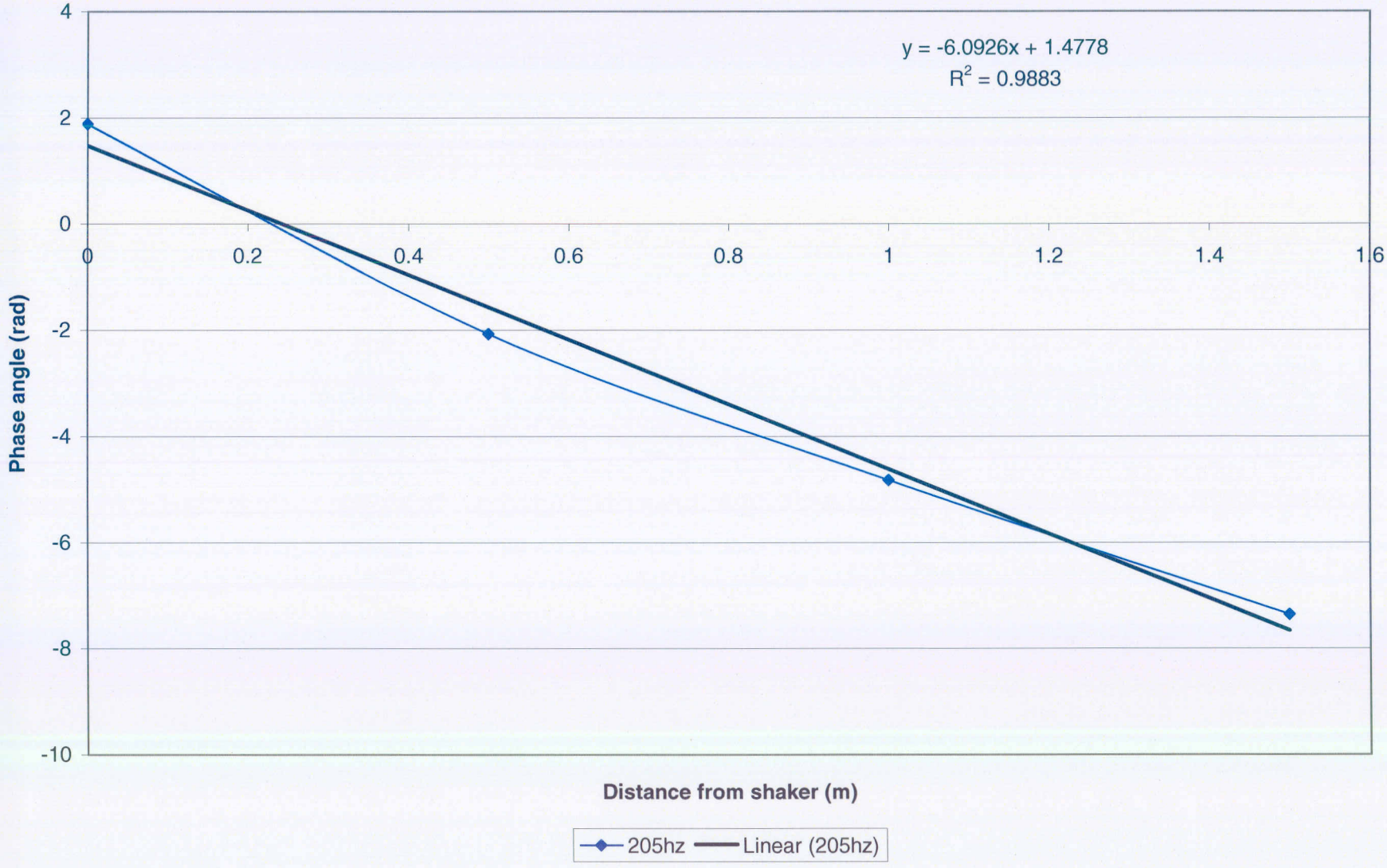

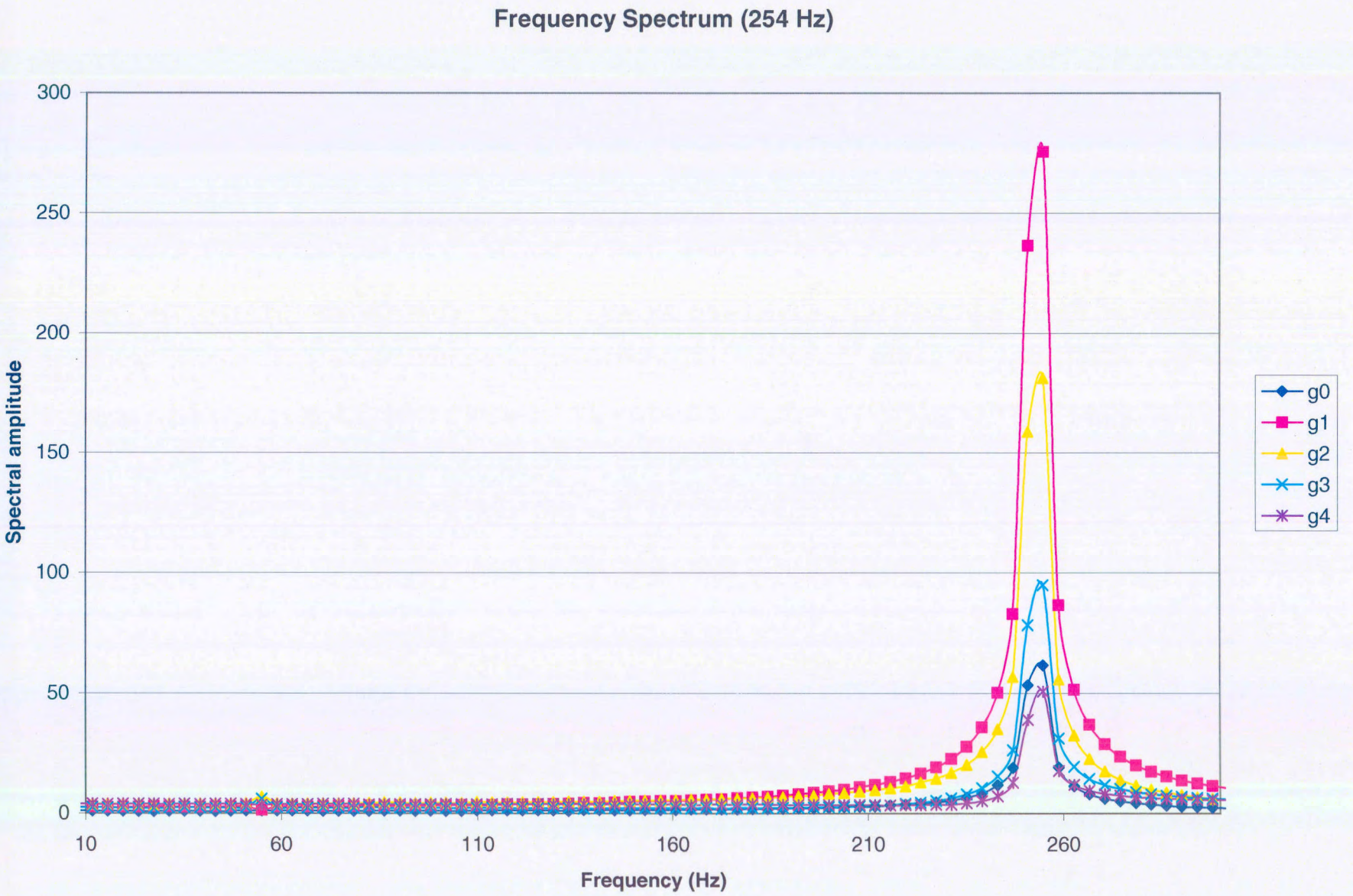

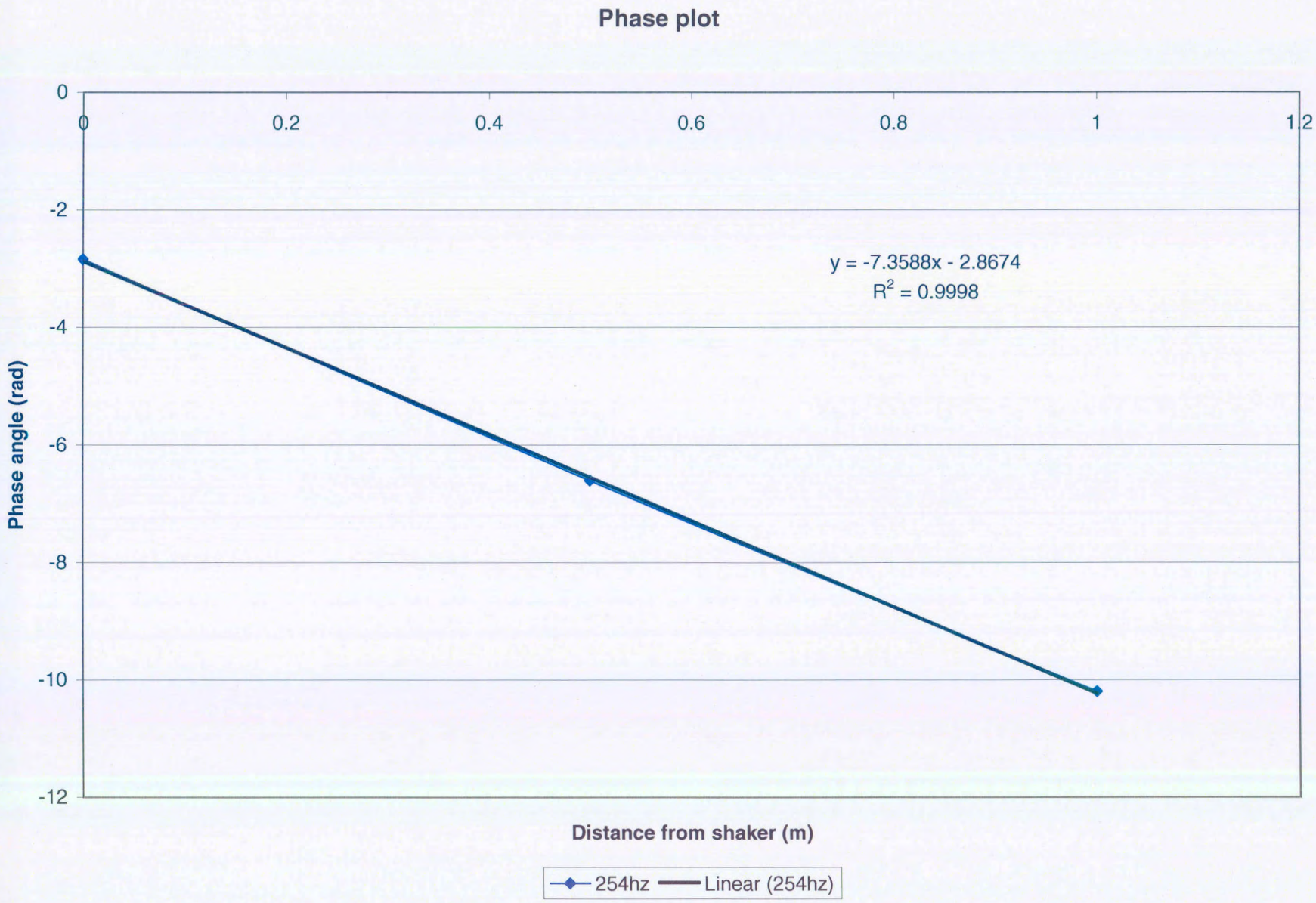

Frequency Spectrum (303 Hz)

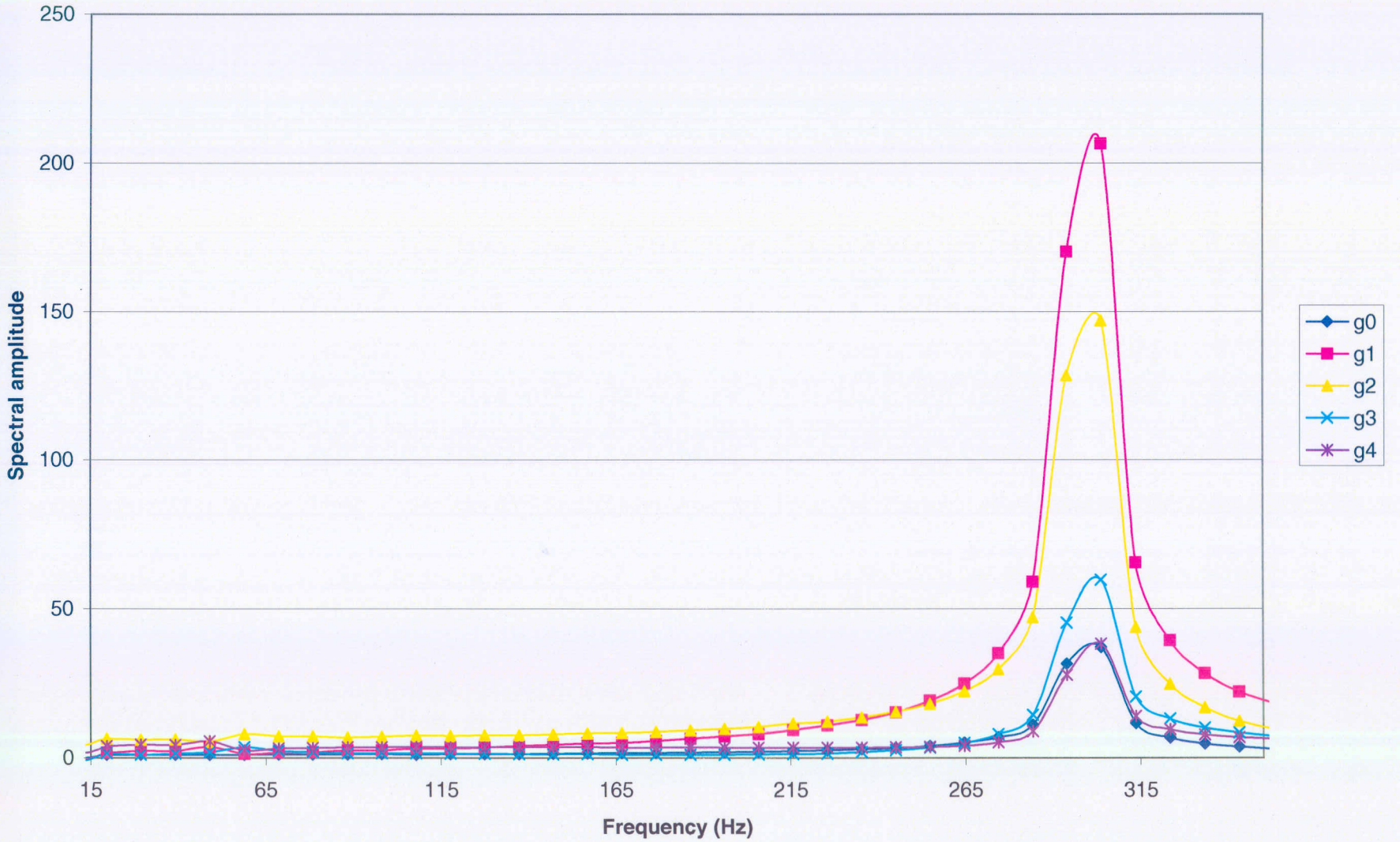

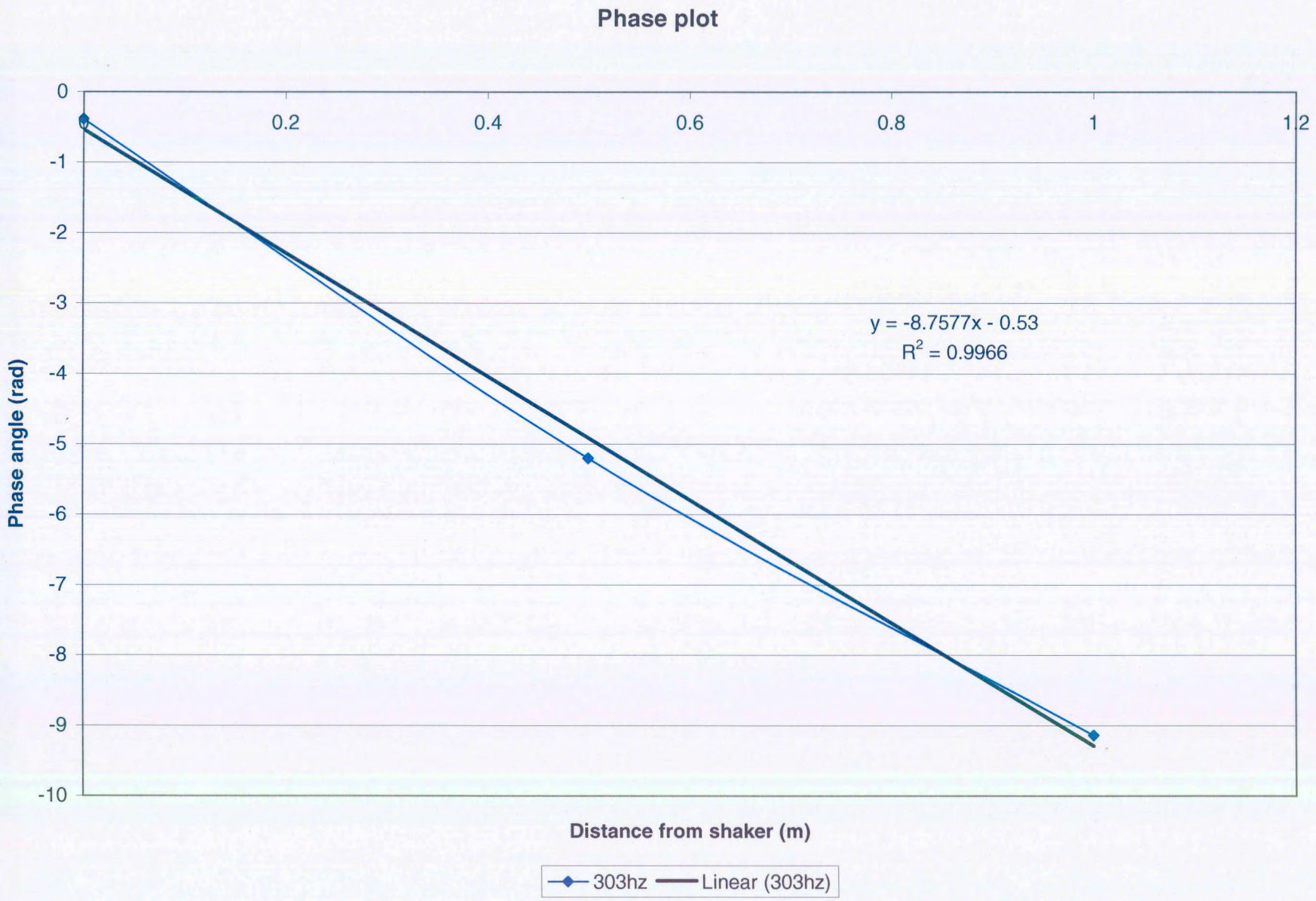

Appendix C

Phase plots and frequency spectrum for the compacted CSW testing